



High diversity of *Diaporthe* species associated with pear shoot canker in China

Y.S. Guo^{1,2,3,4}, P.W. Crous^{5,6,7,8}, Q. Bai⁴, M. Fu⁴, M.M. Yang⁴,
X.H. Wang⁴, Y.M. Du⁴, N. Hong^{1,2,3,4}, W.X. Xu^{1,2,3,4}, G.P. Wang^{1,2,3,4}

Key words

multi-gene phylogeny
pathogenicity
Pyrus
six new taxa
taxonomy

Abstract Species of *Diaporthe* (syn. *Phomopsis*) are important endophytes, saprobes and pathogens, infecting a wide range of plants and resulting in important crop diseases. However, the species occurring on pear remain largely unresolved. In this study, a total of 453 *Diaporthe* isolates were obtained from branches of *Pyrus* plants (including *P. bretschneideri*, *P. communis*, *P. pyrifolia* and *P. ussuriensis* collected from 12 provinces in China) showing shoot canker symptoms. Phylogenetic analyses based on five loci (ITS, *TEF*, *CAL*, *HIS*, and *TUB*) coupled with morphology of 113 representative isolates revealed that 19 *Diaporthe* species were isolated, representing 13 known species (including *D. caryae*, *D. cercidis*, *D. citrichinensis*, *D. eres*, *D. fusicola*, *D. ganjae*, *D. hongkongensis*, *D. padina*, *D. pescicola*, *D. sojae*, *D. taoicola*, *D. unshiuensis* and *D. velutina*) and six new species described here as *D. acuta*, *D. chongqingensis*, *D. fulvicolor*, *D. parvae*, *D. spinosa* and *D. zaobaisu*. Although Koch's postulates confirmed all species to be pathogenic, a high degree of variation in aggressiveness was observed. Moreover, these species have a high diversity, plasticity, and prevalence related to the geographical location and pear species involved.

Article info Received: 29 October 2019; Accepted: 4 December 2019; Published: 6 February 2020.

INTRODUCTION

Species of *Diaporthe* (asexual morph *Phomopsis*) are widely distributed, and infect a broad plant host range, e.g., fruit and forest trees, vegetables, and ornamental plants as endophytes, saprobes or pathogens (Santos & Phillips 2009, Santos et al. 2011, Udayanga et al. 2011, 2012, 2014a, b, Gomes et al. 2013, Gao et al. 2015, Marin-Felix et al. 2019). As plant pathogens *Diaporthe* spp. cause severe diseases, e.g., dieback, cankers, leaf spots, blights, decay or wilt of many economically important plants including *Camellia*, *Citrus*, *Glycine*, *Helianthus*, *Persea*, *Vaccinium*, and *Vitis* (Van Rensburg et al. 2006, Santos & Phillips 2009, Crous et al. 2011, 2016, Santos et al. 2011, Thompson et al. 2011, Grasso et al. 2012, Huang et al. 2013, Lombard et al. 2014, Gao et al. 2015, 2016, Udayanga et al. 2015, Guarnaccia & Crous 2017, 2018, Guarnaccia et al. 2018), resulting in major losses (Van Rensburg et al. 2006, Santos et al. 2011, Thompson et al. 2011). In recent years the taxonomy of *Diaporthe* species has been largely resolved based on multigene phylogenetic analyses including the rDNA internal transcribed spacer (ITS1, 5.8S, ITS2) region, partial translation elongation

factor 1-alpha (*TEF*), beta-tubulin (*TUB*), histone H3 (*HIS*) and calmodulin (*CAL*) genes (Gomes et al. 2013, Marin-Felix et al. 2019). Based on this approach, *Diaporthe* species have been well characterised for those infecting grapevine and citrus in Europe (Guarnaccia & Crous 2017, Guarnaccia et al. 2018) and forest trees in China (Yang et al. 2018). Published results revealed numerous species infecting these crops, with four (*D. bohemiae*, *D. celeris*, *D. hispaniae* and *D. hungariae*), two (*D. limonicola* and *D. melitensis* spp. nov.) and 12 (*D. acerigena*, *D. alangii*, *D. betulina*, *D. caryae*, *D. cercidis*, *D. chensiensis*, *D. cinnamomi*, *D. conica*, *D. fraxinicola*, *D. kadsurae*, *D. padina* and *D. ukurunduensis*) from citrus, grapevine and forest trees, respectively (Guarnaccia & Crous 2017, Guarnaccia et al. 2018, Yang et al. 2018). Moreover, some *Diaporthe* taxa appear to be strictly host specific (Gomes et al. 2013). However, the *Diaporthe* spp. occurring on other economically important crops, such as *Pyrus* (pear), have been poorly studied.

Pear species represent the third most important temperate fruit crop after apple and grape worldwide. Pear originated in the Tertiary period in Western China, and is divided into two major groups: European and Asian pears, with *Pyrus bretschneideri*, *P. communis*, *P. pyrifolia*, *P. sinkiangensis*, and *P. ussuriensis* commercially cultivated (Silva et al. 2014, Ferradini et al. 2017). Three species, including *P. bretschneideri*, *P. communis* and *P. pyrifolia* are the major species cultivated in China, with a pear-cultivation area of 957 321 ha in 2017, producing 16.5 MT fruits, accounting for nearly 70 % of the global pear fruit yield (24.2 MT) (Wu et al. 2013, Zhao et al. 2016, FAO 2017).

Pear shoot canker is a devastating disease caused by *Diaporthe* spp. The disease was initially described on *P. pyrifolia* in Japan (Nasu et al. 1987), infecting pear branches, causing brown canker tissue around buds on the shoots, twigs, or large branches, and always killing the infected shoots or branches and the attached blossom and leaf buds. The disease has resulted in large losses to fruit production in China (Wang et al. 2011, Huang et al. 2014, Bai et al. 2015), and other countries, e.g., Japan and

¹ State Key Laboratory of Agricultural Microbiology, Huazhong Agricultural University, Wuhan 430070, Hubei, China;

corresponding author e-mail: gpwang@mail.hzau.edu.cn.

² Key Laboratory of Horticultural Crop (Fruit Trees) Biology and Germplasm Creation of the Ministry of Agriculture, Wuhan 430070, Hubei, China.

³ Key Lab of Plant Pathology of Hubei Province, Wuhan, Hubei 430070, P. R. China.

⁴ College of Plant Science and Technology, Huazhong Agricultural University, Wuhan 430070, Hubei, China.

⁵ Westerdijk Fungal Biodiversity Institute, Uppsalalaan 8, 3584 CT Utrecht, The Netherlands.

⁶ Microbiology, Department of Biology, Utrecht University, Padualaan 8, 3584 CH Utrecht, The Netherlands.

⁷ Wageningen University and Research Centre (WUR), Laboratory of Phytopathology, Droevendaalsesteeg 1, 6708 PB Wageningen, The Netherlands.

⁸ Department of Biochemistry, Genetics & Microbiology, Forestry & Agricultural Biotechnology Institute (FABI), University of Pretoria, Pretoria, South Africa.

Table 1 Collection details and GenBank accession numbers of isolates included in this study.

Species	Culture no.	Host	Origin	GenBank accession number					Mating type	
				ITS	CAL	HIS	TEF	TUB	MAT1	MAT2
<i>D. acuta</i>	PSCG 045	<i>P. pyrifolia</i>	Wuhan, Hubei	MK626956	MK691123	MK726160	MK654809	MK691223	/	/
	PSCG 046	<i>P. pyrifolia</i>	Wuhan, Hubei	MK626958	MK691124	MK726162	MK654803	MK691224	/	/
	PSCG 047*	<i>P. pyrifolia</i>	Wuhan, Hubei	MK626957	MK691125	MK726161	MK654802	MK691225	/	/
<i>D. caryae</i>	PSCG 380	<i>P. pyrifolia</i>	Nanjing, Jiangsu	MK626951	MK691198	MK726200	MK654893	MK691313	-	+
	PSCG 382	<i>P. pyrifolia</i>	Nanjing, Jiangsu	MK626954	MK691199	MK726201	MK654894	MK691314	-	+
	PSCG 520	<i>P. pyrifolia</i>	Zhenjiang, Jiangsu	MK626952	MK691200	MK726202	MK654895	MK691315	+	-
<i>D. cercidis</i>	PSCG 528	<i>P. pyrifolia</i>	Zhenjiang, Jiangsu	MK626953	MK691201	MK726203	MK654896	MK691316	-	+
	PSCG 259	<i>P. pyrifolia</i>	Yantai, Shandong	MK626847	MK691170	MK726154	MK654795	MK691218	+	-
	PSCG 273	<i>P. pyrifolia</i>	Hangzhou, Zhejiang	MK626848	MK691113	MK726165	MK654808	MK691231	-	+
	PSCG 275	<i>P. pyrifolia</i>	Hangzhou, Zhejiang	MK626853	MK691114	MK726158	MK654805	MK691220	+	+
	PSCG 439	<i>P. pyrifolia</i>	Chongqing, China	MK626852	MK691118	MK726172	MK654813	MK691221	-	+
	PSCG 513	<i>P. pyrifolia</i>	Zhenjiang, Jiangsu	MK626850	MK691117	MK726223	MK654815	MK691219	-	+
<i>D. chongqingensis</i>	PSCG 526	<i>P. pyrifolia</i>	Zhenjiang, Jiangsu	MK626851	MK691121	MK726169	MK654804	MK691228	+	-
	PSCG 435*	<i>P. pyrifolia</i>	Chongqing, China	MK626916	MK691209	MK726257	MK654866	MK691321	-	+
	PSCG 436	<i>P. pyrifolia</i>	Chongqing, China	MK626917	MK691208	MK726256	MK654867	MK691322	-	+
<i>D. citrichinensis</i>	PSCG 462	<i>P. pyrifolia</i>	Guiyang, Guizhou	MK626893	MK691171	MK726248	MK654852	MK691286	+	-
<i>D. eres</i>	PSCG 007	<i>P. pyrifolia</i>	Nanchang, Jiangxi	MK626884	MK691157	MK726216	MK654835	MK691278	+	-
	PSCG 017	<i>P. pyrifolia</i>	Fuzhou, Jiangxi	MK626887	MK691139	MK726232	MK654829	MK691283	-	+
<i>D. fuscicola</i>	PSCG 023	<i>P. pyrifolia</i>	Fuzhou, Jiangxi	MK626878	MK691158	MK726217	MK654821	MK691269	+	-
	PSCG 041	<i>P. bretschneideri</i>	Kunming, Yunnan	MK626880	MK691144	MK726219	MK654840	MK691265	-	+
	PSCG 042	<i>P. bretschneideri</i>	Kunming, Yunnan	MK626881	MK691145	MK726225	MK654845	MK691285	-	+
	PSCG 043	<i>P. bretschneideri</i>	Kunming, Yunnan	MK626879	MK691146	MK726229	MK654844	MK691266	-	+
	PSCG 090	<i>P. communis</i>	Yantai, Shandong	MK626872	MK691159	MK726236	MK654828	MK691281	+	-
	PSCG 092	<i>P. communis</i>	Yantai, Shandong	MK626896	MK691147	MK726227	MK654823	MK691264	-	+
	PSCG 132	<i>P. pyrifolia</i>	Sanming, Fujian	MK626891	MK691133	MK726212	MK654816	MK691250	+	-
	PSCG 135	<i>P. pyrifolia</i>	Sanming, Fujian	MK626873	MK691160	MK726213	MK654837	MK691251	+	-
	PSCG 151	<i>P. pyrifolia</i>	Sanming, Fujian	MK626876	MK691161	MK726239	MK654820	MK691262	+	-
	PSCG 175	<i>P. pyrifolia</i>	Yingtian, Jiangsu	MK626877	MK691165	MK726238	MK654843	MK691259	-	+
	PSCG 202	<i>P. communis</i>	Yantai, Shandong	MK626885	MK691166	MK726237	MK654817	MK691254	-	+
	PSCG 245	<i>P. pyrifolia</i>	Chongqing, China	MK626894	MK691164	MK726224	MK654822	MK691274	+	-
	PSCG 250	<i>P. pyrifolia</i>	Chongqing, China	MK626895	MK691168	MK726245	MK654836	MK691275	-	+
	PSCG 261	<i>P. pyrifolia</i>	Wuhan, Hubei	MK626904	MK691141	MK726241	MK654826	MK691252	+	-
	PSCG 265	<i>P. pyrifolia</i>	Wuhan, Hubei	MK626903	MK691150	MK726214	MK654842	MK691282	+	-
	PSCG 276	<i>P. pyrifolia</i>	Hangzhou, Zhejiang	MK626909	MK691163	MK726226	MK654841	MK691263	+	-
	PSCG 299	<i>P. pyrifolia</i>	Changli, Hebei	MK626900	MK691154	MK726246	MK654818	MK691255	-	+
	PSCG 300	<i>P. pyrifolia</i>	Changli, Hebei	MK626901	MK691155	MK726247	MK654819	MK691253	-	+
	PSCG 306	<i>P. communis</i>	Yantai, Shandong	MK626898	MK691138	MK726243	MK654839	MK691279	-	+
	PSCG 321	<i>P. pyrifolia</i>	Nanyang, Henan	MK626874	MK691167	MK726228	MK654827	MK691267	-	+
	PSCG 322	<i>P. pyrifolia</i>	Nanyang, Henan	MK626875	MK691162	MK726244	MK654824	MK691268	-	+
	PSCG 324	<i>P. pyrifolia</i>	Nanyang, Henan	MK626906	MK691149	MK726220	MK654830	MK691272	-	+
	PSCG 325	<i>P. pyrifolia</i>	Nanyang, Henan	MK626905	MK691153	MK726222	MK654838	MK691273	-	+
	PSCG 346	<i>P. pyrifolia</i>	Nanyang, Henan	MK626882	MK691134	MK726234	MK654848	MK691270	-	+
	PSCG 358	<i>P. ussuriensis</i>	Yingkou, Liaoning	MK626889	MK691143	MK726231	MK654849	MK691260	-	+
	PSCG 362	<i>P. pyrifolia</i>	Yingkou, Liaoning	MK626907	MK691151	MK726235	MK654846	MK691280	+	-
	PSCG 376	<i>P. pyrifolia</i>	Hangzhou, Zhejiang	MK626899	MK691142	MK726218	MK654834	MK691257	-	+
	PSCG 377	<i>P. pyrifolia</i>	Hangzhou, Zhejiang	MK626886	MK691137	MK726221	MK654833	MK691276	+	-
	PSCG 381	<i>P. pyrifolia</i>	Nanchang, Jiangxi	MK626897	MK691148	MK726215	MK654847	MK691277	-	+
PSCG 440	<i>P. pyrifolia</i>	Wuhan, Hubei	MK626908	MK691140	MK726230	MK654825	MK691256	+	-	
PSCG 512	<i>P. pyrifolia</i>	Zhenjiang, Jiangsu	MK626883	MK691135	MK726240	MK654832	MK691271	+	-	
PSCG 521	<i>P. pyrifolia</i>	Zhenjiang, Jiangsu	MK626888	MK691136	MK726233	MK654850	MK691284	-	+	
PSCG 529	<i>P. pyrifolia</i>	Zhenjiang, Jiangsu	MK626902	MK691156	MK726242	MK654831	MK691258	-	+	
<i>D. fulvicolor</i>	PSCG 051*	<i>P. pyrifolia</i>	Wuhan, Hubei	MK626859	MK691132	MK726163	MK654806	MK691236	-	+
	PSCG 057	<i>P. pyrifolia</i>	Wuhan, Hubei	MK626858	MK691131	MK726164	MK654810	MK691233	-	+
<i>D. ganjae</i>	PSCG 015	<i>P. pyrifolia</i>	Fuzhou, Jiangxi	MK626915	MK691210	MK726254	MK654861	MK691320	-	+
	PSCG 030	<i>P. pyrifolia</i>	Fuzhou, Jiangxi	MK626914	MK691211	MK726255	MK654864	MK691323	-	+
	PSCG 118	<i>P. pyrifolia</i>	Sanming, Fujian	MK626910	MK691204	MK726250	MK654860	MK691317	-	+
	PSCG 178	<i>P. pyrifolia</i>	Yingtian, Jiangxi	MK626913	MK691206	MK726251	MK654862	MK691324	-	+
	PSCG 179	<i>P. pyrifolia</i>	Yingtian, Jiangxi	MK626912	MK691207	MK726252	MK654863	MK691318	-	+
	PSCG 371	<i>P. pyrifolia</i>	Hangzhou, Zhejiang	MK626911	MK691205	MK726253	MK654865	MK691319	-	+
	PSCG 489	<i>P. pyrifolia</i>	Guiyang, Guizhou	MK626955	MK691202	MK726204	MK654897	MK691287	-	+
<i>D. hongkongensis</i>	PSCG 001	<i>P. pyrifolia</i>	Nanchang, Jiangxi	MK626846	MK691103	MK726150	MK654788	MK691240	+	-
	PSCG 026	<i>P. pyrifolia</i>	Fuzhou, Jiangxi	MK626861	MK691106	MK726153	MK654789	MK691241	+	-
	PSCG 114	<i>P. pyrifolia</i>	Sanming, Fujian	MK626867	MK691104	MK726146	MK654785	MK691212	-	+
	PSCG 130	<i>P. pyrifolia</i>	Sanming, Fujian	MK626862	MK691105	MK726151	MK654786	MK691239	-	+
	PSCG 141	<i>P. pyrifolia</i>	Sanming, Fujian	MK626854	MK691110	MK726147	MK654787	MK691213	+	+
	PSCG 290	<i>P. pyrifolia</i>	Hangzhou, Zhejiang	MK626870	MK691107	MK726152	MK654794	MK691214	+	+
	PSCG 465	<i>P. pyrifolia</i>	Sanming, Fujian	MK626863	MK691109	MK726148	MK654790	MK691242	-	+
	PSCG 466	<i>P. pyrifolia</i>	Sanming, Fujian	MK626864	MK691111	MK726149	MK654792	MK691217	-	+
	PSCG 472	<i>P. pyrifolia</i>	Sanming, Fujian	MK626865	MK691108	/	MK654793	MK691215	/	/
	PSCG 473	<i>P. pyrifolia</i>	Sanming, Fujian	MK626866	MK691112	MK726187	MK654791	MK691216	-	+
	PSCG 160	<i>P. pyrifolia</i>	Nanchang, Jiangxi	MK626892	MK691172	MK726249	MK654851	MK691261	-	+
<i>D. padina</i>	PSCG 034*	<i>P. bretschneideri</i>	Kunming, Yunnan	MK626919	/	MK726210	MK654858	MK691248	+	-
	PSCG 035	<i>P. bretschneideri</i>	Kunming, Yunnan	MK626920	MK691169	MK726211	MK654859	MK691249	+	-
<i>D. pescicola</i>	PSCG 036	<i>P. bretschneideri</i>	Kunming, Yunnan	MK626855	MK691116	MK726159	MK654796	MK691226	+	-
	PSCG 037	<i>P. bretschneideri</i>	Kunming, Yunnan	MK626857	MK691130	MK726157	MK654799	MK691230	-	+
<i>D. sojiae</i>	PSCG 177	<i>P. pyrifolia</i>	Yingtian, Jiangxi	MK626940	MK691188	MK726189	MK654882	MK691302	+	+
	PSCG 283	<i>P. pyrifolia</i>	Hangzhou, Zhejiang	MK626950	MK691189	MK726191	MK654890	MK691303	+	+

Table 1 (cont.)

Species	Culture no.	Host	Origin	GenBank accession number					Mating type	
				ITS	CAL	HIS	TEF	TUB	MAT1	MAT2
<i>D. sojae</i> (cont.)	PSCG 481	<i>P. pyrifolia</i>	Guiyang, Guizhou	MK626944	MK691196	MK726196	MK654887	MK691307	+	+
	PSCG 486	<i>P. pyrifolia</i>	Guiyang, Guizhou	MK626949	MK691190	MK726192	MK654888	MK691308	+	+
	PSCG 488	<i>P. pyrifolia</i>	Guiyang, Guizhou	MK626946	MK691197	MK726197	MK654884	MK691304	+	+
	PSCG 490	<i>P. pyrifolia</i>	Guiyang, Guizhou	MK626947	MK691195	MK726194	MK654885	MK691306	+	+
	PSCG 492	<i>P. pyrifolia</i>	Guiyang, Guizhou	MK626948	MK691203	MK726199	MK654886	MK691305	+	+
	PSCG 502	<i>P. pyrifolia</i>	Zhenjiang, Jiangsu	MK626941	MK691191	MK726193	MK654891	MK691309	+	+
	PSCG 510	<i>P. pyrifolia</i>	Zhenjiang, Jiangsu	MK626942	MK691192	MK726190	MK654889	MK691311	+	+
	PSCG 518	<i>P. pyrifolia</i>	Zhenjiang, Jiangsu	MK626945	MK691192	MK726198	MK654883	MK691312	+	+
	PSCG 530	<i>P. pyrifolia</i>	Zhenjiang, Jiangsu	MK626943	MK691194	MK726195	MK654892	MK691310	+	+
	<i>D. spinosa</i>	PSCG 279	<i>P. pyrifolia</i>	Hangzhou, Zhejiang	MK626925	MK691126	MK726155	MK654801	MK691235	+
PSCG 383*		<i>P. pyrifolia</i>	Nanjing, Jiangsu	MK626849	MK691129	MK726156	MK654811	MK691234	–	+
PSCG 388		<i>P. pyrifolia</i>	Nanjing, Jiangsu	MK626860	MK691128	MK726171	MK654798	MK691229	–	+
PSCG 491		<i>P. pyrifolia</i>	Guiyang, Guizhou	MK626856	MK691127	MK726170	MK654807	MK691237	–	+
<i>D. taicola</i>	PSCG 292	<i>P. pyrifolia</i>	Hangzhou, Zhejiang	MK626871	MK691115	MK726168	MK654800	MK691232	–	+
	PSCG 386	<i>P. pyrifolia</i>	Nanjing, Jiangsu	MK626868	MK691122	MK726166	MK654797	MK691222	+	–
	PSCG 413	<i>P. pyrifolia</i>	Guiyang, Guizhou	MK626890	MK691119	MK726167	MK654814	MK691238	–	+
	PSCG 485	<i>P. pyrifolia</i>	Guiyang, Guizhou	MK626869	MK691120	MK726173	MK654812	MK691227	–	+
<i>D. unshiuensis</i>	PSCG 039	<i>P. bretschneideri</i>	Kunming, Yunnan	MK626932	MK691183	MK726177	MK654871	MK691290	+	–
	PSCG 059	<i>P. pyrifolia</i>	Wuhan, Hubei	MK626938	MK691185	MK726178	MK654873	MK691297	+	–
	PSCG 060	<i>P. pyrifolia</i>	Wuhan, Hubei	MK626929	MK691179	MK726185	MK654875	MK691292	+	–
	PSCG 120	<i>P. pyrifolia</i>	Sanming, Fujian	MK626926	MK691174	MK726174	MK654868	MK691288	+	+
	PSCG 121	<i>P. pyrifolia</i>	Sanming, Fujian	MK626936	MK691175	MK726180	MK654876	MK691289	+	+
	PSCG 128	<i>P. pyrifolia</i>	Sanming, Fujian	MK626927	MK691184	MK726175	MK654880	MK691295	+	+
	PSCG 131	<i>P. pyrifolia</i>	Sanming, Fujian	MK626934	MK691176	MK726176	MK654869	MK691293	+	–
	PSCG 331	<i>P. pyrifolia</i>	Sanming, Fujian	MK626937	MK691186	MK726182	MK654870	MK691291	+	+
	PSCG 335	<i>P. pyrifolia</i>	Sanming, Fujian	MK626933	MK691177	MK726186	MK654881	MK691299	–	+
	PSCG 339	<i>P. pyrifolia</i>	Sanming, Fujian	MK626928	MK691181	MK726188	MK654879	MK691300	+	–
	PSCG 341	<i>P. pyrifolia</i>	Sanming, Fujian	MK626935	MK691182	MK726183	MK654878	MK691296	+	+
	PSCG 344	<i>P. pyrifolia</i>	Sanming, Fujian	MK626931	MK691187	MK726181	MK654874	MK691298	+	+
	PSCG 468	<i>P. pyrifolia</i>	Sanming, Fujian	MK626939	MK691180	MK726184	MK654872	MK691301	–	+
	PSCG 511	<i>P. pyrifolia</i>	Zhenjiang, Jiangsu	MK626930	MK691178	MK726179	MK654877	MK691294	–	+
	<i>D. velutina</i>	PSCG 134	<i>P. pyrifolia</i>	Sanming, Fujian	MK626918	MK691173	MK726205	MK654853	MK691243	+
PSCG 417		<i>P. pyrifolia</i>	Guiyang, Guizhou	MK626921	MK691152	MK726206	MK654854	MK691244	–	+
<i>D. zaobaisu</i>	PSCG 031*	<i>P. bretschneideri</i>	Kunming, Yunnan	MK626922	/	MK726207	MK654855	MK691245	+	–
	PSCG 032	<i>P. bretschneideri</i>	Kunming, Yunnan	MK626923	/	MK726208	MK654856	MK691246	+	–
	PSCG 033	<i>P. bretschneideri</i>	Kunming, Yunnan	MK626924	/	MK726209	MK654857	MK691247	+	–

* = Ex-type culture. Newly described taxa and deposited sequences are in bold.

Korea (Tanaka & Endo 1930, Nasu et al. 1987). In our previous study, we preliminarily identified five *Diaporthe* species from pear samples collected from six provinces in China based on three loci including *TEF*, *ACT* and ITS sequences (Bai et al. 2015). However, these loci proved to be insufficiently robust to identify these species. Therefore, the species associated with pear shoot canker remain largely unresolved. The aims of the present study were thus as follows:

- make an extensive survey of *Diaporthe* species associated with pear shoot canker in the major pear-cultivation provinces in China;
- resolve the species identity based on multi-locus DNA sequence data;
- characterise the morphology and evaluate the pathogenicity of the species involved; and
- get insight into the diversity, incidence and biology of the *Diaporthe* species associated with pear shoot canker.

MATERIALS AND METHODS

Sampling and isolation

From May 2014 to December 2017, pear twigs, branches and trunks showing shoot canker symptoms were collected from 40 pear orchards in 15 provinces (including Chongqing, Fujian, Guizhou, Hebei, Henan, Hubei, Jiangsu, Jiangxi, Jilin, Liaoning, Shandong, Shanxi, Xinjiang, Yunnan and Zhejiang) of China. The pear species and varieties involved in the collection include *P. pyrifolia* cultivars (cvs.) Aigansui, Cuiyu, Cuiguan, Chuxialv, Huanghua, Hohsui, Jinqiu, Jinshui, Jinshui No. 2, Kousui, Minfu, Niitaka, Wanqiu Huang, Whangkeumbae, Yuanhuang and

Yujing, *P. bretschneideri* cvs. Bayuesu, Dangshansu, Huangguan, Qingxiang, Wanyu, Yali and Zaobaisu, *P. ussuriensis* cv. Xiaonanguo, and *P. communis* cvs. Docteur Jule Guyot, Packham, J6, J23 and Winter decana.

The collected samples were subjected to fungal isolation as previously described (Bai et al. 2015). Briefly, infected tissues (4–5 mm²) were excised from the xylem or phloem under the canker lesions neighbouring the asymptomatic regions after surface-sterilised with 75 % ethanol for 45 s and 75 % NaClO for 45 s and then rinsed twice with sterilised water. The excised tissues were placed on potato dextrose agar (PDA, 20 % diced potatoes, 2 % glucose and 1.5 % agar) Petri dishes and incubated at 25 °C in the dark for 3–5 d. When colonies formed, each colony was transferred to a new PDA Petri dish and assigned a number. Each isolate was further purified by culturing a colony from a single conidium (Choi et al. 1999). The obtained isolates were stored in 25 % glycerol at -80 °C for later use. Type specimens of new species from this study were deposited in the Mycological Herbarium, Institute of Microbiology, Chinese Academy of Sciences, Beijing, China (HMAS), and ex-type living cultures were deposited in the China General Microbiological Culture Collection Centre (CGMCC), Beijing, China.

DNA extraction, PCR amplification and sequencing

Total genomic DNA was extracted from pure cultures using a modified cetyltrimethylammonium bromide (CTAB) protocol (Freeman et al. 1996), and subjected to PCR amplification of partial regions of five loci including partial ITS, *TUB*, *TEF*, *CAL* and *HIS* gene regions using corresponding primer pairs, e.g.,

Table 2 List of isolates of the *Diaporthe* species used in this study, with details about host/substrate, country, and GenBank accession numbers.

Species	Culture ¹	Host	Country	GenBank accession no.				
				ITS	CAL	HIS	TEF	TUB
<i>D. acaciurum</i>	CBS138862*	<i>Acacia tortilis</i>	Tanzania	KP004460	–	KP004504	–	KP004509
<i>D. alleghaniensis</i>	CBS495.72 = ATCC 24097*	<i>Betula alleghaniensis</i>	Canada	KC343007	KC343249	KC343491	KC343733	KC343975
<i>D. alnea</i>	CBS 146.46*	<i>Alnus sp.</i>	Netherlands	KC343008	KC343250	KC343492	KC343734	KC343976
<i>D. ampelina</i>	CBS 114016*	<i>Vitis vinifera</i>	France	AF230751	JX197443	–	AY745056	JX275452
<i>D. amygdali</i>	CBS 126679*	<i>Prunus dulcis</i>	Portugal	KC343022	KC343264	KC343506	KC343748	KC343990
	CBS 115620 = FAU 1005	<i>Prunus persica</i>	USA:	KC343020	KC343262	KC343504	KC343746	KC343988
<i>D. anacardii</i>	CBS 720.97*	<i>Anacardium occidentale</i>	East Africa	KC343024	KC343266	KC343508	KC343750	KC343992
<i>D. angelicae</i>	CBS 111592*	<i>Heracleum sphondylium</i>	Austria	KC343027	KC343269	KC343511	KC343753	KC343995
<i>D. apiculatum</i>	CGMCC 3.17533*	<i>Camellia sinensis</i>	China	KP267896	–	–	KP267970	KP293476
<i>D. arctii</i>	DP0482*	<i>Arctium lappa</i>	Austria	KJ590736	KJ612133	KJ659218	KJ590776	KJ610891
<i>D. arecae</i>	CBS 161.64*	<i>Areca catechu</i>	India	KC343032	KC343274	KC343516	KC343758	KC344000
	ZJUD65	<i>Citrus sinensis</i>	China	KJ490600	–	KJ490542	KJ490479	KJ490421
	ZJUD55	<i>Citrus sinensis</i>	China	KJ490590	–	KJ490532	KJ490469	KJ490411
	CBS 535.75	<i>Citrus sp.</i>	Suriname	KC343033	KC343275	KC343517	KC343759	KC344001
<i>D. arengae</i>	CBS 114979*	<i>Arenga engleri</i>	Hong Kong	KC343034	KC343276	KC343518	KC343760	KC344002
<i>D. baccae</i>	CBS 136972*	<i>Vaccinium corymbosum</i>	Italy	KJ160565	MG281695	MF418264	KJ160597	MF418509
<i>D. batatas</i>	CBS 122.21*	<i>Ipomoea batatas</i>	USA	KC343040	KC343282	KC343524	KC343766	KC344008
<i>D. beilharziae</i>	BRIP 54792*	<i>Indigofera australis</i>	Australia	JX862529	–	–	JX862535	KF170921
<i>D. betulae</i>	CFCC 50469*	<i>Betula platyphylla</i>	China	KT732950	KT732997	–	KT733016	KT733020
<i>D. betulina</i>	CFCC 52560*	<i>Betula albosinensis</i>	China	MH121495	MH121419	MH121455	MH121537	MH121577
<i>D. bicincta</i>	CBS 121004*	<i>Juglans sp.</i>	USA	KC343134	KC343376	KC343618	KC343760	KC344102
<i>D. biguttusis</i>	CGMCC 3.17081*	<i>Lithocarpus glabra</i>	China	KF576282	–	–	KF576257	KF576306
<i>D. camptothecicola</i>	CFCC 51632	<i>Camptotheca acuminata</i>	China	KY203726	KY228877	KY228881	KY228887	KY228893
<i>D. caryae</i>	CFCC 52563*	<i>Carya illinoensis</i>	China	MH121498	MH121422	MH121458	MH121540	MH121580
	CFCC 52564	<i>Carya illinoensis</i>	China	MH121499	MH121423	MH121459	MH121541	MH121581
<i>D. castaneae</i>	DNP 128*	<i>Castanea mollissima</i>	China	JF957786	JX197430	–	JX275401	JX275438
<i>D. celastrina</i>	CBS 139.27*	<i>Celastrus sp.</i>	USA	KC343047	KC343289	KC343531	KC343773	KC344015
<i>D. celeris</i>	CPC 28262	<i>Vitis vinifera</i>	Czech Republic	MG281017	MG281712	MG281363	MG281538	MG281190
<i>D. cercidis</i>	CFCC 52565*	<i>Cercis chinensis</i>	China	MH121500	MH121424	MH121460	MH121542	MH121582
	CFCC 52566	<i>Cercis chinensis</i>	China	MH121501	MH121425	MH121461	MH121543	MH121583
<i>D. chamaeropsis</i>	CBS 454.81*	<i>Chamaerops humilis</i>	Greece	KC343048	KC343290	KC343532	KC343774	KC344016
	CBS 753.70	<i>Spartium junceum</i>	Croatia	KC343049	KC343291	KC343533	KC343775	KC344017
<i>D. charlesworthii</i>	BRIP 54884m*	<i>Rapistrum rugostrum</i>	Australia	KJ197288	–	–	KJ197250	KJ197268
<i>D. chensiensis</i>	CFCC 52567*	<i>Abies chensiensis</i>	China	MH121502	MH121426	MH121462	MH121544	MH121584
<i>D. citri</i>	CBS 135422*	<i>Citrus sp.</i>	USA	KC843311	KC843157	KJ490523	KC843071	KC843187
<i>D. citrichinensis</i>	ZJUD96	<i>Citrus sp.</i>	China	KJ490631	–	KJ490573	KJ490511	KJ490452
<i>D. convolvuli</i>	CBS 124654 = DP0727*	<i>Convolvulus arvensis</i>	Turkey	KC343054	KC343296	KC343538	KC343780	KC344022
<i>D. cotoneastri</i>	DP0667	<i>Juglans cinerea</i>	USA	KC843328	KC843155	–	KC84312	KC843229
<i>D. cuppatae</i>	CBS 117499 = STE-U 5431*	<i>Aspalathus linearis</i>	South Africa	KC343057	KC343299	KC343541	KC343783	KC344025
<i>D. cytosporella</i>	FAU461*	<i>Citrus limon</i>	Italy	KC843307	KC843141	MF418283	KC843116	KC843221
<i>D. dorycnii</i>	MFLUCC 17-1015*	<i>Dorycnium hirsutum</i>	Italy	KY964215	–	–	KY964171	KY964099
<i>D. ellipicola</i>	CGMCC 3.17084*	<i>Lithocarpus glabra</i>	China	KF576270	–	–	KF576245	KF576294
<i>D. endophytica</i>	CBS 133811 = LGMF916*	<i>Schinus terebinthifolius</i>	Brazil	KC343065	KC343307	KC343549	KC343791	KC344033
<i>D. eres</i>	AR5193*	<i>Ulmus sp.</i>	Germany	KJ210529	KJ434999	KJ420850	KJ210550	KJ420799
	CBS 101742	<i>Fraxinus sp.</i>	Netherlands	KC343073	KC343315	KC343557	KC343799	KC344041
	DLR12A	<i>Vitis vinifera</i>	France	KJ210518	KJ434996	KJ420833	KJ210542	KJ420783
	DP0438	<i>Ulmus minor</i>	Netherlands	KJ210532	KJ435016	KJ420886	KJ210553	KJ420816
	FAU506	<i>Cornus florida</i>	USA	KJ210526	KJ435012	KJ420842	JQ807403	KJ420792
<i>D. eugeniae</i>	CBS 444.82	<i>Eugenia aromatica</i>	Indonesia	KC343098	KC343340	KC343582	KC343824	KC344066
<i>D. foeniculina</i>	CBS 111553*	<i>Foeniculum vulgare</i>	Spain	KC343101	KC343343	KC343585	KC343827	KC344069
	FAU460	<i>Citrus limon</i>	Spain	KC843304	KC843138	–	KC843113	KC843218
	AR5151	<i>Citrus latifolia</i>	USA	KC843303	KC843137	–	KC843112	KC843217
<i>D. fraxini-angustifoliae</i>	MFLUCC 15-0748	<i>Vitis vinifera</i>	China	KT459428	KT459462	–	KT459446	960500551
<i>D. fukushii</i>	MAFF 625034	<i>Pyrus pyrifolia</i>	Japan	JQ807469	–	–	JQ807418	–
<i>D. fusicola</i>	CGMCC 3.17087*	<i>Lithocarpus glabra</i>	China	KF576281	KF576233	–	KF576256	KF576305
	CGMCC 3.17088	<i>Lithocarpus glabra</i>	China	KF576263	KF576221	–	KF576238	KF576287
<i>D. ganjae</i>	CBS 180.91*	<i>Cannabis sativa</i>	USA	KC343112	KC343354	KC343596	KC343838	KC344080
<i>D. gulyae</i>	BRIP 54025*	<i>Helianthus annuus</i>	Australia	JF431299	–	–	JN645803	–
<i>D. helianthi</i>	CBS 592.81*	<i>Helianthus annuus</i>	Serbia	KC343115	KC343357	KC343599	KC343841	KC344083
<i>D. helicis</i>	AR5211= CBS 138596*	<i>Hedera helix</i>	France	KJ210538	KJ435043	KJ420875	KJ210559	KJ420828
<i>D. hongkongensis</i>	CBS 115448*	<i>Dichroa febrifuga</i>	China	KC343119	KC343361	KC343603	KC343845	KC344087
	ZJUD74	<i>Citrus unshiu</i>	China	KJ490609	–	–	KJ490488	KJ490430
<i>D. incompleta</i>	CGMCC 3.18288*	<i>Camellia sinensis</i>	China	KX986794	KX999289	KX999265	KX999186	KX999226
<i>D. inconspicua</i>	CBS 133813*	<i>Maytenus ilicifolia</i>	Brazil	KC343123	KC343365	KC343607	KC343849	KC344091
<i>D. infecunda</i>	LGMF912 = CPC 20288	<i>Schinus terebinthifolius</i>	Brazil	KC343128	KC343370	KC343612	KC343854	KC344096
<i>D. juglandicola</i>	CFCC 51134*	<i>Juglans mandshurica</i>	China	KU985101	KX024616	KX024622	KX024628	KX024634
<i>D. kadsurae</i>	CFCC 52586*	<i>Kadsura longipedunculata</i>	China	MH121521	MH121439	MH121479	MH121563	MH121600
	CFCC 52587	<i>Kadsura longipedunculata</i>	China	MH121522	MH121440	MH121480	MH121564	MH121601
<i>D. kongii</i>	BRIP 54031*	<i>Helianthus annuus</i>	Australia	JF431301	–	–	JN645797	–
<i>D. limonicola</i>	CPC 28200 = CBS 142549*	<i>Citrus limon</i>	Malta	MF418422	MF418256	MF418342	MF418501	MF418582
<i>D. litichicola</i>	BRIP 54900*	<i>Litchi chinensis</i>	Australia	JX862533	–	–	JX862539	KF170925
<i>D. lithocarpus</i>	CGMCC 3.15175*	<i>Lithocarpus glabra</i>	China	KC153104	KF576235	–	KC153095	KF576311
	CGMCC 3.17098	<i>Lithocarpus glabra</i>	China	KF576276	KF576228	–	KF576251	KF576300

Table 2 (cont.)

Species	Culture ¹	Host	Country	GenBank accession no.				
				ITS	CAL	HIS	TEF	TUB
<i>D. longicicola</i>	CGMCC 3.17089*	<i>Lithocarpus glabra</i>	China	KF576267	–	–	KF576242	KF576291
<i>D. longicolla</i>	FAU644	<i>Glycine max</i>	USA	KJ590730	KJ612126	KJ659190	KJ590769	KJ610885
	FAU599	<i>Glycine max</i>	USA	KJ590728	KJ612124	KJ659188	KJ590767	KJ610883
<i>D. lusitanicae</i>	CBS 123212*	<i>Foeniculum vulgare</i>	Portugal	KC343136	KC343378	KC343620	KC343862	KC344104
<i>D. mahothocarpus</i>	CGMCC 3.15181*	<i>Lithocarpus glabra</i>	China	KC153096	KT459461	–	KC153087	KF576312
<i>D. maritima</i>	NB464-3A	<i>Picea rubens</i>	Canada	KU552027	–	–	KU552022	KU574616
<i>D. masirevicii</i>	BRIP 57892a*	<i>Helianthus annuus</i>	Australia	KJ197277	–	–	KJ197239	KJ197257
<i>D. melitensis</i>	CPC 27873 = CBS 142551	<i>Citrus limon</i>	Malta	MF418424	MF418258	MF418344	MF418503	MF418584
<i>D. melonis</i>	CBS 507.78*	<i>Glycine soja</i>	USA	KC343141	KC343383	KC343625	KC343867	KC344109
<i>D. middletonii</i>	BRIP 54884e*	<i>Rapistrum rugostrum</i>	Australia	KJ197286	–	–	KJ197248	KJ197266
<i>D. miricidae</i>	BRIP 54736j*	<i>Helianthus annuus</i>	Australia	KJ197282	–	–	KJ197244	KJ197262
<i>D. momicola</i>	MFLUCC 16-0113	<i>Prunus persica</i>	China	KU557563	KU557611	–	KU557631	KU557587
<i>D. musigena</i>	CBS 129519*	<i>Musa sp.</i>	Australia	KC343143	KC343385	KC343627	KC343869	KC344111
<i>D. neilliae</i>	CBS 144.27*	<i>Spiraea sp.</i>	USA	KC343144	KC343386	KC343628	KC343870	KC344112
<i>D. neoarctii</i>	CBS 109490*	<i>Ambrosia trifida</i>	USA	KC343145	KC343387	KC343629	KC343871	KC344113
<i>D. neotheicola</i>	CBS 123209	<i>Foeniculum vulgare</i>	Portugal	GQ250192	–	–	GQ250316	–
<i>D. nobilis</i>	CBS 200.39	<i>Laurus nobilis</i>	Germany	KC343151	KC343393	KC343635	KC343877	KC344119
	CBS 587.79	<i>Pinus pantepella</i>	Japan	KC343153	KC343395	KC343637	KC343879	KC344121
<i>D. novem</i>	CBS 127270*	<i>Glycine max, seed</i>	Croatia	KC343156	KC343398	KC343640	KC343882	KC344124
<i>D. ovoicicola</i>	CGMCC 3.17093*	<i>Citrus sp.</i>	China	KF576265	KF576223	–	KF576240	KF576289
<i>D. padina</i>	CFCC 52590*	<i>Padus racemosa</i>	China	MH121525	MH121443	MH121483	MH121567	MH121604
<i>D. pascoei</i>	BRIP 54847*	<i>Persea americana</i>	Australia	JX862532	–	–	JX862538	KF170924
<i>D. passifloricola</i>	CBS 141329*	<i>Passiflora foetida</i>	Malaysia	KX228292	–	KX228367	–	KX228387
<i>D. penetratum</i>	CGMCC 3.17532	<i>Camellia sinensis</i>	China	KP267879	–	KP293532	KP267953	KP293459
<i>D. perseae</i>	CBS 151.73*	<i>Persea gratissima</i>	Netherlands	KC343173	KC343415	KC343657	KC343899	KC344141
<i>D. pescicola</i>	MFLUCC 16-0105*	<i>Prunus persica</i>	China	KU557555	KU557603	–	KU557623	KU557579
	MFLUCC 16-0106	<i>Prunus persica</i>	China	KU557556	KU557604	–	KU557624	KU557580
<i>D. phaseolorum</i>	CBS 116019 = STAM 30	<i>Caperonia palustris</i>	USA	KC343175	KC343417	KC343659	KC343901	KC344143
<i>D. phragmitis</i>	CBS 138897*	<i>Phragmites australis</i>	China	KP004445	–	KP004503	–	KP004507
<i>D. podocarpimacrophylli</i>	LC6200	<i>Podocarpus macrophyllus</i>	China	KX986769	KX999276	KX999240	KX999161	KX999201
<i>D. pseudomangiferae</i>	CBS 101339*	<i>Mangifera indica</i>	Dominican Republic	KC343181	KC343423	KC343665	KC343907	KC344149
<i>D. pseudophoenicicola</i>	CBS 462.69*	<i>Phoenix dactylifera</i>	Spain	KC343183	KC343425	KC343667	KC343909	KC344151
	LC6150	<i>Phoenix canariensis</i>	Uruguay	KY011891	–	–	KY011902	–
<i>D. pterocarpus</i>	MFLUCC 10-0571*	<i>Pterocarpus indicus</i>	Thailand	JQ619899	JX197451	–	JX275416	JX275460
<i>D. pterocarpicola</i>	MFLUCC 10-0580a*	<i>Pterocarpus indicus</i>	Thailand	JQ619887	JX197433	–	JX275403	JX275441
<i>D. pulla</i>	CBS 338.89*	<i>Hedera helix</i>	Yugoslavia	KC343152	KC343394	KC343636	KC343878	KC344120
<i>D. ravennica</i>	MFLUCC 15–0480	<i>Tamarix sp.</i>	Italy	KU900336	–	–	KX426703	KX377688
<i>D. rhusicola</i>	CBS 129528*	<i>Rhus pendulina</i>	South Africa	JF951146	KC843124	–	KC843100	KC843205
<i>D. sackstonii</i>	BRIP 54669b*	<i>Helianthus annuus</i>	Australia	KJ197287	–	–	KJ197249	KJ197267
<i>D. schini</i>	CBS 133181*	<i>Schinus terebinthifolius</i>	Brazil	KC343191	KC343433	KC343675	KC343917	KC344159
<i>D. sennae</i>	CFCC 51636*	<i>Senna bicapsularis</i>	China	KY203724	KY228875	KY228879	KY228885	KY228891
<i>D. sennicola</i>	CFCC 51634*	<i>Senna bicapsularis</i>	China	KY203722	–	KY228873	KY228883	KY228889
<i>D. serafinae</i>	BRIP 55665a*	<i>Helianthus annuus</i>	Australia	KJ197274	–	–	KJ197236	KJ197254
<i>D. sojae</i>	FAU635*	<i>Glycine max</i>	USA	KJ590719	KJ612116	KJ659208	KJ590762	KJ610875
	FAU455	<i>Stokesia laevis</i>	USA	KJ590712	KJ612109	KJ659201	KJ590755	KJ610868
	DP0601	<i>Glycine max</i>	USA	KJ590706	KJ612103	KJ659195	KJ590749	KJ610862
<i>D. stewartii</i>	AR3602	<i>Cucumis melo</i>	Japan	KJ590714	KJ612111	KJ659203	KJ590757	KJ610870
	CBS 193.36	<i>Cosmos bipinnatus</i>	USA	FJ889448	JX197415	–	GQ250324	JX275421
<i>D. subclavata</i>	ZJUD95*	<i>Citrus sp.</i>	China	KJ490630	–	KJ490572	KJ490509	KJ490451
<i>D. subordinaria</i>	CBS 464.90*	<i>Plantago lanceolata</i>	New Zealand	KC343214	KC343456	KC343698	KC343940	KC344182
<i>D. taoicola</i>	MFLUCC 16-0117*	<i>Prunus persica</i>	China	KU557567	–	–	KU557635	KU557591
<i>D. tectonendophytica</i>	MFLUCC 13–0471*	<i>Tectona grandis</i>	China	KU712439	KU749354	KX999266	KU749367	KU743986
<i>D. tectonigena</i>	LC6512	<i>Camellia sinensis</i>	China	KX986782	KX999284	KX999254	KX999174	KX999215
<i>D. terebinthifolii</i>	CBS 133180*	<i>Schinus terebinthifolius</i>	Brazil	KC343216	KC343458	KC343700	KC343942	KC344184
<i>D. thunbergiicola</i>	MFLUCC 12–0033*	<i>Thunbergia laurifolia</i>	Thailand	KP715097	–	–	KP715098	–
<i>D. ueckerae</i>	FAU656*	<i>Cucumis melo</i>	USA	KJ590726	KJ612122	KJ659215	KJ590747	KJ610881
<i>D. unshiuensis</i>	ZJUD52*	<i>Citrus sp.</i>	China	KJ490587	–	KJ490529	KJ490466	KJ490408
<i>D. unshiuensis</i>	ZJUD49	<i>Citrus sp.</i>	China	KJ490584	–	KJ490526	KJ490463	KJ490405
	CFCC 52595	<i>Carya illinoensis</i>	China	MH121530	–	MH121488	MH121572	MH121607
<i>D. vaccinii</i>	CBS 160.32 = IFO 32646*	<i>Oxycoccus macrocarpos</i>	USA	KC343228	KC343470	KC343712	KC343954	KC344196
<i>D. velutina</i>	CGMCC 3.18286 = LC 4421*	<i>Neolitsea sp.</i>	China	KX986790	–	–	KX999182	KX999223
<i>D. vexans</i>	FAU597	<i>Solanum sp.</i>	Dominican Republic	KJ590734	KJ612131	KJ659216	KJ590774	KJ610889
<i>D. virgilliae</i>	CMW40748	<i>Virgilia oroboides</i>	South Africa	KP247566	–	–	–	KP247575
<i>Diaporthe corylina</i>	CBS 121124*	<i>Corylus sp.</i>	China	KC343004	KC343246	KC343488	KC343730	KC343972

¹ AR, DP, FAU: Isolates in culture collection of Systematic Mycology and Microbiology Laboratory, USDA-ARS, Beltsville, Maryland, USA; BRIP: Queensland Plant Pathology herbarium/culture collection, Australia; CBS: Culture collection of the Centraalbureau voor Schimmelcultures, Fungal Biodiversity Centre, Utrecht, The Netherlands; CFCC: China Forestry Culture Collection Center, China; CGMCC: China General Microbiological Culture Collection; CMW: culture collection of the Forestry and Agricultural Biotechnology Institute; DNP: First author's personal collection (deposited in MFLUCC); LC: Corresponding author's personal collection (deposited in laboratory State Key Laboratory of Mycology, Institute of Microbiology, Chinese Academy of Sciences); LGMF: Culture collection of Laboratory of Genetics of Microorganisms, Federal University of Parana, Curitiba, Brazil; MAFF: MAFF Genebank Project, Ministry of Agriculture, Forestry and Fisheries, Tsukuba, Japan; MFLU: Herbarium of Mae Fah Luang University, Chiang Rai, Thailand; MFLUCC: Mae Fah Luang University Culture Collection, Chiang Rai, Thailand; ZJUD: Zhejiang University.

* = Ex-type culture.

Table 3 Nucleotide substitution models used in the phylogenetic analyses.

Loci/Genes	Eres clade	Sojae clade	Arecae clade and other taxa
ITS	–	SYM+I+G	SYM+I+G
TEF	HKY+G	HKY+I+G	HKY+I+G
CAL	HKY+G	HKY+G	GTR+I+G
HIS	GTR+I+G	GTR+G	GTR+I+G
TUB	HKY+G	HKY+I+G	HKY+G

ITS1/ITS4 (White et al. 1990), Bt2a/Bt2b (Glass & Donaldson 1995), EF1-728F/EF1-986R (Carbone & Kohn 1999), CAL-228F/CAL-737R (Carbone & Kohn 1999) and CYLH3F/H3-1b (Glass & Donaldson 1995, Crous et al. 2004), respectively. PCR parameters were initiated with 95 °C for 5 min, followed by 34 cycles of denaturation at 95 °C for 30 s, annealing at a suitable temperature for 30 s (56 °C for ITS, 52 °C for TEF, 54 °C for CAL, 57 °C for HIS and 60 °C for TUB), and extension at 72 °C for 30 s, and terminated with a final elongation step at 72 °C for 10 min. The PCR amplicons were purified and sequenced at the Sangon Biotech (Shanghai, China) Company, Ltd. The obtained sequences were analysed on DNAMAN (v. 9.0; Lynnon Biosoft), and deposited in GenBank (Table 1).

Phylogenetic analyses

New sequences generated in this study were blasted against the NCBI GenBank nucleotide database to determine the closest relatives for a taxonomic framework of the studied isolates. Alignments of different gene regions, including sequences obtained from this study and sequences downloaded from GenBank (Table 2), were initially performed by using the MAFFT v. 7 online server (<http://mafft.cbrc.jp/alignment/server/index.html>) (Katoh & Standley 2013) with default settings, and then manually adjusted in MEGA v. 7 (Kumar et al. 2016).

Three phylogenetic analyses were conducted based on concatenated loci for the *D. eres* species complex, *D. sojae* species complex and the remaining species. Of these, concatenated ITS, TEF, CAL, HIS and TUB were used for the *D. sojae* species complex and the remaining isolates except for the *D. eres* species complex, for which only TEF, CAL, HIS and TUB were analysed. Bayesian inference (BI) was used to construct phylogenies using MrBayes v. 3.1.2 (Ronquist & Huelsenbeck 2003). The best-fit models of nucleotide substitution for each partition were determined using MrModeltest v. 2.3 (Nylander 2004) and incorporated into the analyses (Table 3). Two analyses of four Markov Chain Monte Carlo (MCMC) chains were conducted from random trees with 15×10^6 generations for the *D. eres* species complex, 2×10^6 for the *D. sojae* species complex, and 15×10^6 generations for the remainder of the *Diaporthe* species. The analyses were sampled every 1000 generations, which were stopped once the average standard deviation of split frequencies was below 0.01. The first 25 % of the trees were discarded as the burn-in phase of each analysis, and the remaining trees were summarised to calculate the posterior probabilities (PP) of each clade being monophyletic.

Additionally, maximum parsimony analyses (MP) were performed on the multi-locus alignment using PAUP (Phylogenetic Analysis Using Parsimony) v. 4.0b10 (Swofford 2002). Phylogenetic trees were generated using the heuristic search option with Tree Bisection Reconnection (TBR) branch swapping and 1000 random sequence additions. Max trees were set up to 5000, branches of zero length collapsed, and all multiple parsimonious trees were saved. Clade stability was assessed using a bootstrap analysis with 1000 replicates. Afterwards, tree length (TL), consistency index (CI), retention index (RI), rescaled con-

sistency index (RC), and homoplasy index (HI) were calculated. Furthermore, IQtree v. 1.6.8 was used for maximum likelihood (ML) analysis. The analysis was performed with a GTR site substitution model. The branch support was evaluated with a bootstrapping (BS) method of 1000 replicates (Hillis & Bull 1993). Phylogenetic trees were visualised in FigTree v. 1.4.2 (Rambaut 2014). The alignments and phylogenetic trees were deposited in TreeBASE (Study 24313).

Morphological analyses

Fungal morphology was accessed by culturing a 4-d-old mycelial disc (5 mm diam) on a Petri dish containing PDA, oatmeal agar (OA; Crous et al. 2019), synthetic nutrient-poor agar medium (SNA; Nirenberg 1976), and 2 % tap water agar supplemented with sterile pine needles (PNA; Smith et al. 1996), wild fennel stems (Santos et al. 2010), and alfalfa stems (Udayanga et al. 2014a), respectively. Cultures were incubated at 25 °C with a 14/10 h fluorescent light/dark cycle. Growth rate (mm/d) was determined by similarly establishing each isolate on PDA and colony diameters were measured daily for 3 d. The colony morphologies were recorded after 14 d. Colony colours were rated according to Rayner (1970). Moreover, the shapes, colours and sizes of sporocarps, conidia, conidiophores, asci and ascospores were observed under a compound microscope (Olympus BX63 or Olympus SZX16, Japan), and 30–50 conidia or ascospores were measured to determine their sizes unless no or less spores were produced.

Prevalence

The prevalence of *Diaporthe* species in sampled provinces and the *Pyrus* spp. involved was calculated as previously described (Fu et al. 2019). The Isolation Rate (R') was calculated for each species with the formula, $R' \% = (N^s/N^i) \times 100$, where N^s was the number of isolates from the same species, and N^i was the total number of isolates from each sample-collected region or *Pyrus* sp. (Fu et al. 2019).

Pathogenicity

Host ranges were determined on detached shoots of *P. pyrifolia* cv. Hohsui, *P. bretschneideri* cv. Xuehua, *P. ussuriensis* cv. Hanxiang, *P. communis* cv. Docteur Jules Guyot, *P. sinkiangensis* cv. Kuerlexiangli, and other host plants, including *Citrus reticulata* cv. Rihui, *Malus pumila* cv. Hong Fushi, *Prunus persica* cv. Jinxiu, and *Actinidia chinensis* cv. Hongyang. Briefly, plant shoots 7.0 to 11.0 mm diam were disinfested with 75 % ethanol, and wounded between two of the closer buds with a punch (5 mm diam) on each shoot. Colonised PDA discs (5 mm diam) were excised from the colony margins after being cultured on PDA at 25 °C for 3 d, and inoculated in the hole of each shoot. Non-colonised PDA discs were used in parallel as controls. The inoculated shoots were incubated at 25 °C in plastic containers covered with a plastic film. Six branches were used for each inoculation treatment. A total of 31 isolates were used, namely: *D. acuta* (PSCG045), *D. caryae* (PSCG520), *D. cercidis* (PSCG275), *D. chongqingensis* (PSCG435), *D. citrichinensis* (PSCG462), *D. eres* (PSCG092, PSCG017, PSCG322, PSCG440), *D. fulvicolor* (PSCG051), *D. fusicola* (PSCG371, PSCG118), *D. ganjae* (PSCG489), *D. hongkongensis* (PSCG130, PSCG141, PSCG465), *D. padina* (PSCG160), *D. parvae* (PSCG034), *D. pescicola* (PSCG036), *D. sojae* (PSCG510, PSCG481, PSCG490), *D. spinosa* (PSCG279, PSCG388, PSCG491), *D. taoicola* (PSCG485), *D. unshiuensis* (PSCG511, PSCG120, PSCG059), *D. velutina* (PSCG134) and *D. zaobaisu* (PSCG031). The symptoms were recorded by taking photos, and the lesion lengths were measured at 8 dpi.



Fig. 1 Representative symptoms of pear shoot canker on branches in the field. a. Newly developed reddish brown canker lesion around a bud of *P. pyrifolia* cv. Cuiguan; b–c. dieback symptoms resulting from lesion expansion around the branches of *P. communis* cv. Packham (b) and *P. pyrifolia* cv. Cuiguan (c); d. reddish brown necrosis at the cut of *P. pyrifolia* cv. Cuiguan; e. annular reddish brown lesion on branch of *P. pyrifolia* cv. Cuiguan; f. light-yellow spore tendrils released from pycnidia.

Pathogenicity tests were conducted by inoculating colonised PDA discs on intact shoots of 1-yr-old seedlings of *P. pyrifolia* cv. Cuiguan as described above. After inoculation, the seedlings were cultivated outdoors where the average daily lowest temperature was 15 °C and the highest temperature was 26 °C, with average humidity at 60 %. The tests were conducted in six repeats at two independent times. One representative isolate of each species was selected, namely: *D. acuta* (PSCG047), *D. caryae* (PSCG520), *D. cercidis* (PSCG275), *D. chongqingensis* (PSCG435), *D. citrichinensis* (PSCG462), *D. eres* (PSCG261), *D. fulvicolor* (PSCG051), *D. fusicola* (PSCG371), *D. ganjae* (PSCG489), *D. hongkongensis* (PSCG465), *D. padina* (PSCG160), *D. parvae* (PSCG034), *D. pescicola* (PSCG036), *D. sojiae* (PSCG481), *D. spinosa* (PSCG491), *D. taoicola* (PSCG485), *D. unshiuensis* (PSCG120), *D. velutina* (PSCG134) and *D. zaobaisu* (PSCG033).

Mating-type test

The mating types (heterothallic or homothallic) were determined with a PCR-based mating type assay as previously described (Santos et al. 2010). The primers MAT1-1-1FW/MAT1-1-1RV were used for amplification of partial $\alpha 1$ box domain of the mating gene (*MAT*) *MAT1-1-1*, and primers MAT1-2-1FW/MAT1-2-1RV for amplification of partial HMG domain of the *MAT1-2-1* gene.

RESULTS

Diaporthe isolates associated with pear shoot canker

In the surveyed pear orchards, pear shoot canker showed symptoms including reddish brown canker lesions around buds (Fig. 1a, e), branch necrosis with oval or long cankers around branches (Fig. 1b–c), twig or branch cutting dieback (Fig. 1d), and curly white spore tendrils after rainfall in late summer (Fig. 1f). A total of 286 pear samples (shoots, branches, and twigs) affected by pear shoot canker collected from 12 provinces including Chongqing, Fujian, Guizhou, Hebei, Henan, Hubei, Jiangsu, Jiangxi, Liaoning, Shandong, Yunnan and Zhejiang provinces in China were subjected to fungal isolation, resulting in a total of 453 *Diaporthe* isolates identified based on morphology and ITS sequence data (see Appendix). However, no *Diaporthe* isolates were obtained from the samples collected from Jilin, Shanxi and Xinjiang provinces. A total of 113 representative isolates were chosen for further phylogenetic and taxonomic analyses (Table 1).

Phylogenetic analyses

The 113 representative isolates (Table 1) were subjected to multi-locus phylogenetic analyses with concatenated ITS, *TEF*, *CAL*, *HIS* and *TUB* sequences together with 137 reference isolates from previously described species (Table 2). Results showed that these isolates clustered together with 19 species in three species complexes including *D. eres* (36 isolates),



Fig. 2 A Bayesian inference phylogenetic tree of 37 isolates in the *D. eres* species complex. The species *D. citri* (CBS 135422) was selected as an outgroup. The tree was built using concatenated sequences of the *TEF*, *CAL*, *HIS* and *TUB* genes. Bayesian posterior probability (PP \geq 0.90), MP bootstrap support values (ML \geq 50 %) and RAxML bootstrap support values (ML \geq 50 %) were shown at the nodes (PP/ML/MP). Ex-type strains were emphasized in **bold**. Coloured blocks indicate clades containing isolates from *Pyrus* spp. in this study. The scale bar indicates 0.3 expected changes per site.

D. sojiae (30) and *D. arecae* (21), and seven singleton species (26) (Fig. 2–4).

In the phylogenetic tree constructed for the *D. eres* species complex, 37 isolates clustered in three clades corresponding to *D. eres* (35 isolates), *D. padina* (1) and *D. citrichinensis* (1) with a total of 1504 characters including gaps (318 for *TEF*, 352 for *CAL*, 391 for *HIS* and 443 for *TUB*) included in the phylogenetic analysis (Fig. 2). Furthermore, *D. biguttus* (CGMCC 3.17081), *D. camptothecicola* (CFCC 51632), *D. ellipicola* (CGMCC 3.17084), *D. longicicola* (CGMCC 3.17089), *D. mahothocarpus* (CGMCC 3.15181) and *D. momicola* (MFLUCC 16-0113) clustered together with *D. eres*, indicating that these species are synonyms of *D. eres* as previously proposed (Yang et al. 2018). In the *D. sojiae* species complex, 30 isolates clustered into four clades corresponding to *D. sojiae* (11 isolates), *D. unshiuensis* (14), *D. caryae* (4) and *D. ganjae* (1) (Fig. 3),

with a total of 2 445 characters including gaps (480 for ITS, 380 for *TEF*, 560 for *CAL*, 539 for *HIS* and 482 for *TUB*) included in the phylogenetic analysis. In the *D. arecae* species complex, 12 isolates were assigned to three species, including *D. cercidis* (6), *D. taicola* (4), *D. pescicola* (2), whereas nine isolates formed distinct clades with a highly supported subclade (1.00/100/100), which were identified as novel species and named *D. spinosa* (4), *D. fulvicolor* (2), and *D. acuta* (closely related to *D. pescicola*) (3), respectively. A total of 2 130 characters including gaps (510 for ITS, 296 for *TEF*, 437 for *CAL*, 465 for *HIS*, and 422 for *TUB*) were included in the multi-locus dataset. For the remaining isolates, 18 isolates were assigned to three species, including *D. hongkongensis* (10), *D. fusicola* (6) and *D. velutina* (2), whereas seven isolates formed distinct clades, and are identified as novel species, described as *D. zaobaisu* (3 isolates, closely related to *D. ravennica*), *D. parvae* (2) and *D. chongqingensis* (2, close to *D. fusicola*), respectively (Fig. 4).

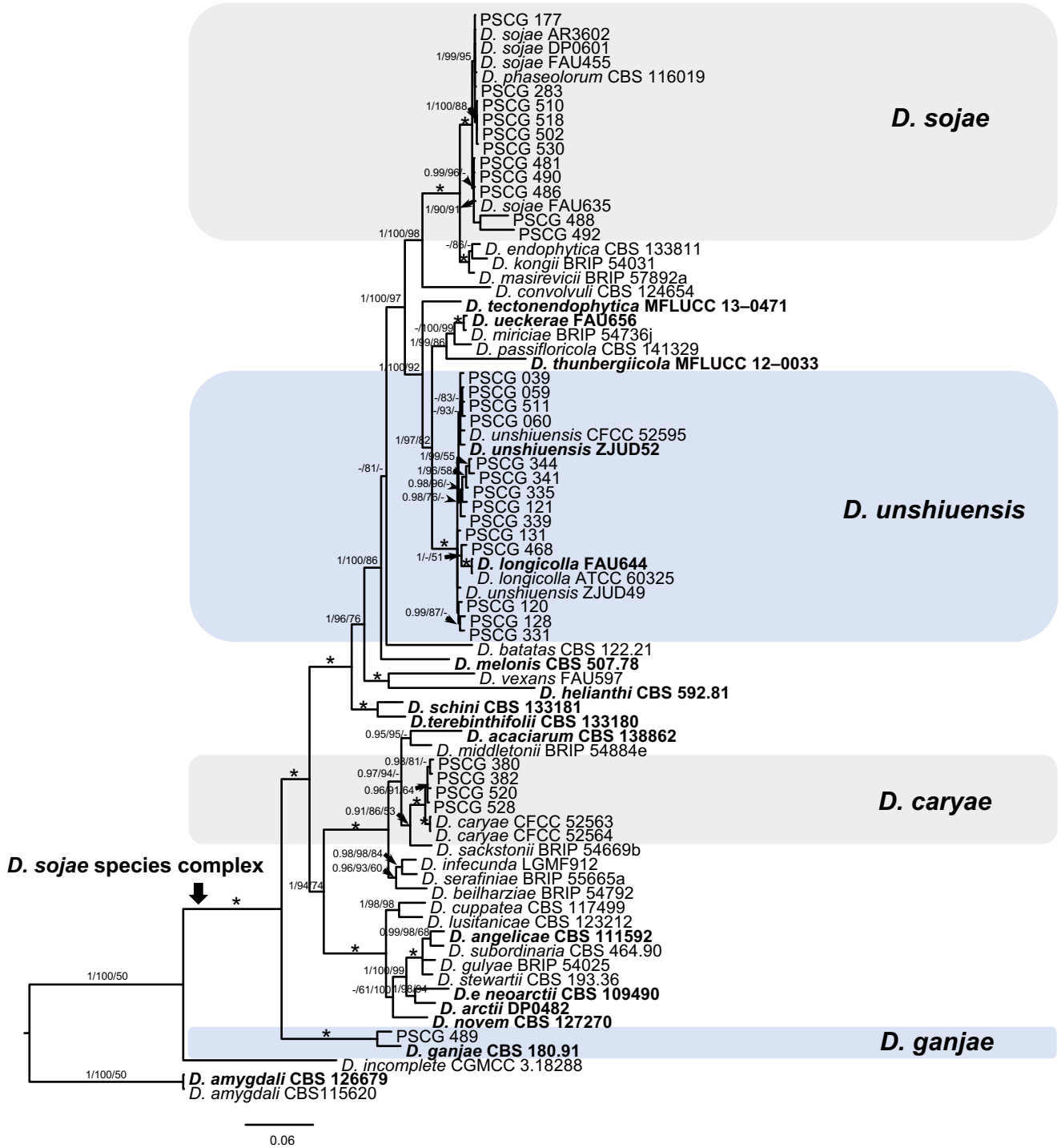


Fig. 3 A Bayesian inference phylogenetic tree of 30 isolates in the *D. sojae* species complex. The species *D. amygdali* (CBS 115620, CBS 126679) was selected as an outgroup. The tree was built using concatenated sequences of the ITS, *TEF*, *CAL*, *HIS* and *TUB* genes. Bayesian posterior probability (PP \geq 0.90), MP bootstrap support values (ML \geq 50 %) and RAxML bootstrap support values (ML \geq 50 %) were shown at the nodes (PP/ML/MP). The asterisk symbol (*) represents full support (1/100/100). Ex-type strains were emphasized in **bold**. Coloured blocks indicate clades containing isolates from *Pyrus* spp. in this study. The scale bar indicates 0.06 expected changes per site.

TAXONOMY

Based on the morphology and multi-locus phylogeny, the 113 isolates were assigned to 19 species, including six newly described species. All species studied in culture are characterised below.

Diaporthe acuta Y.S. Guo & G.P. Wang, *sp. nov.* — MycoBank MB830655; Fig. 5

Etymology. Named after the acute shape of both ends of its alpha conidia.

Sexual morph not observed. *Asexual morph* on alfalfa stems. *Pycnidial conidiomata* globose or irregular, solitary or aggregated, exposed on the alfalfa stems surface, dark brown to black, 230–544 μm diam. *Alpha conidia* hyaline, aseptate, fusiform to oval, acutely round at both ends, bi- or multi-guttulate, 6–9.5 \times 2–3 μm , mean \pm SD = 7.8 \pm 0.6 \times 2.6 \pm 0.2 μm , L/W ratio = 3 (n = 50). *Beta* and *gamma conidia* not observed.

Culture characteristics — Colonies on PDA with flattened mycelium, aerial mycelium scarce, flocculent scattered distribution, surface and reverse luteous. Colony diam 63–67 mm in 3 d at 28 $^{\circ}\text{C}$. On OA with aerial mycelium white, fluffy, sulphur yellow pigment accumulation in the centre, pure white at the colony margin.

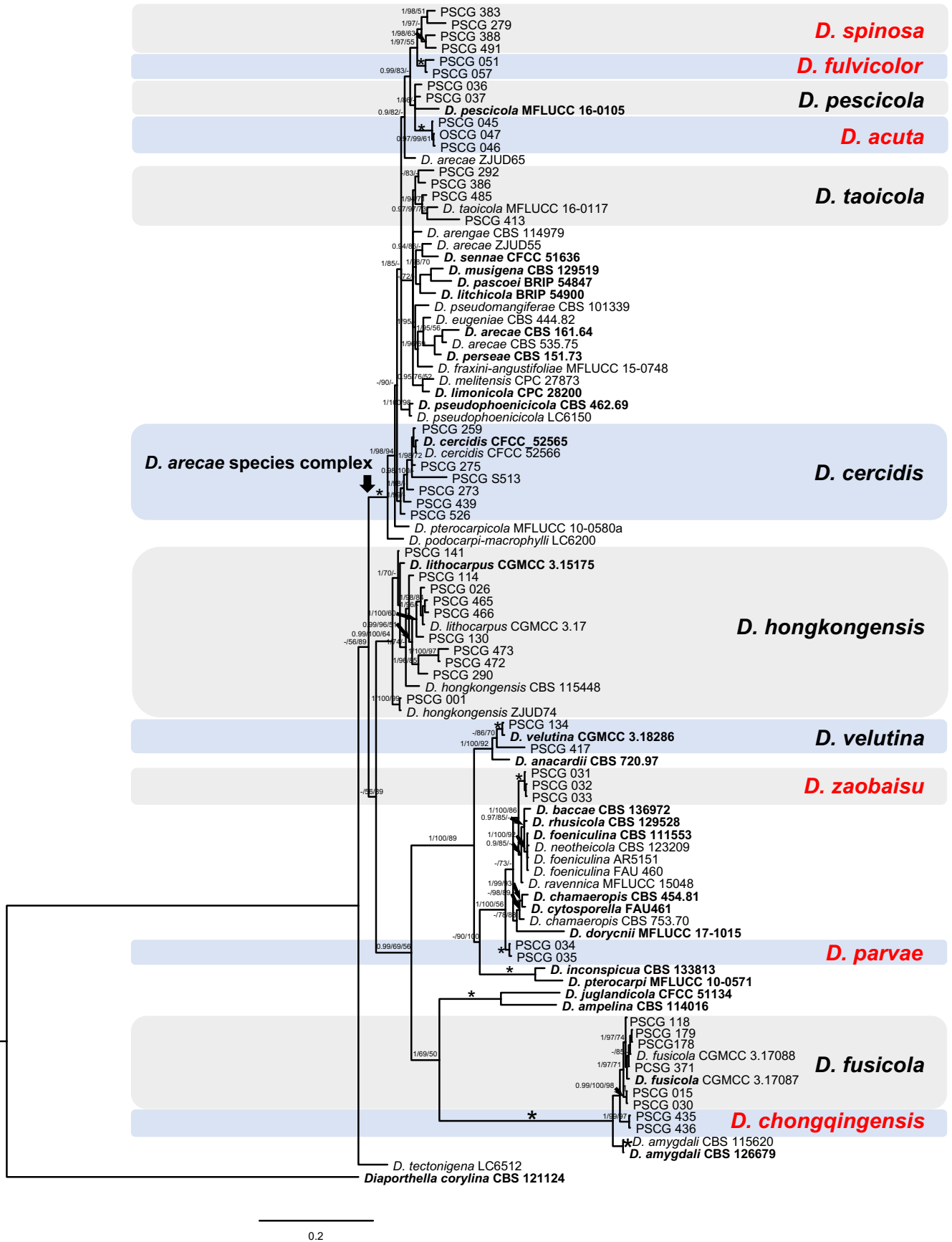


Fig. 4 Phylogenetic tree generated by Bayesian analysis based on combined ITS, *TEF*, *CAL*, *HIS* and *TUB* sequence alignments of *Diaporthe* spp. The species *Diaporthe corylina* (CBS 121124) was selected as an outgroup. Bayesian posterior probability (PP \geq 0.90), MP bootstrap support values (ML \geq 50 %) and RAxML bootstrap support values (ML \geq 50 %) were shown at the nodes (PP/ML/MP). The asterisk symbol (*) represents full support (1/100/100). Ex-type strains were emphasized in **bold**. Coloured blocks indicate clades containing isolates from *Pyrus* spp. in this study. The scale bar indicates 0.2 expected changes per site.

Materials examined. CHINA, Hubei Province, Wuhan City, on branches of *P. pyrifolia* cv. Cuiguang, 1 Sept. 2014, Q. Bai (holotype HMAS 248147, culture ex-type CGMCC 3.19600 = PSCG 047); *ibid.*, culture PSCG 045 and PSCG 046.

Notes — Three isolates were identified as *D. acuta* in a well-supported clade in the *D. arecae* species complex. This species is most closely related to *D. pescicola*, *D. fulvicolor* and *D. spinosa*, but easily distinguished from *D. pescicola* by 85 nucleotides difference in the concatenated alignment (40 in the ITS region, 6 *TEF*, 38 *CAL* and 1 *TUB*), from *D. fulvicolor* by 82 nucleotides difference (43 in the ITS region, 3 *TEF*, 17 *CAL*, 3 *HIS* and 16 *TUB*) and from *D. spinosa* by 24 nucleotides difference (13 in the ITS region, 7 *CAL* and 4 *TUB*). Moreover, *D. acuta* differs from *D. pescicola* in morphology, namely having smaller conidiomata (230–544 vs 637–881 µm), larger alpha conidia (6–9.5 × 2–3 vs 6–8 × 2–2.5 µm) (Table 4) and lacking beta conidia. However, its pycnidial conidiomata are larger than those of *D. fulvicolor* (230–544 vs 174–316 µm) and *D. spinosa* (230–544 vs 124–172 µm).

***Diaporthe caryae* C.M. Tian & Q. Yang, MycoKeys 39: 124. 2018 — Fig. 6**

Description & Illustration — Yang et al. (2018).

Materials examined. CHINA, Jiangsu Province, Nanjing City, on branches of *P. pyrifolia* cv. Cuiguang, 22 Aug. 2016, Y.S. Guo (culture PCSG 380, PCSG 382); Zhenjiang City, on branches of *P. pyrifolia* cv. Hohsui, 18 Nov. 2017, Y.S. Guo (culture PCSG 520, PCSG 528).

Notes — *Diaporthe caryae* was first reported on symptomatic twigs of *Carya illinoensis* in Jiangsu province, China (Yang et al. 2018). In this study, four isolates were identified as this species, and this is the first report of *D. caryae* responsible for pear shoot canker.

Pycnidial conidiomata of the isolate PSCG 528 are similar to the ex-type isolate CFCC 52563 (375–922 vs 450–836 µm). Alpha conidia of the isolate PSCG 528 are shorter than in isolate CFCC 52563 (5–7 × 2–3 vs 7–8.5 × 2–2.5 µm).

Table 4 Conidial sizes of *Diaporthe* spp. studied.

Species	Isolate No.	Conidia size ranges					
		Alpha conidia (µm)		Beta conidia		Means ± SD of conidia	
		Length (µm)	Width (µm)	Length (µm)	Width (µm)	Alpha conidia	Beta conidia
<i>D. acuta</i>	PSCG 047	6.14–9.53	2.20–2.94	/	/	7.76 ± 0.64 × 2.58 ± 0.17	/
<i>D. caryae</i>	PSCG 528	5.23–7.07	2.16–3.00	24.36–30.82	0.99–1.50	6.17 ± 0.40 × 2.55 ± 0.19	27.56 ± 2.28 × 1.21 ± 0.15
<i>D. cercidis</i>	PSCG 259	6.25–8.86	2.18–2.96	/	/	7.51 ± 0.67 × 2.50 ± 0.20	/
<i>D. chongqingensis</i>	PSCG 435	5.27–7.69	2.08–2.94	/	/	6.39 ± 0.47 × 2.34 ± 0.18	/
<i>D. citrichinensis</i>	PSCG 462	6.80–8.38	2.29–3.67	22.49–30.84	1.07–1.26	7.46 ± 0.42 × 2.74 ± 0.35	27.77 ± 4.60 × 1.17 ± 0.10
<i>D. eres</i>	PSCG 321	5.14–7.15	2.00–2.89	/	/	6.23 ± 0.42 × 2.38 ± 0.18	/
	PSCG 377	6.22–8.11	2.28–3.39	21.50–30.34	1.08–1.86	7.07 ± 0.48 × 2.67 ± 0.24	32.98 ± 3.87 × 1.31 ± 0.17
	PSCG 044	6.83–9.37	2.02–2.70	20.06–38.31	1.19–1.88	7.77 ± 0.58 × 2.38 ± 0.16	32.45 ± 5.31 × 1.43 ± 0.20
	PSCG 250	5.43–8.27	1.92–2.78	30.34–37.31	1.10–1.40	6.49 ± 0.70 × 2.38 ± 0.21	33.45 ± 3.54 × 1.28 ± 0.16
	PSCG 265	/	/	18.89–29.68	1.01–2.03	/	23.53 ± 2.69 × 1.51 ± 0.20
	PSCG 276	6.08–8.68	2.58–3.37	21.50–30.34	1.08–1.86	7.46 ± 0.74 × 3.03 ± 0.32	26.14 ± 2.53 × 1.44 ± 0.16
	PSCG 300	6.66–8.90	2.32–3.62	24.07–31.38	1.26–1.31	7.65 ± 0.54 × 3.05 ± 0.28	27.72 ± 5.16 × 1.29 ± 0.04
	PSCG 325	6.58–7.92	2.22–3.04	/	/	7.14 ± 0.40 × 2.51 ± 0.18	/
	PSCG 440	5.12–7.71	2.05–3.50	26.22–37.66	1.07–1.91	6.37 ± 0.69 × 2.62 ± 0.33	32.06 ± 2.93 × 1.32 ± 0.24
	PSCG 529	5.74–7.51	2.11–2.90	24.96–36.81	1.13–1.57	6.41 ± 0.47 × 2.48 ± 0.22	29.95 ± 2.06 × 1.36 ± 0.12
	PSCG 041	5.29–8.78	1.82–2.68	20.16–38.18	0.94–1.54	6.63 ± 0.67 × 2.25 ± 0.17	28.70 ± 3.83 × 1.29 ± 0.17
	PSCG 092	7.06–9.13	2.48–3.63	/	/	8.10 ± 0.55 × 3.14 ± 0.26	/
	PSCG 322	6.66–8.53	2.38–3.06	/	/	7.62 ± 0.46 × 2.69 ± 0.17	/
	PSCG 358	5.96–7.17	2.25–2.83	28.94–39.48	1.05–1.60	6.58 ± 0.31 × 2.59 ± 0.15	33.84 ± 2.89 × 1.28 ± 0.18
PSCG 378	5.72–7.94	2.04–2.68	20.74–50.93	0.69–1.43	6.81 ± 0.48 × 2.34 ± 0.14	34.37 ± 8.27 × 1.20 ± 0.19	
<i>D. fulvicolor</i>	PSCG 051	7.00–8.86	2.08–2.85	/	/	7.78 ± 0.44 × 2.52 ± 0.16	/
<i>D. fusicola</i>	PSCG 015	5.18–7.15	1.76–2.44	/	/	6.20 ± 0.45 × 2.11 ± 0.16	/
	PSCG 118	4.86–6.89	1.76–3.17	/	/	5.83 ± 0.49 × 2.29 ± 0.27	/
	PSCG 371	5.61–9.00	1.82–2.86	/	/	6.78 ± 0.68 × 2.22 ± 0.24	/
<i>D. ganjae</i>	PSCG 489	5.31–7.25	2.16–3.01	/	/	6.44 ± 0.41 × 2.62 ± 0.21	/
<i>D. hongkongensis</i>	PSCG 465	5.44–8.32	1.89–2.69	14.01–22.64	0.93–1.46	6.88 ± 0.63 × 2.24 ± 0.17	16.75 ± 2.68 × 1.20 ± 0.18
	PSCG 466	6.06–8.98	1.79–2.87	14.67–23.92	0.80–1.35	7.15 ± 0.63 × 2.36 ± 0.22	19.20 ± 3.18 × 1.06 ± 0.17
	PSCG 141	6.28–8.71	1.99–2.73	16.04–19.20	1.14–1.69	7.43 ± 0.63 × 2.29 ± 0.18	17.27 ± 1.42 × 1.41 ± 0.22
<i>D. padina</i>	PSCG 160	7.29–10.08	2.16–3.52	25.92–41.59	1.07–1.74	8.40 ± 0.63 × 2.86 ± 0.34	34.33 ± 3.32 × 1.33 ± 0.15
<i>D. pescicola</i>	PSCG 036	6.05–7.77	1.93–2.75	21.17–30.63	1.12–1.74	6.99 ± 0.44 × 2.42 ± 0.17	24.99 ± 3.07 × 1.29 ± 0.21
<i>D. sojae</i>	PSCG 486	6.29–7.83	2.32–3.20	14.58–23.09	1.09–1.81	7.00 ± 0.38 × 2.78 ± 0.19	18.78 ± 2.15 × 1.40 ± 0.17
<i>D. spinosa</i>	PSCG 383	5.68–8.12	2.11–3.36	18.74–30.60	1.13–1.61	7.02 ± 0.64 × 2.58 ± 0.27	25.06 ± 2.76 × 1.34 ± 0.13
	PSCG 491	2.37	1.89–3.08	12.06–24.75	0.88–1.90	7.26 ± 0.85 × 2.78 ± 0.26	19.89 ± 3.25 × 1.41 ± 0.22
<i>D. taoicola</i>	PSCG 485	6.50–11.19	1.77–2.74	/	/	8.34 ± 0.94 × 2.31 ± 0.19	/
<i>D. unshiuensis</i>	PSCG 120	5.48–6.72	2.12–2.61	/	/	5.94 ± 0.27 × 2.35 ± 0.13	/
	PSCG 128	4.22–6.84	2.18–2.83	/	/	5.44 ± 0.51 × 2.45 ± 0.15	/
	PSCG 511	5.21–7.20	2.42–3.13	/	/	6.21 ± 0.52 × 2.81 ± 0.18	/
	PSCG 468	5.08–7.01	2.25–2.83	21.07–32.33	1.16–1.43	5.92 ± 0.47 × 2.55 ± 0.15	27.56 ± 4.76 × 1.29 ± 0.13
	PSCG 055	5.74–7.65	2.29–3.04	/	/	6.70 ± 0.53 × 2.62 ± 0.17	/
	PSCG 059	4.53–6.35	2.01–2.77	/	/	5.53 ± 0.52 × 2.41 ± 0.20	/
<i>D. velutina</i>	PSCG 134	5.59–7.39	2.03–2.77	/	/	6.50 ± 0.43 × 2.41 ± 0.15	/
<i>D. zaobaisu</i>	PSCG 032	5.23–6.90	2.12–2.58	21.43–28.16	0.86–1.44	5.96 ± 0.40 × 2.35 ± 0.09	24.52 ± 1.50 × 1.14 ± 0.14
	PSCG 033	5.38–8.45	1.89–2.90	/	/	6.83 ± 0.71 × 2.35 ± 0.27	/

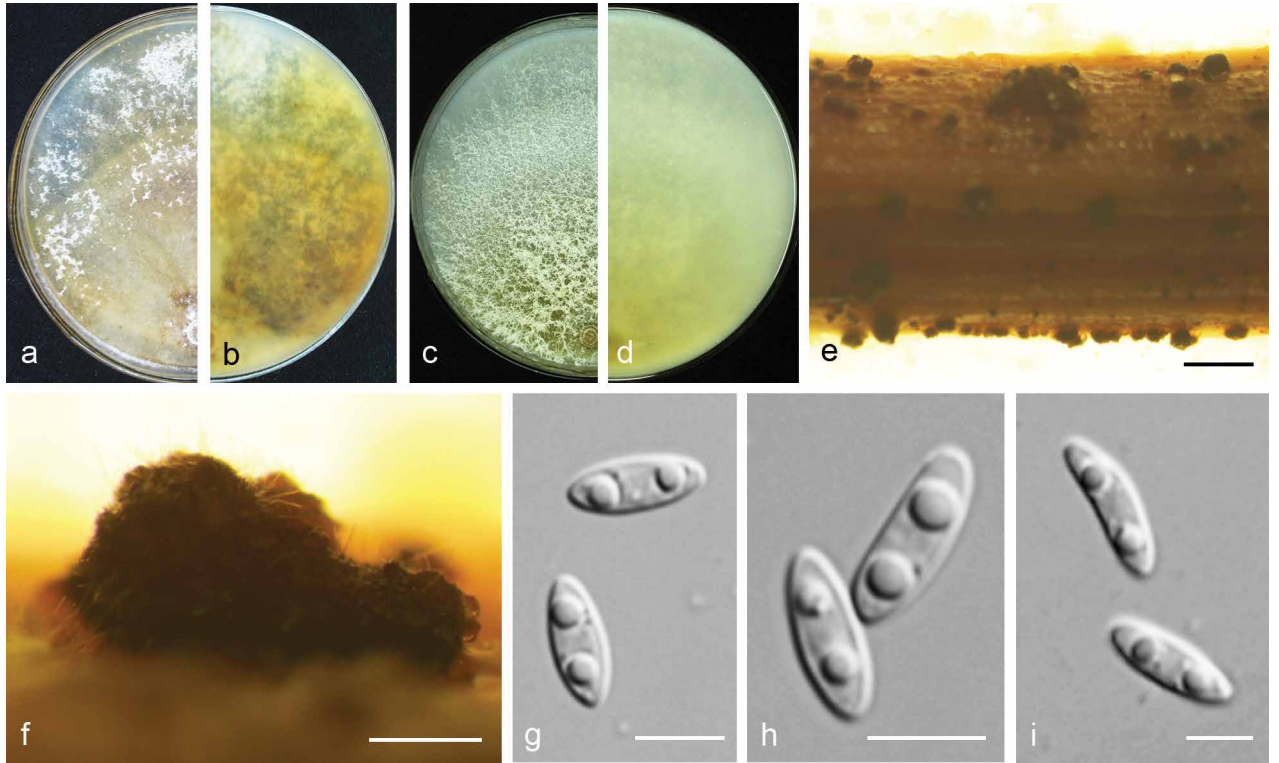


Fig. 5 *Diaporthe acuta* (CGMCC 3.19600). a–d. Front and back view, respectively of colonies on PDA (a, b) and OA (c, d); e. conidiomata on alfalfa stems; f. conidiomata; g–i. alpha conidia. — Scale bars: e = 1 mm; f = 200 μ m; g–i = 5 μ m.

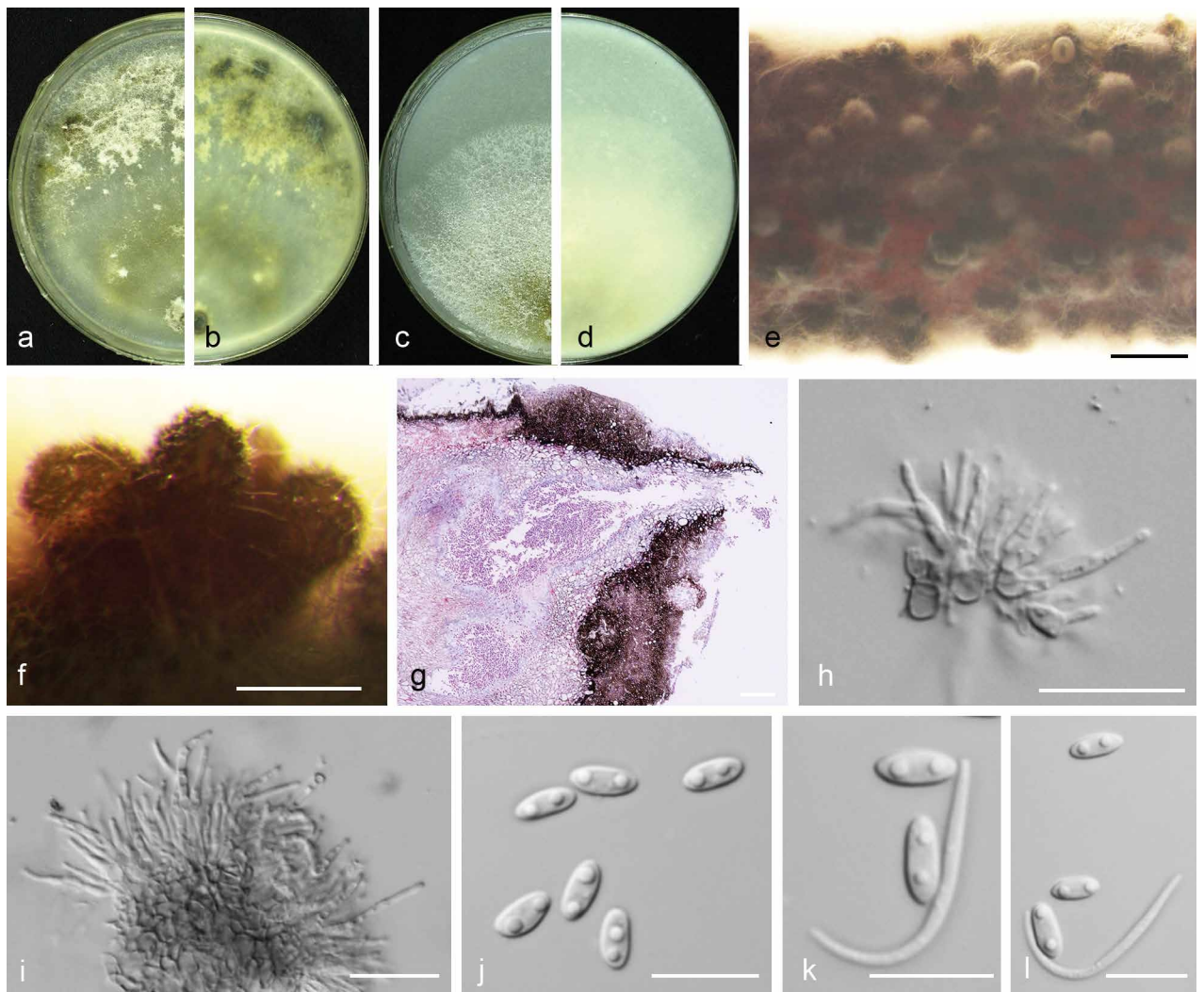


Fig. 6 *Diaporthe caryae* (PSCG 528). a–d. Front and back view, respectively of colonies on PDA (a, b) and OA (c, d); e. conidiomata on alfalfa stems; f. conidiomata; g. section view of conidiomata; h–i. conidiophores; j. alpha conidia; k–l. alpha and beta conidia. — Scale bars: e = 1 mm; f–g = 200 μ m; h–i = 20 μ m; j–l = 10 μ m.

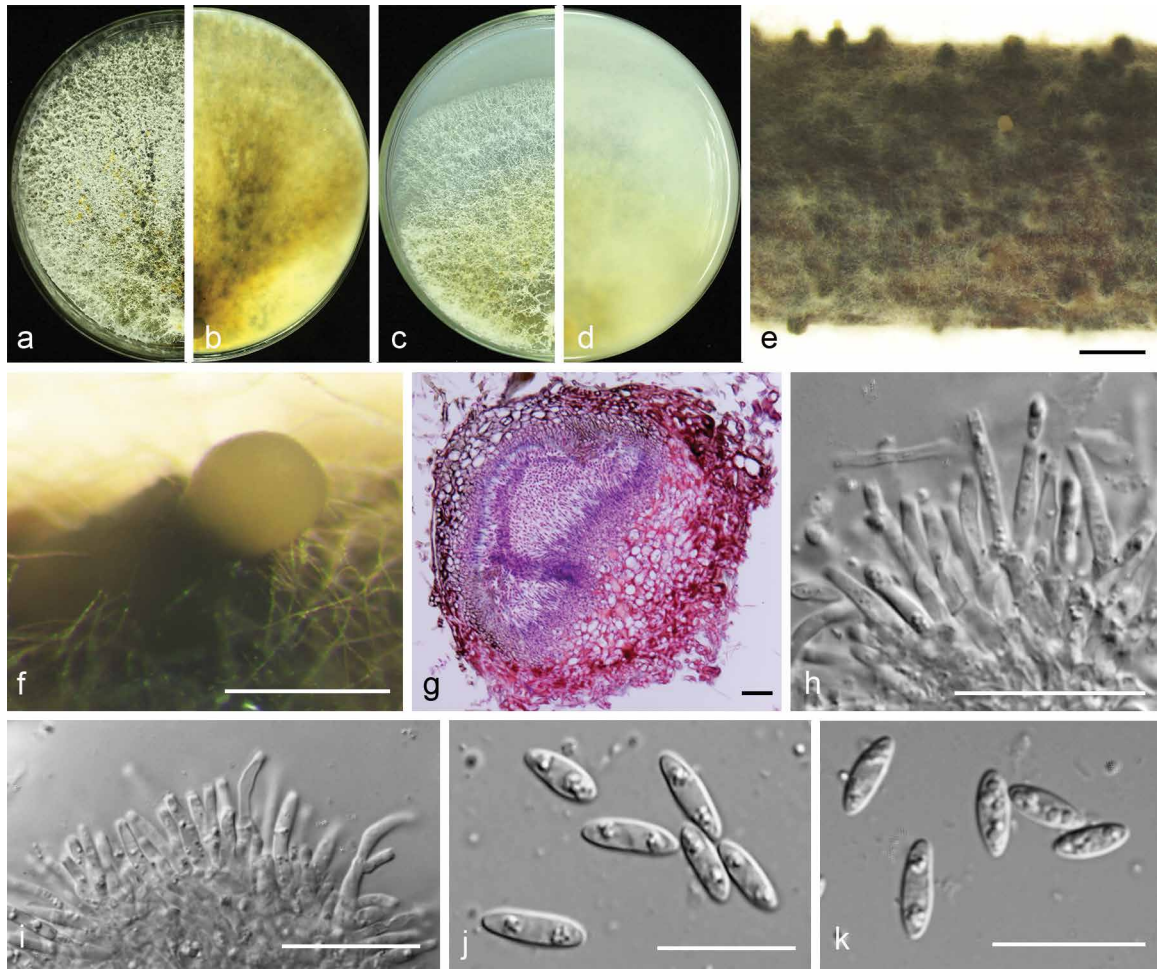


Fig. 7 *Diaporthe cercidis* (PSCG 259). a–d. Front and back view, respectively of colonies on PDA (a, b) and OA (c, d); e. conidiomata on alfalfa stems; f. conidiomata; g. section view of conidiomata; h–i. conidiophores; j–k. alpha conidia. — Scale bars: e = 1 mm; f = 200 μ m; g–h = 20 μ m; j–k = 10 μ m.

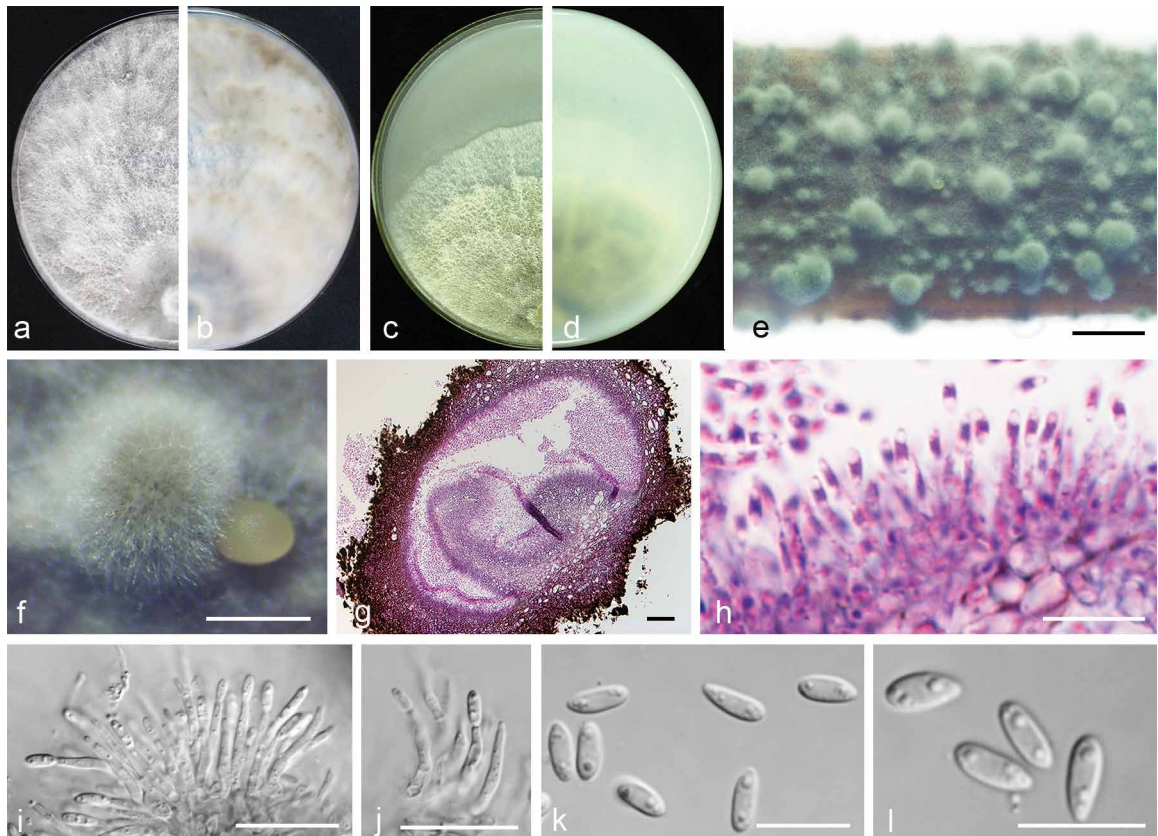


Fig. 8 *Diaporthe chongqingensis* (CGMCC 3.19603). a–d. Front and back view, respectively of colonies on PDA (a, b) and OA (c, d); e. conidiomata on alfalfa stems; f. conidiomata; g. section view of conidiomata; h–j. conidiophores; k–l. alpha conidia. — Scale bars: e = 2 mm; f = 500 μ m; g = 50 μ m; i–j = 20 μ m; h, k–l = 10 μ m.

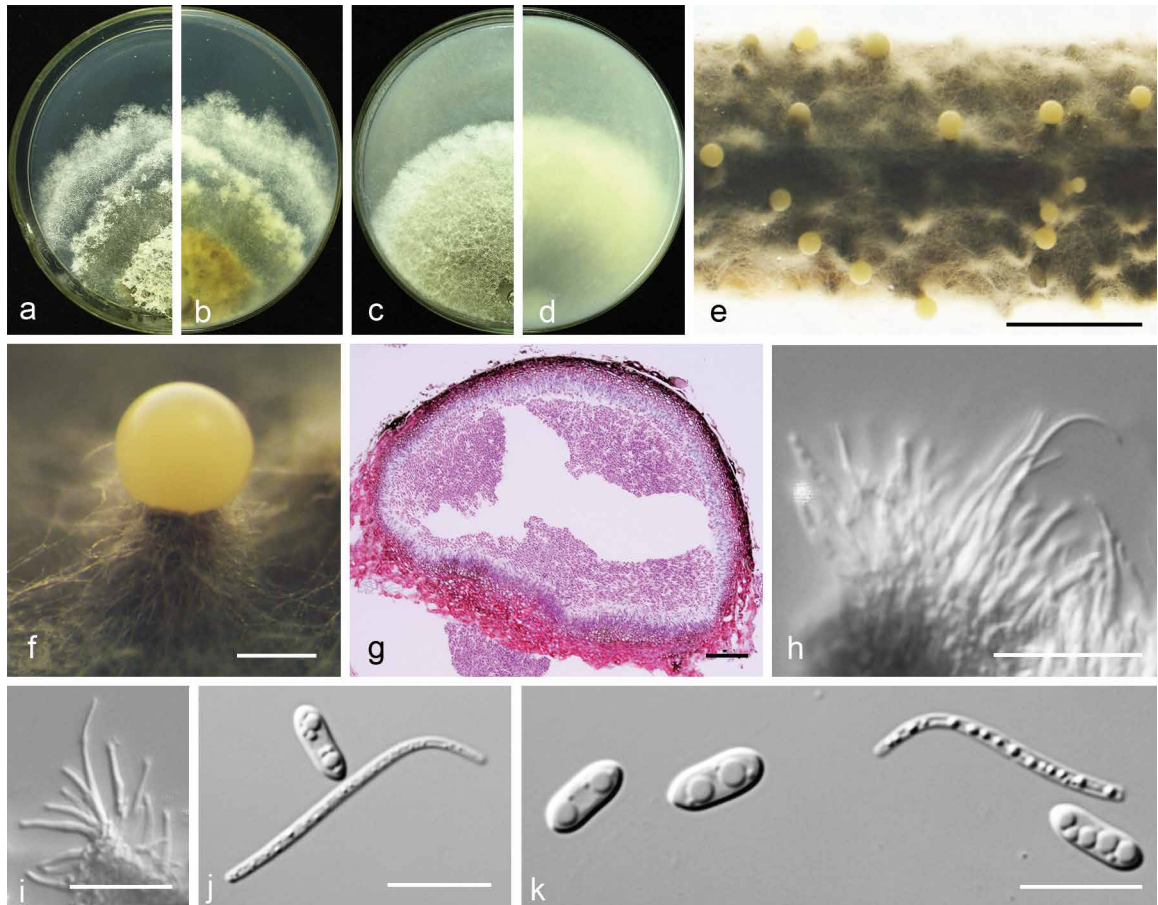


Fig. 9 *Diaporthe citrichinensis* (PSCG 462). a–d. Front and back view, respectively of colonies on PDA (a, b) and OA (c, d); e. conidiomata on alfalfa stems; f. conidiomata; g. section view of conidiomata; h–i. conidiophores; j–k. alpha and beta conidia. — Scale bars: e = 2 mm; f = 200 μ m; g = 50 μ m; h–i = 20 μ m; j–k = 10 μ m.

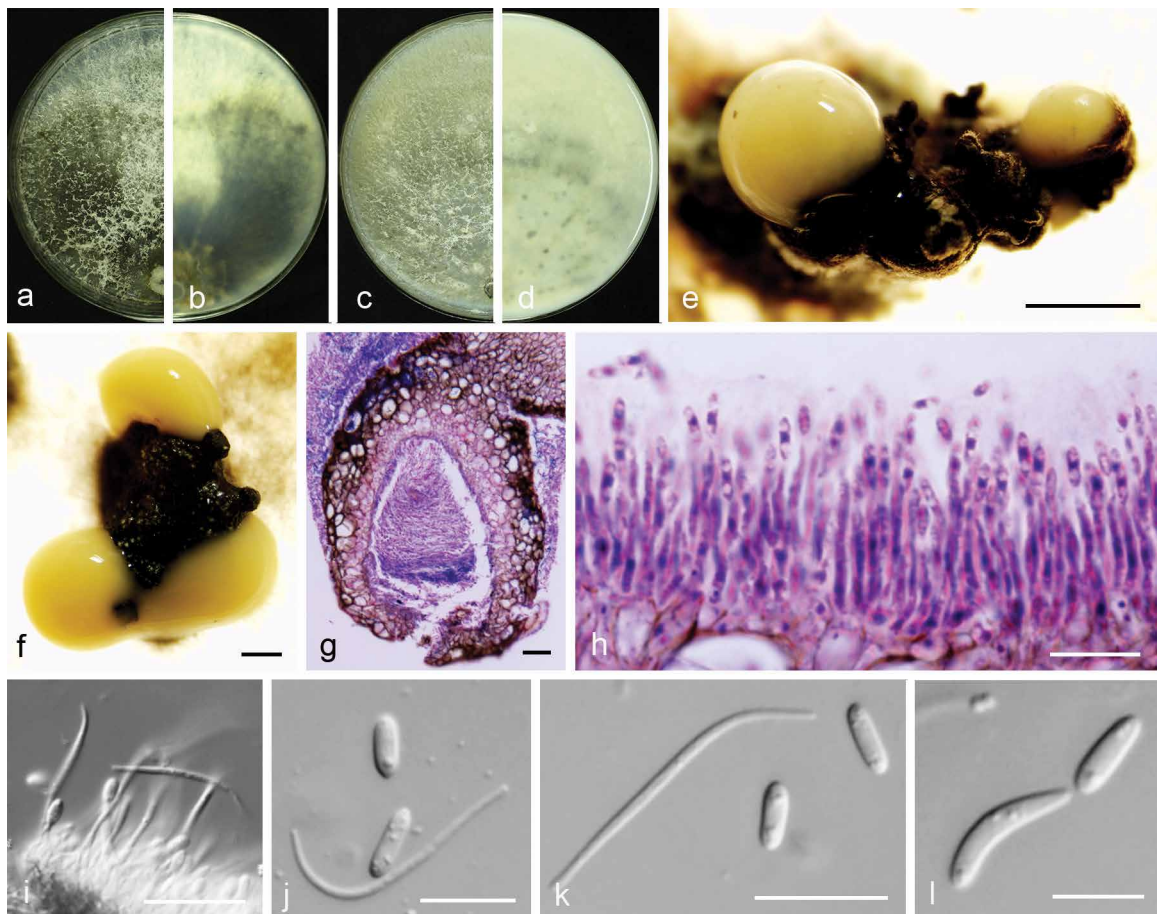


Fig. 10 *Diaporthe eres* (PSCG 041). a–d. Front and back view, respectively of colonies on PDA (a, b) and OA (c, d); e–f. conidiomata; g. section view of conidiomata; h–i. conidiophores; j–k. alpha and beta conidia; l. alpha and gamma conidia. — Scale bars: e = 1 mm; f = 500 μ m; g, i–j = 20 μ m; h, k–l = 10 μ m.

Diaporthe cercidis C.M. Tian & Q. Yang, MycoKeys 39: 124. 2018 — Fig. 7

Description & Illustration — Yang et al. (2018).

Materials examined. CHINA, Shandong Province, Yantai City, on branches of *P. communis* cv. Winter decana, 27 Nov. 2015, Y.S. Guo (culture PSCG 259); Zhejiang Province, Hangzhou City, on branches of *P. pyrifolia* cv. Cuiyu, 7 Mar. 2016, Y.S. Guo (culture PSCG 273, PSCG 275); Chongqing City, on branches of *P. pyrifolia* cv. Huanghua, 29 Mar. 2017, Y.S. Guo (culture PSCG 439); Jiangsu Province, Zhenjiang City, on branches of *P. pyrifolia* cv. Aigansui, 18 Nov. 2017, Y.S. Guo (culture PCSG 513); *ibid.*, on branches of *P. pyrifolia* cv. Hohsui, 18 Nov. 2017, Y.S. Guo (culture PCSG 526).

Notes — *Diaporthe cercidis* was first reported on twigs and branches of *Cercis chinensis* in Jiangsu province, China (Yang et al. 2018). In this study, six isolates were identified as belonging to this species, and this is the first report of *D. cercidis* responsible for pear shoot canker. The conidial size and morphology are similar to the ex-type isolate CFCC 52565, but the alpha conidia are multi-guttulate.

Diaporthe chongqingensis Y.S. Guo & G.P. Wang, *sp. nov.* — MycoBank MB830656; Fig. 8

Etymology. Referring to the city, Chongqing, where it was collected.

Sexual morph not observed. *Asexual morph* on alfalfa stems. *Pycnidial conidiomata* globose, solitary or aggregated, wrapped in hyphae embedded in alfalfa stems surface, grey to black, 285–744 µm diam, yellowish translucent conidial drops exuded from the ostioles. *Conidiophores* hyaline, smooth, 1-septate, densely aggregated, unbranched, ampulliform, 6.5–12.5 × 2–6 µm. *Conidiogenous cells* phialidic, hyaline, terminal, cylindrical, straight, 14–26 × 1.5–2.5 µm, tapered towards the apex. *Alpha conidia* hyaline, aseptate, fusiform, biguttulate or multi-guttulate, acutely round at one end, 5.5–7.5 × 2–3 µm, mean ± SD = 6.4 ± 0.5 × 2.3 ± 0.2 µm, L/W ratio = 2.8 (n = 50). *Beta* and *gamma conidia* not observed.

Culture characteristics — Colony on PDA with flattened mycelium, white, smoke grey in the centre, reverse with smoke grey coloured pigments formed in the shape of a concentric ring pattern. Colony diam 40–49 mm in 3 d at 28 °C. On OA, colony with entire margin, grey olivaceous in the centre and white margin, reverse grey olivaceous pigments formed in the centre.

Materials examined. CHINA, Chongqing City, on branches of *P. pyrifolia* cv. Huanghua, 29 Mar. 2017, Y.S. Guo (holotype HMAS 248148, culture ex-type CGMCC 3.19603 = PSCG 435); *ibid.*, culture PSCG 436.

Notes — *Diaporthe chongqingensis* is introduced based on the multi-locus phylogenetic analysis, with two isolates clustering separately in a well-supported clade (BI/ML/MP = 1/100/100). *Diaporthe chongqingensis* is most closely related to *D. fusicola*, but distinguished based on ITS and *TEF* loci from *D. fusicola* (96.6 % in ITS and 97 % in *CAL*) by 24 nucleotides in the concatenated alignment, in which 15 are distinct in the ITS region, six in the *TEF* region and three in the *TUB* region. Morphologically, *D. chongqingensis* differs from *D. fusicola* in its smaller alpha conidia (5.5–7.5 × 2–3 vs 5.5–9 × 2–3 µm).

Diaporthe citrichinensis F. Huang et al., Fungal Diversity 61: 247. 2013 — Fig. 9

Description & Illustration — Huang et al. (2013).

Materials examined. CHINA, Guizhou Province, Guiyang City, on branches of *P. pyrifolia* cv. Jinqiu, 5 Mar. 2018, Y.S. Guo (culture PSCG 462).

Notes — *Diaporthe citrichinensis* was originally described from deadwood of *Citrus unshiu* in Shaanxi province, China (Huang et al. 2013). Isolate PSCG 462 clustered together

with *D. citrichinensis* (ZJUD34) in the multi-locus phylogenetic tree. This is the first report of *D. citrichinensis* responsible for pear shoot canker. Pycnidial conidiomata of the ex-type isolate are slightly larger than those of the ex-type isolate ZJUD34 (375–922 vs 165–435 µm), and alpha and beta conidia of the ex-type are multi-guttulate.

Diaporthe eres Nitschke, Pyrenomyc. Germ. 2: 245. 1870 — Fig. 10

Synonym. *Diaporthe nobilis* Sacc. & Spég., *Michelia* 1(4): 386. 1878.

Description & Illustration — Udayanga et al. (2014b).

Materials examined. CHINA, Henan Province, Nanyang City, on branches of *P. pyrifolia* cv. Wanqiu Huang, 17 Apr. 2016, Y.S. Guo (culture PCSG 321, PCSG 322, PCSG 325); Zhejiang Province, Hangzhou City, on branches of *P. pyrifolia* cv. Cuiguan, 7 Mar. 2016, Y.S. Guo (PCSG 276); *ibid.*, 22 Aug. 2016, Y.S. Guo (PCSG 377); Yunnan Province, Kunming City, on branches of *P. bretschneideri* cv. Zaobaisu, 17 Oct. 2014, Q. Bai (PCSG 041, PCSG 042); Chongqing City, on branches of *P. pyrifolia* cv. Huangguan, 27 Nov. 2016, Y.S. Guo (PCSG 250); Hubei Province, Wuhan City, on branches of *P. pyrifolia* cv. Jinshui, 27 Nov. 2016, Y.S. Guo (PCSG 265); *ibid.*, on branches of *P. pyrifolia* cv. Yuanhuang, 10 Apr. 2017, Y.S. Guo (PCSG 440); Hebei Province, Cangzhou City, on branches of *P. pyrifolia* cv. Wanyu, 10 May 2016, Y.S. Guo (PCSG 300); Jiangsu Province, Zhenjiang City, on branches of *P. pyrifolia* cv. Hohsui, 18 Nov. 2017, Y.S. Guo (PCSG 529); Shandong Province, Yantai City, on branches of *P. communis* cv. Packham, 17 Oct. 2014, Q. Bai (PCSG 092); Liaoning Province, Yingkou City, on branches of *P. pyrifolia* cv. Huangjin, 29 June 2016, Y.S. Guo (PCSG 358).

Notes — *Diaporthe eres* is the type species of *Diaporthe*. It was described by Nitschke (1870) and collected from *Ulmus* sp. in Germany. It has a wide distribution and a broad host range as pathogen, endophyte or saprobe, and can cause a variety of plant diseases (Udayanga et al. 2014b). Recent studies indicated that *D. biguttusis*, *D. camptothecicola*, *D. ellipticola*, *D. longicola*, *D. mahothocarpus* and *D. momicola* should be treated as synonyms of *D. eres* (Fan et al. 2018, Yang et al. 2018). The results of this study are consistent with the above. A large number of isolates clustered in *D. eres*. Bai et al. (2015) identified this species as responsible for pear shoot canker, and some of the isolates previously identified as *P. fukushii* were identified as *D. eres* in this study.

Diaporthe fulvicolor Y.S. Guo & G.P. Wang, *sp. nov.* — MycoBank MB830657; Fig. 11

Etymology. From Latin *fulvi* 'tawny', referring to tawny pigment accumulated in the centre of the colony.

Sexual morph not observed. *Asexual morph* on alfalfa stems. *Pycnidial conidiomata* globose or irregular, solitary or aggregated, exposed on the alfalfa stems surface, dark brown to black, 174–316 µm diam. *Conidiophores* hyaline, smooth, 1-septate, densely aggregated, unbranched, cylindrical, straight, 5.5–8 × 2.5–3.5 µm. *Conidiogenous cells* phialidic, hyaline, terminal, ampulliform, 6.5–10 × 1.5–2.5 µm, tapered towards the apex. *Alpha conidia* hyaline, aseptate, fusiform to oval, acutely round at both ends, biguttulate or multi-guttulate, 7–9 × 2–3 µm, mean ± SD = 7.8 ± 0.4 × 2.5 ± 0.2 µm, L/W ratio = 3.1 (n = 50). *Beta* and *gamma conidia* not observed.

Culture characteristics — Colonies on PDA with aerial mycelium white, fluffy, reverse tawny pigment accumulation in the centre, surrounded by amber, pure white at the colony margin. Colony diam 52–55 mm in 3 d at 28 °C. On OA with entire margin, greyish yellow-green in the centre and white margin.

Materials examined. CHINA, Hubei Province, Wuhan City, on branches of *P. pyrifolia* cv. Cuiguan, 1 Sept. 2014, Q. Bai (holotype HMAS 248149, culture ex-type CGMCC 3.19601 = PSCG 051); *ibid.*, culture PSCG 057.

Notes — *Diaporthe fulvicolor* forms an independent clade in the *D. arecae* species complex (Fig. 4) and is phylogenetically

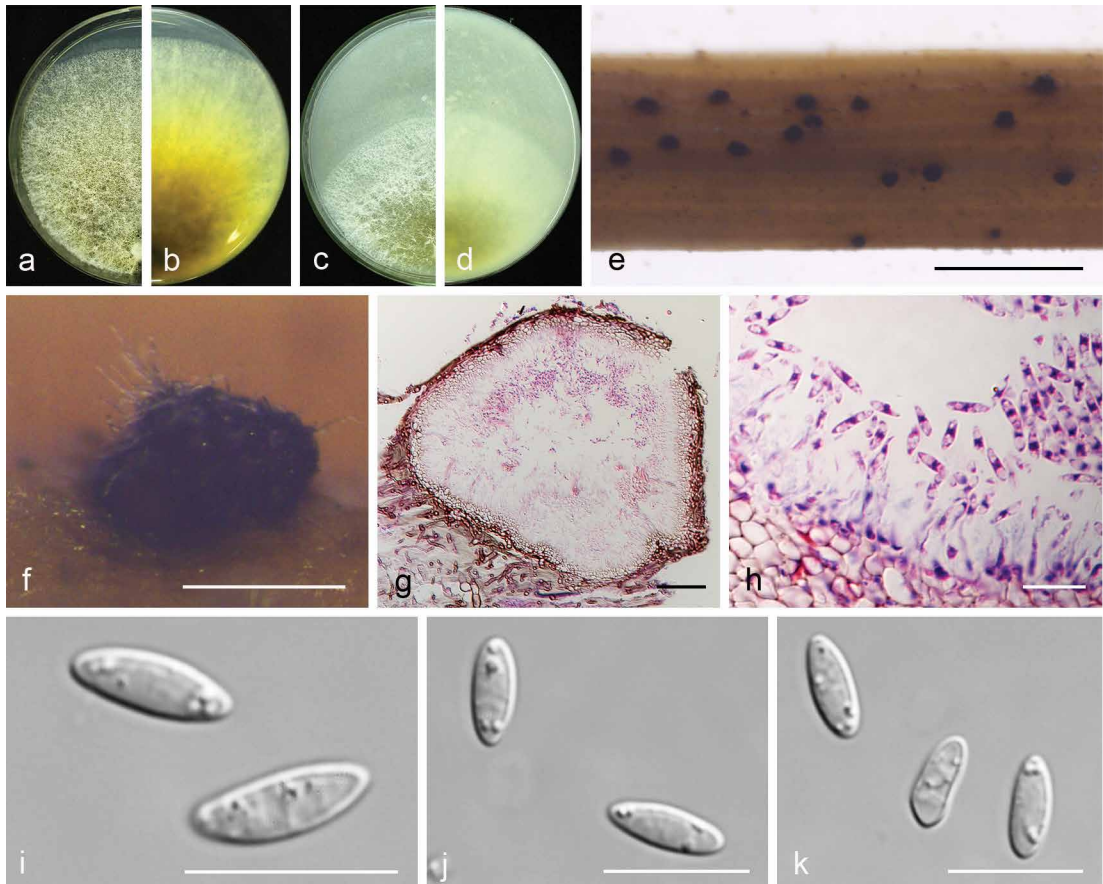


Fig. 11 *Diaporthe fulvicolor* (CGMCC 3.19601). a–d. Front and back view, respectively of colonies on PDA (a, b) and OA (c, d); e. conidiomata on alfalfa stems; f. conidiomata; g. section view of conidiomata; h. conidiophores; i–k. alpha conidia. — Scale bars: e = 2 mm; f = 200 μ m; g = 50 μ m; h–k = 10 μ m.

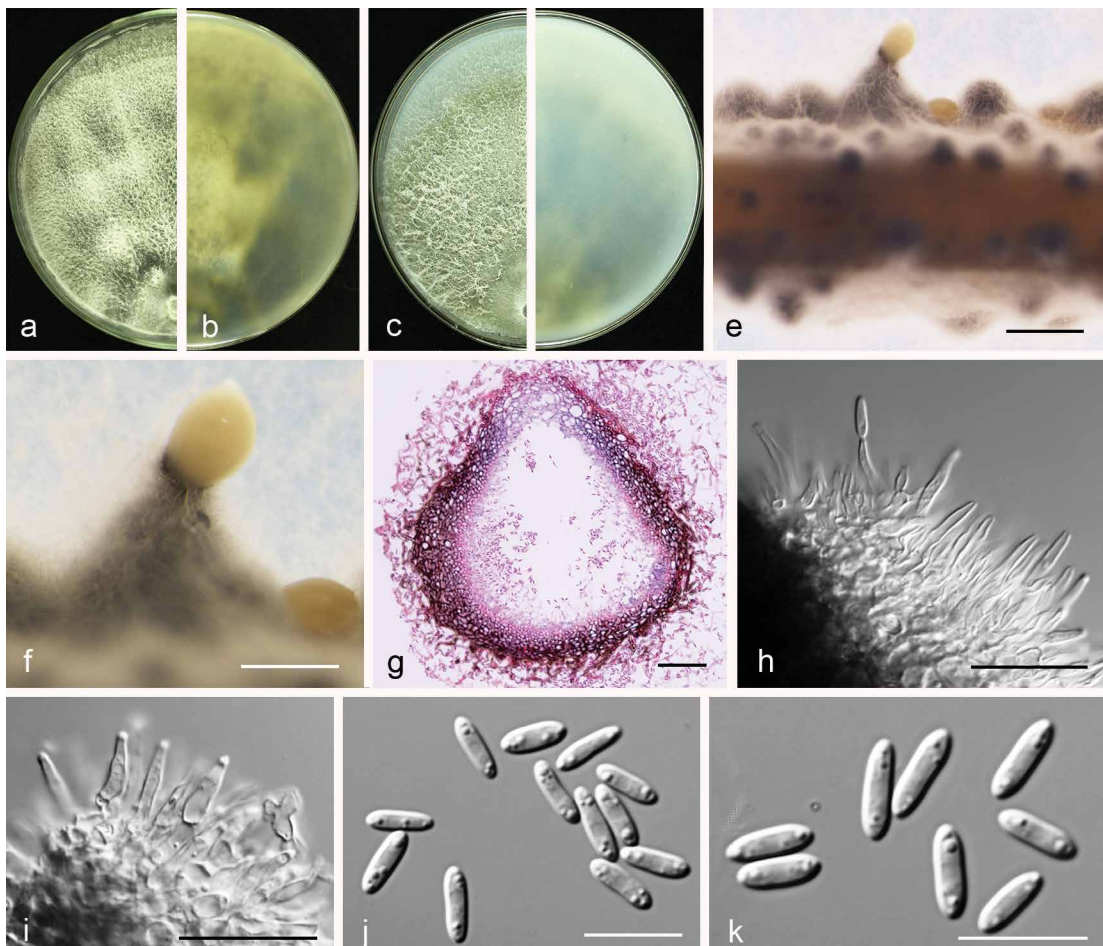


Fig. 12 *Diaporthe fuscicola* (PSCG 371). a–d. Front and back view, respectively of colonies on PDA (a, b) and OA (c, d); e. conidiomata on alfalfa stems; f. conidiomata; g. section view of conidiomata; h–i. conidiophores; j–k. alpha conidia. — Scale bars: e = 1 mm; f = 500 μ m; g = 50 μ m; h–i = 20 μ m; j–k = 10 μ m.

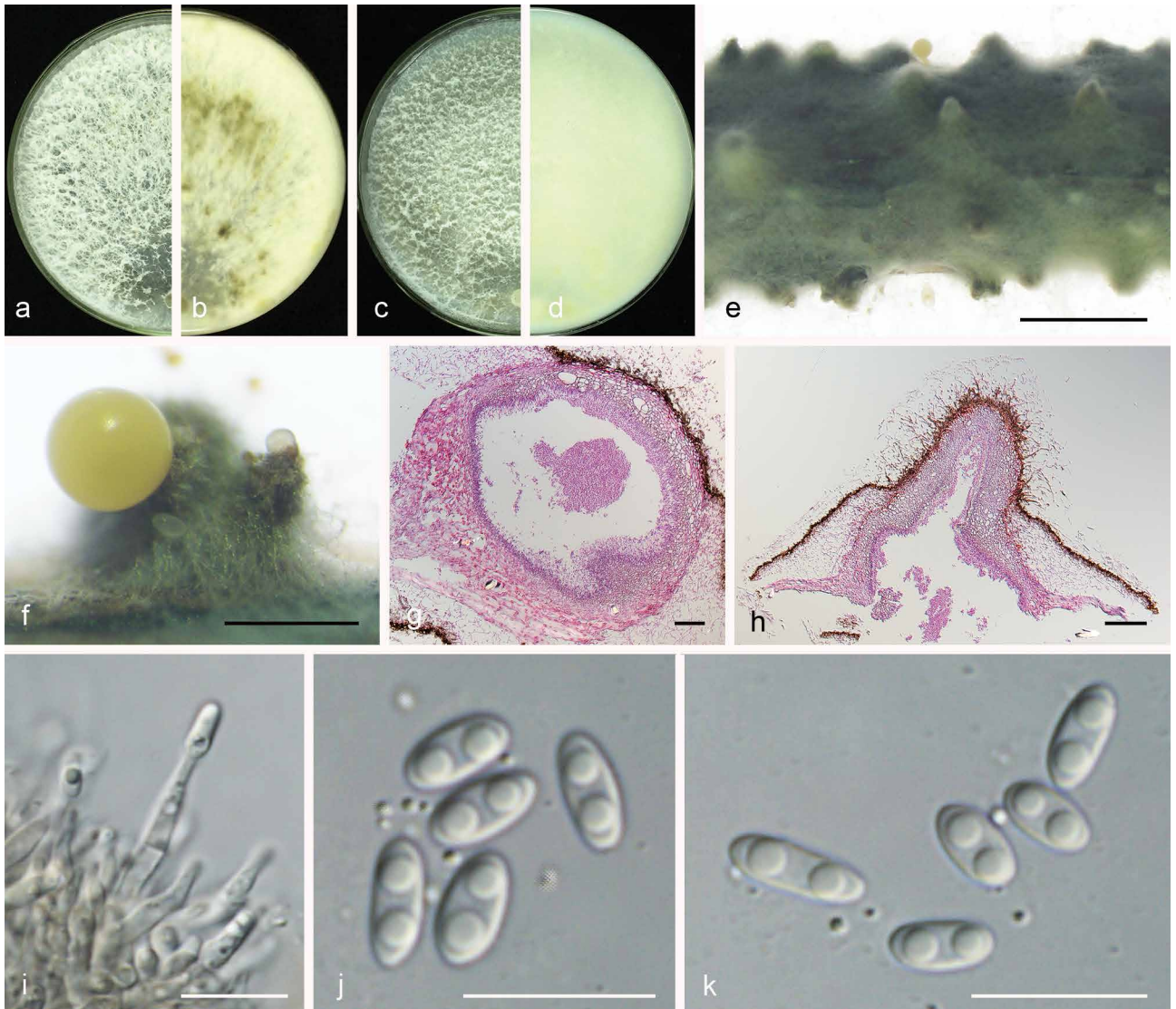


Fig. 13 *Diaporthe ganjiae* (PSCG 489). a–d. Front and back view, respectively of colonies on PDA (a, b) and OA (c, d); e. conidiomata on alfalfa stems; f. conidiomata; g–h. section view of conidiomata; i. conidiophores; j–k. alpha conidia. — Scale bars: e = 2 mm; f = 500 μ m; g = 50 μ m; h = 100 μ m; i–k = 10 μ m.

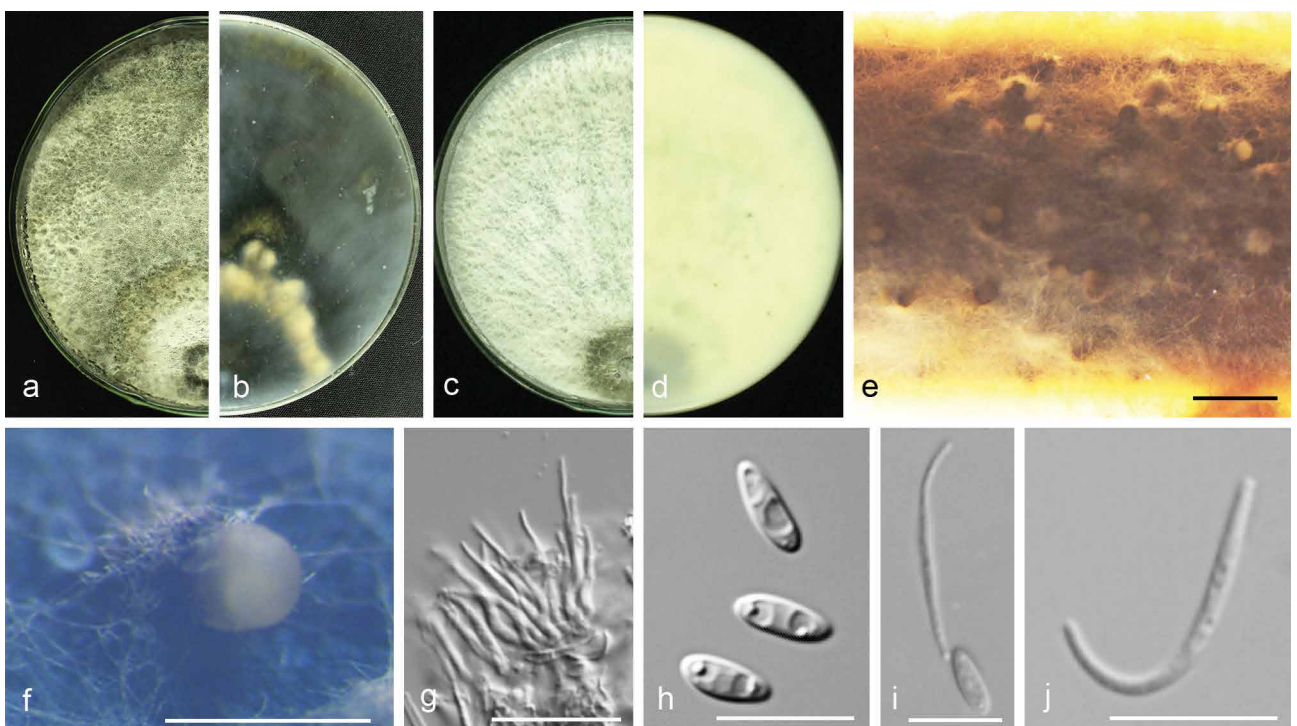


Fig. 14 *Diaporthe hongkongensis* (PSCG 466). a–d. Front and back view, respectively of colonies on PDA (a, b) and OA (c, d); e. conidiomata on alfalfa stems; f. conidiomata; g. conidiophores; h. alpha conidia; i. alpha and beta conidia; j. beta conidia. — Scale bars: e = 1 mm; f = 200 μ m; g = 20 μ m; h–j = 10 μ m.

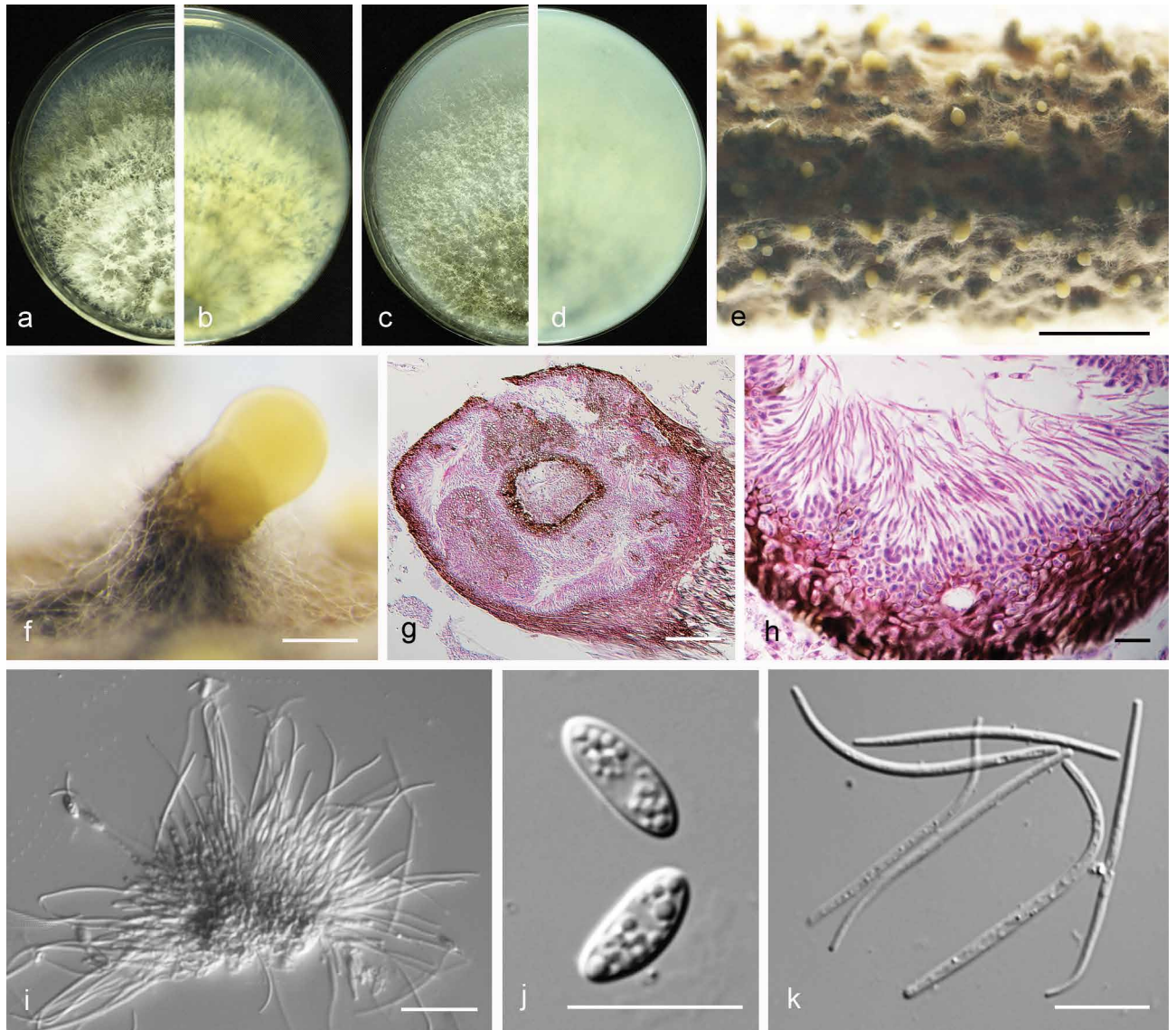


Fig. 15 *Diaporthe padina* (PSCG 160). a–d. Front and back view, respectively of colonies on PDA (a, b) and OA (c, d); e. conidiomata on alfalfa stems; f. conidiomata; g. section view of conidiomata; h–i. conidiophores; j. alpha conidia; k. beta conidia. — Scale bars: e = 2 mm; f = 200 μm; g = 100 μm; i = 20 μm; h, j–k = 10 μm.

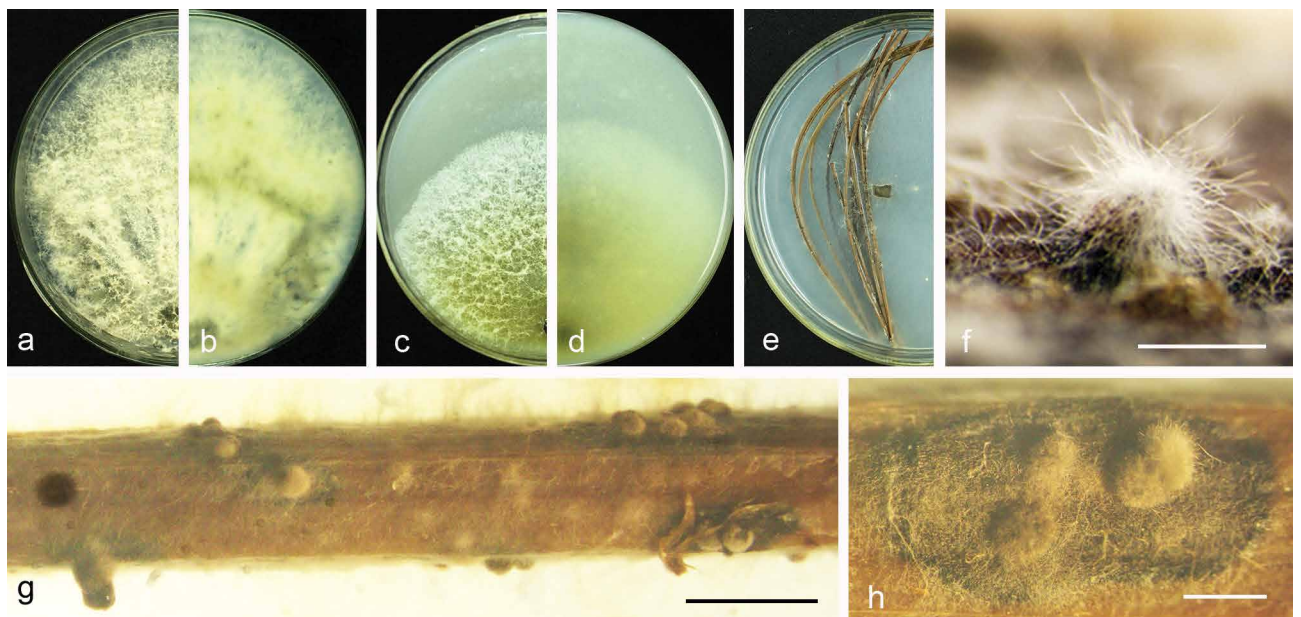


Fig. 16 *Diaporthe parvae* (CGMCC 3.19599). a–d. Front and back view, respectively of colonies on PDA (a, b) and OA (c, d); e. conidiomata on PNA medium; f–h. conidiomata on alfalfa stems. — Scale bars: f = 100 μm; g = 5 mm; h = 1 mm.

distinct from *D. pescicola* and *D. spinosa* (described below). *Diaporthe fulvicolor* can be distinguished from *D. pescicola* in *CAL* and *TUB* loci by 57 nucleotide differences in concatenated alignment (40 in *CAL* and 17 in *TUB*), and from *D. spinosa* in *CAL* loci by 15 nucleotides (93 % in *CAL*). Moreover, *D. fulvicolor* differs from *D. pescicola* in having smaller conidiomata (174–316 vs 637–881 μm), and larger alpha conidia (7–9 \times 2–3 vs 6–8 \times 2–2.5 μm). Furthermore, *D. fulvicolor* differs from *D. spinosa* in its longer alpha conidia (7–9 \times 2–3 vs 5.5–8 \times 2–3.5 μm).

Diaporthe fusicola Y.H. Gao & L. Cai, Fungal Biol. 119: 300. 2015 — Fig. 12

Description & Illustration — Gao et al. (2015).

Materials examined. CHINA, Jiangxi Province, Fuzhou City, on branches of *P. pyrifolia* cv. Cuiyu, 2 Sept. 2014, Q. Bai (culture PSCG 015); Fujian

Province, Sanming City, on branches of *P. pyrifolia* cv. Cuiyu, 10 Nov. 2014, Q. Bai (PSCG 118); Zhejiang Province, Hangzhou City, on branches of *P. pyrifolia* cv. Cuiguan, 22 Aug. 2016, Y.S. Guo (PSCG 371).

Notes — *Diaporthe fusicola* was first described on leaves of *Lithocarpus glabra* in Zhejiang province, China (Gao et al. 2015). In this study, six isolates were identified as belonging to this species, and this is the first report of *D. fusicola* responsible for pear shoot canker. Bai et al. (2015) identified some of the isolates as *P. amygdali*, but they were identified as *D. fusicola* in this study.

Diaporthe ganjae R.R. Gomes et al., Persoonia 31: 22. 2013 — Fig. 13

Sexual morph not observed. *Asexual morph* on alfalfa stems. *Pycnidial conidiomata* globose, conical or irregular, solitary or aggregated, exposed on the alfalfa stems surface, dark brown

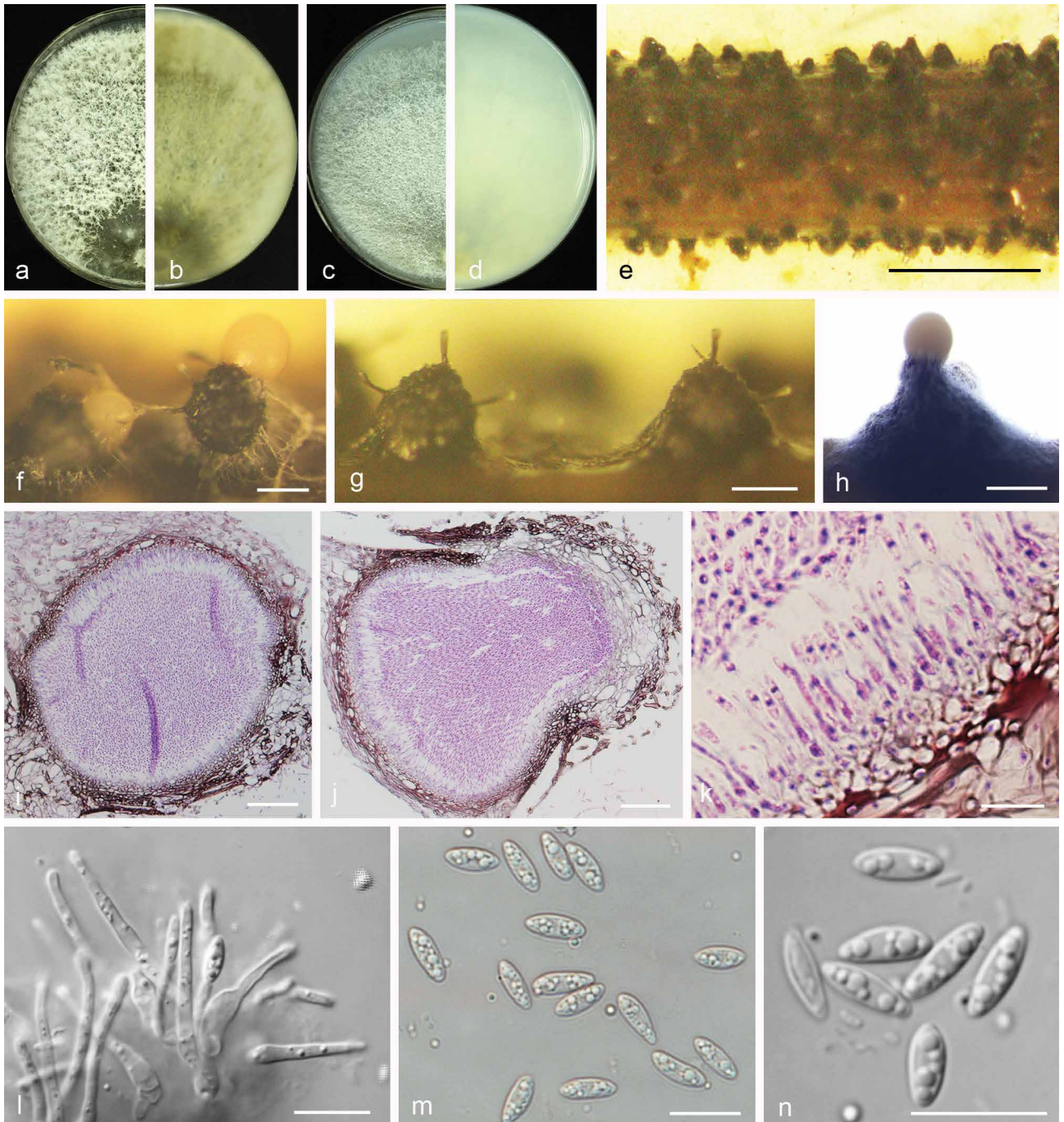


Fig. 17 *Diaporthe pescicola* (PSCG 036). a–d. Front and back view, respectively of colonies on PDA (a, b) and OA (c, d); e. conidiomata on alfalfa stems; f–h. conidiomata; i–j. section view of conidiomata; k–l. conidiophores; m–n. alpha conidia. — Scale bars: e = 5 mm; f–g = 200 μm ; h = 500 μm ; i–j = 50 μm ; k–n = 10 μm .

to black, 229–634 μm diam. *Conidiophores* hyaline, smooth, 1-septate, densely aggregated, unbranched, ampulliform, 5.5–7 \times 2–4 μm . *Conidiogenous cells* phialidic, hyaline, terminal, cylindrical, 10.5–16 \times 1.5–2.5 μm , tapered towards the apex. *Alpha conidia* hyaline, aseptate, fusiform to oval, obtuse rounded at both ends, biguttulate, 5.5–7.5 \times 2–3 μm , mean \pm SD = 6.4 \pm 0.4 \times 2.6 \pm 0.2 μm , L/W ratio = 2.5 (n = 50). *Beta* and *gamma conidia* not observed.

Culture characteristics — Cultures on PDA with aerial mycelium white, fluffy, reverse with a mottled tawny pigment. Colony diam 79–81 mm in 3 d at 28 °C. On OA, colony with white aerial mycelium and lacking pigmentation.

Materials examined. CHINA, Guizhou Province, Guiyang City, on branches of *P. pyrifolia* cv. Yuanhuang, 8 Nov. 2017, Y.S. Guo (culture PSCG 489).

Notes — *Diaporthe ganjae* was first reported from dead leaves of *Cannabis sativa* in Illinois, USA (Gomes et al. 2013). In this study, one isolate (PSCG 489) clustered together with the ex-type culture of *D. ganjae* (CBS 180.91) in the multi-locus phylogenetic tree (Fig. 3). This is the first description of its asexual morph and culture characteristics. Furthermore, this is the first report of *D. ganjae* responsible for pear shoot canker.

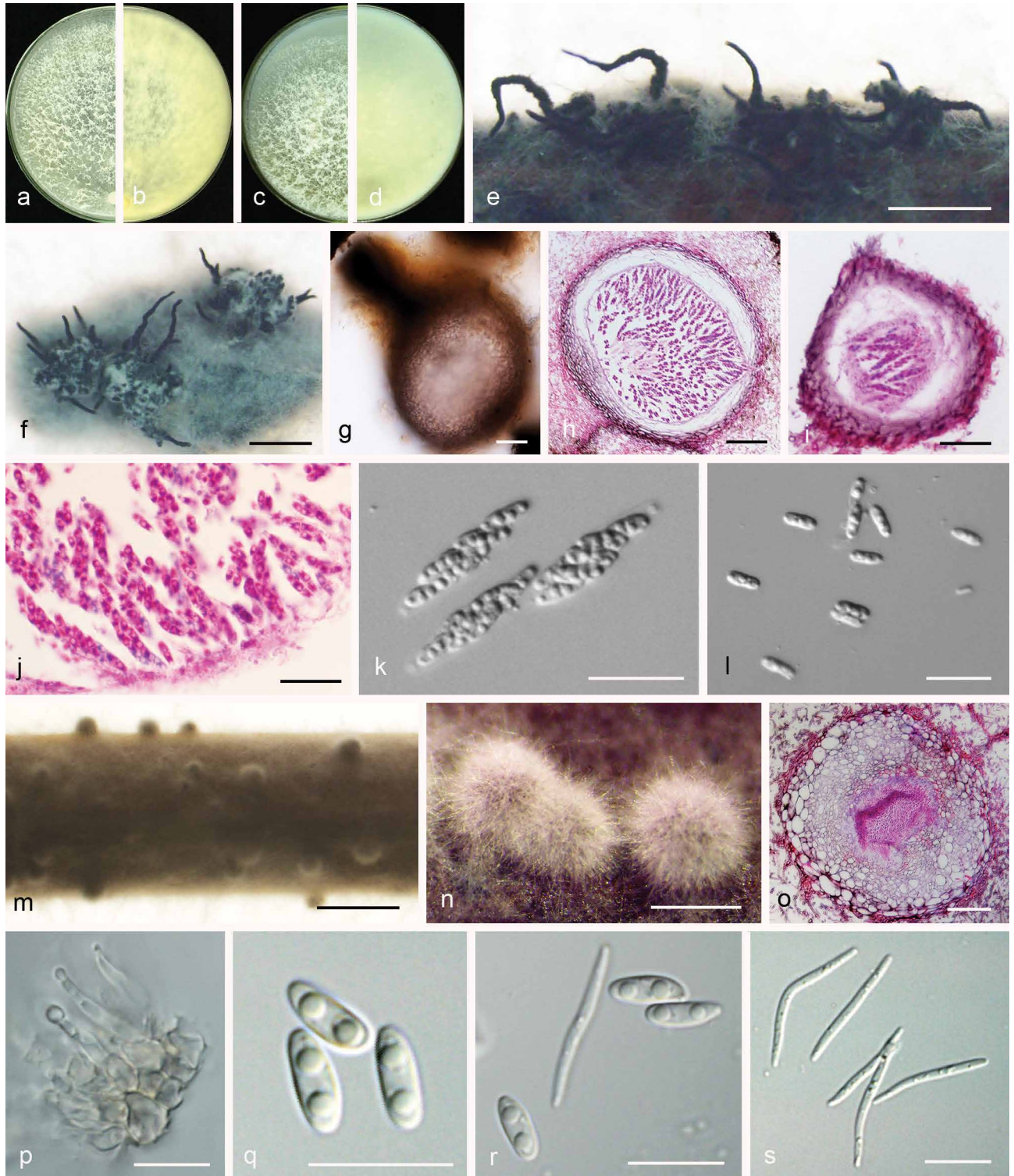


Fig. 18 *Diaporthe sojae* (PSCG 486). a–d. Front and back view, respectively, of colonies on PDA (a, b) and OA (c, d); e. ascomata on alfalfa stems; f. ascomata; g. ascoma; h–i. section view of ascoma; j–k. asci; l. ascospores; m. conidiomata on alfalfa stems; n. conidiomata; o. section view of conidiomata; p. conidiophores; q. alpha conidia; r. alpha and beta conidia; s. beta conidia. — Scale bars: e–f = 1 mm; g–h, o = 50 μm ; i = 30 μm ; j–l = 20 μm ; m = 2 mm; n = 500 μm ; p–s = 10 μm .

Diaporthe hongkongensis R.R. Gomes et al., *Persoonia* 31:
23. 2013 — Fig. 14

Synonym. *Diaporthe lithocarpi* (Y.H. Gao et al.) Y.H. Gao & L. Cai, *Fungal Biol.* 119: 306. 2015. Nom. inval., Arts 41.1, F.5.1 (Shenzhen).

Description & Illustration — Gomes et al. (2013).

Materials examined. CHINA, Fujian Province, Sanming City, on branches of *P. pyrifolia* cv. Cuiyu, 10 Nov. 2014, Q. Bai (PSCG 114); *ibid.*, on branches of *P. pyrifolia* cv. Huanghua, 10 Nov. 2014, Q. Bai (culture PSCG 130, PSCG 141); Zhejiang Province, Hangzhou City, on branches of *P. pyrifolia* cv. Cuiyu, 7 Mar. 2016, Y.S. Guo (culture PSCG 290); Fujian Province, Sanming City, on branches of *P. pyrifolia* cv. Cuiyu, 25 Nov. 2017, Y.S. Guo (PSCG 465, PSCG 466).

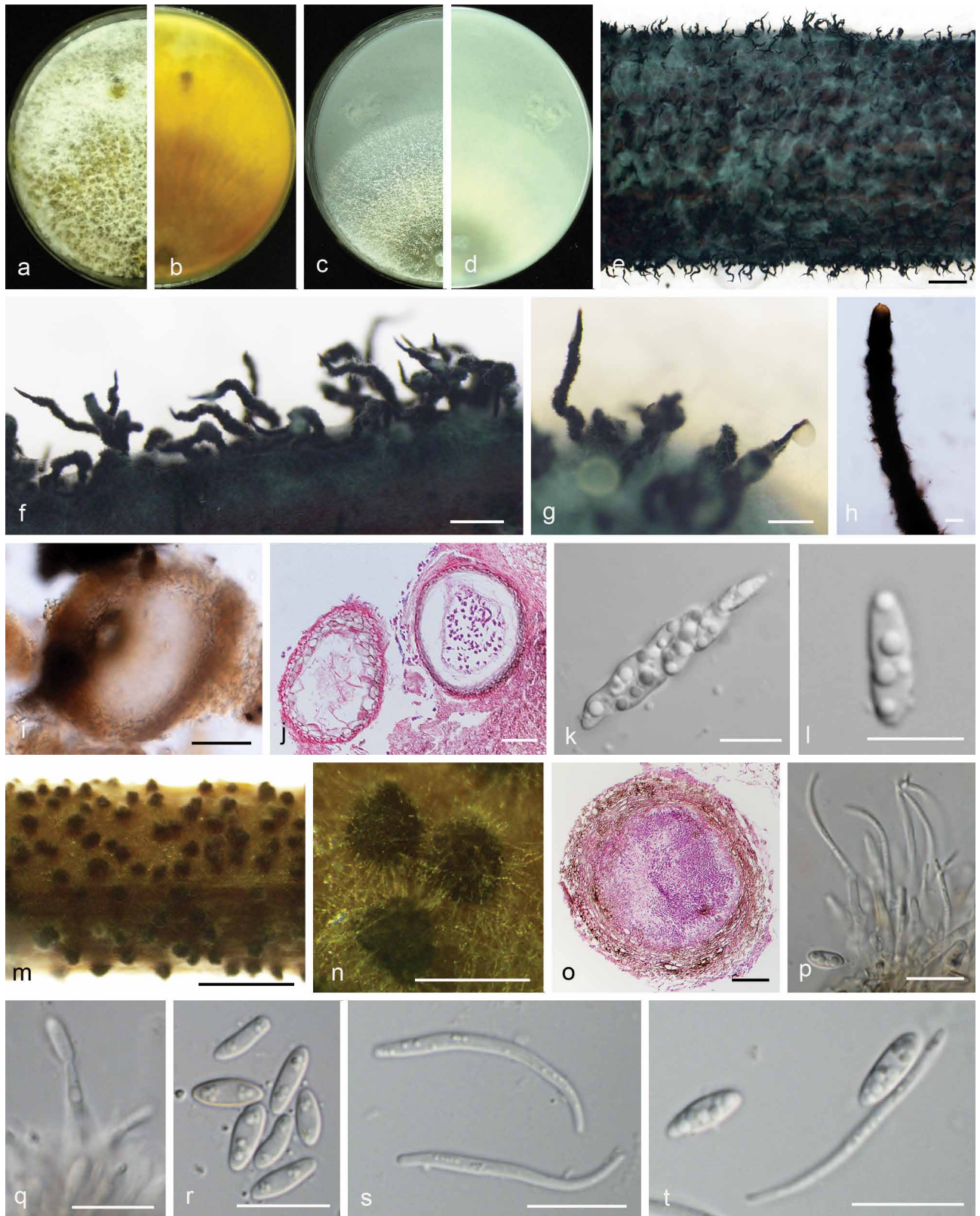


Fig. 19 *Diaporthe spinosa*. a–d. Front and back view, respectively of colonies on PDA (a, b) and OA (c, d); e. ascomata on alfalfa stems; f–g. ascomata; h. perithecial neck; i. ascoma; j. section view of ascoma; k. asci; l. ascospores; m. conidiomata on alfalfa stems; n. conidiomata; o. section view of conidiomata; p–q. conidiophores; r. alpha conidia; s. beta conidia; t. alpha and beta conidia (a–d, m–t. isolate PSCG 383; e–l. PSCG 491). — Scale bars: e, m = 2 mm; f–g, n = 500 μ m; h–j, o = 50 μ m; k–l, p–t = 10 μ m.

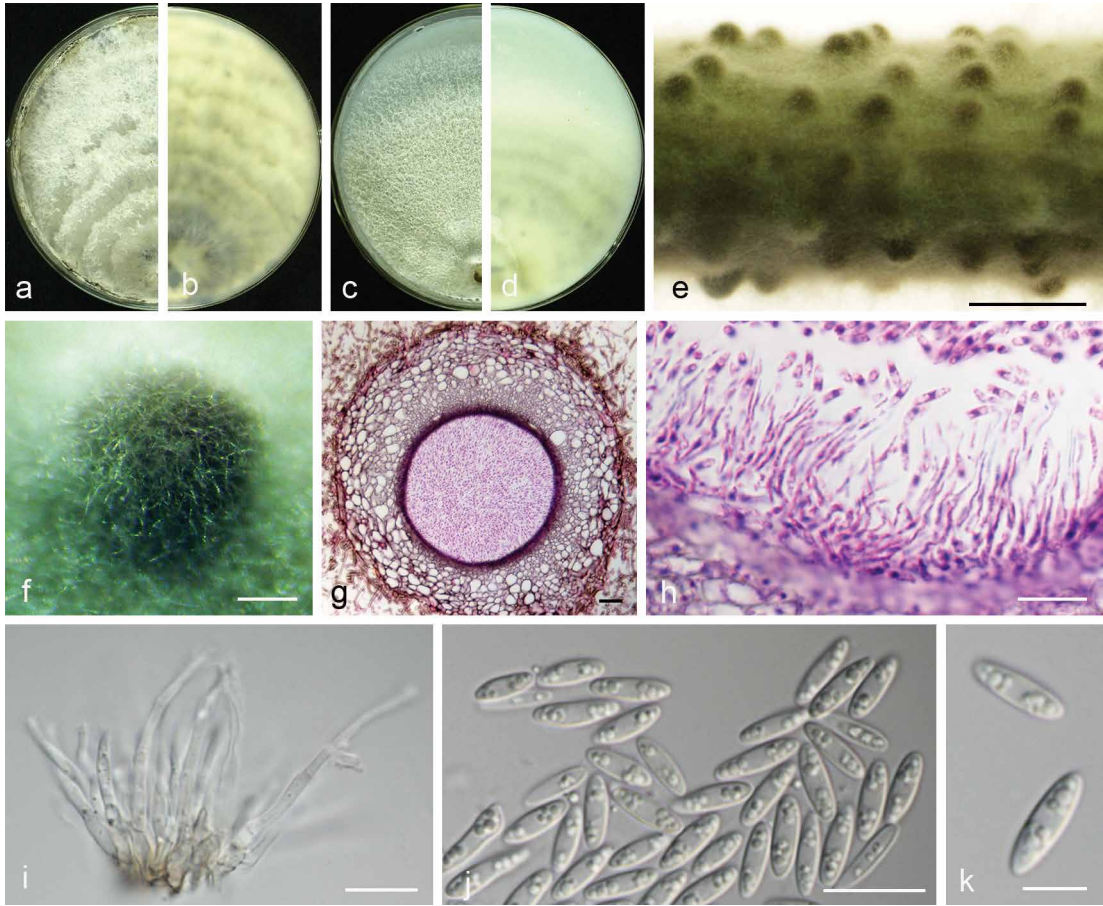


Fig. 20 *Diaporthe taicicola* (PSCG 485). a–d. Front and back view, respectively of colonies on PDA (a, b) and OA (c, d); e. conidiomata on alfalfa stems; f. conidiomata; g. section view of conidiomata; h–i. conidiophores; j–k. alpha conidia. — Scale bars: e = 2 mm; f = 200 μ m; g = 20 μ m; h–j = 10 μ m; k = 5 μ m.

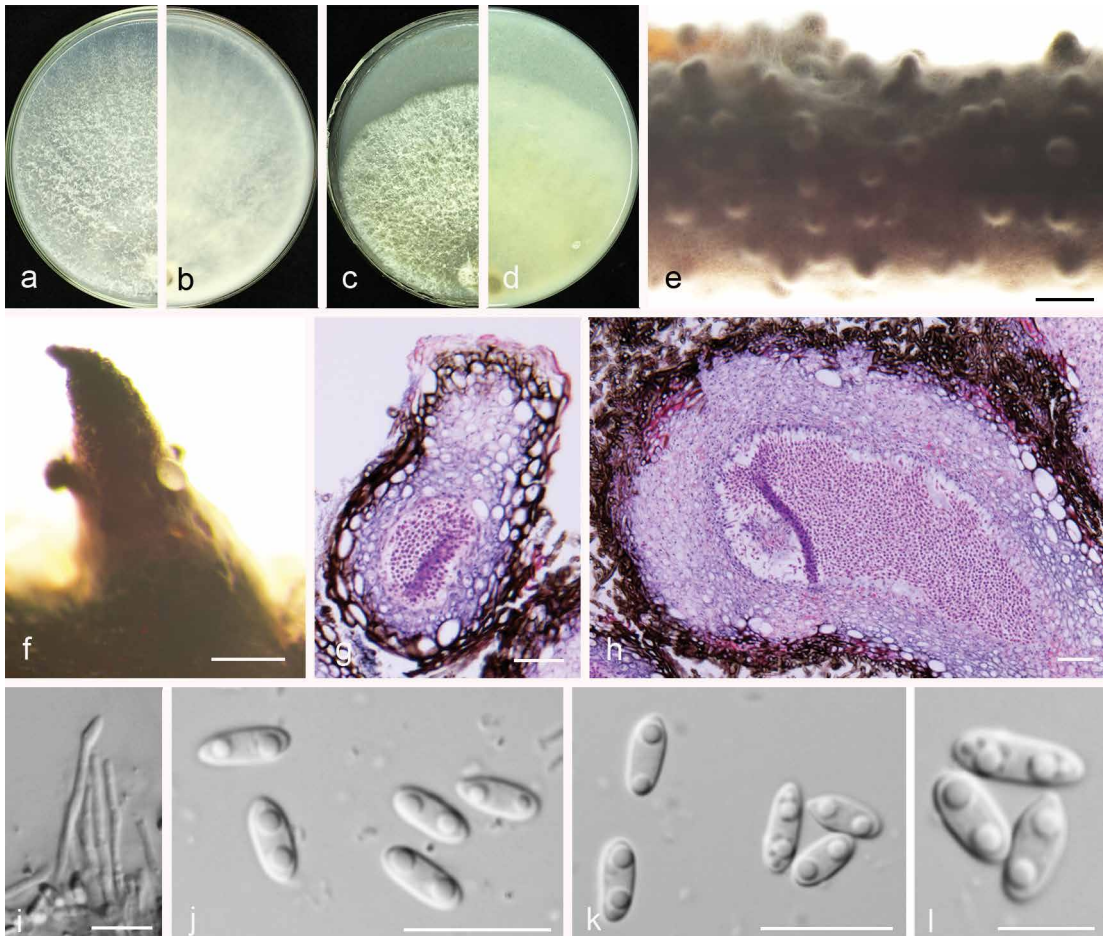


Fig. 21 *Diaporthe unshiuensis* (PSCG 120). a–d. Front and back view, respectively of colonies on PDA (a, b) and OA (c, d); e. conidiomata on alfalfa stems; f. conidiomata; g–h. section view of conidiomata; i. conidiophores; j–l. alpha conidia. — Scale bars: e = 1 mm; f = 200 μ m; g–h = 20 μ m; i–k = 10 μ m; l = 5 μ m.

Notes — *Diaporthe hongkongensis* was first described from fruit of *Dichroa febrifuga* in Hong Kong, China (Gomes et al. 2013). This species often causes trunk diseases. In this study, 10 isolates were identified as belonging to this species, and this is the first report of *D. hongkongensis* responsible for pear shoot canker.

Diaporthe padina C.M. Tian & Q. Yang, MycoKeys 39: 137. 2018 — Fig. 15

Description & Illustration — Yang et al. (2018).

Materials examined. CHINA, Jiangxi Province, Nanchang City, on branches of *P. pyrifolia* cv. Cuiquan, 27 Nov. 2014, Q. Bai (culture PSCG 160).

Notes — *Diaporthe padina* was first described from symptomatic twigs of *Padus racemosa* in Heilongjiang Province, China (Yang et al. 2018). In this study, one isolate was identified as belonging to this species, and this is the first report of *D. padina* responsible for pear shoot canker. Compared with the description of ex-type isolate CFCC 52590, pycnidial conidiomata of the isolate PSCG 160 are larger than CFCC 52590 (455–994 vs 330–520 µm), and conidiophores are longer (28–32 × 1–1.5 vs 5.5–12.5 × 1–1.5 µm). Alpha and beta conidia are both multi-guttulate, and longer than in isolate CFCC 52590 (alpha 7.5–10 × 2–3.5 vs 7–8 × 1.5–2 µm, beta 26–41.5 × 1–1.5 vs 21–24 × 1 µm).

Diaporthe parvae Y.S. Guo & G.P. Wang, *sp. nov.* — MycoBank MB830658; Fig. 16

Etymology. From Latin *parva* 'small', referring to smaller conidiomata.

Sexual morph not observed. *Asexual morph* on alfalfa stems. *Pycnidial conidiomata* globose or irregular, solitary or aggregated, exposed on the alfalfa stems surface, dark brown to black, 253–455 µm diam. *Alpha*, *beta* and *gamma conidia* not observed.

Culture characteristics — Colony on PDA with flattened mycelium, white, reverse with non-uniform accumulation of citrine pigments. Colony 35.5–40 mm diam in 3 d at 28 °C. On OA with entire margin, aerial mycelium white, fluffy, citrine in the centre and white margin.

Materials examined. CHINA, Yunnan Province, Kunming City, on branches of *P. bretschneideri* cv. Zaobaisu, 17 Oct. 2014, Q. Bai (holotype HMAS 248150, culture ex-type CGMCC 3.19599 = PSCG 034); *ibid.*, culture PSCG 035.

Notes — *Diaporthe parvae* forms a distinct clade with high support (BI/ML/MP = 1/100/100), and differed with the closely related species (*D. chamaeropsis* and *D. cytospora*) on ITS and *CAL* loci (96 % in ITS and 83 % in *CAL*; and 98 % in ITS and 80 % in *CAL*, respectively). This species formed conidiomata-like structures, but remained sterile on various media including SNA, OA, PNA, fennel stems, alfalfa stems, pear stems and barleycorn at varied conditions, e.g., induced at black light and low temperatures, producing no conidiophores, conidiogenous cells and conidia.

Diaporthe pescicola Dissanayake et al., Mycosphere 8: 542. 2017 — Fig. 17

Description & Illustration — Dissanayake et al. (2017).

Materials examined. CHINA, Shandong Province, Yantai City, on branches of *P. bretschneideri* cv. Zaobaisu, 17 Oct. 2014, Q. Bai (cultures PSCG 036, PSCG 037).

Notes — *Diaporthe pescicola* was first described from diseased shoots of *Prunus persica* in Hubei province, China (Dissanayake et al. 2017). In this study, two isolates (PSCG 036,

PSCG 037) clustered together with the ex-type culture of *D. pescicola* (MFLUCC 16-0105) in the multi-locus phylogenetic tree (Fig. 4), and this is the first report of *D. pescicola* responsible for pear shoot canker.

Diaporthe sojiae Lehman, Ann. Missouri Bot. Gard. 10: 128. 1923 — Fig. 18

Description & Illustration — Udayanga et al. (2015).

Materials examined. CHINA, Zhejiang Province, Hangzhou City, on branches of *P. pyrifolia* cv. Cuiyu, 7 Mar. 2016, Y.S. Guo (culture PSCG 283); Guizhou Province, Guiyang City, on branches of *P. pyrifolia* cv. Yuanhuang, 8 Nov. 2017, Y.S. Guo (culture PSCG 481, PSCG 486, PSCG 488); Jiangsu Province, Zhenjiang City, on branches of *P. pyrifolia* cv. Hohsui, 18 Nov. 2017, Y.S. Guo (culture PCSG 502, PCSG 518); *ibid.*, on branches of *P. pyrifolia* cv. Aigansui, 18 Nov. 2017, Y.S. Guo (culture PCSG 510); *ibid.*, on branches of *P. pyrifolia* cv. Kousui, 18 Nov. 2017, Y.S. Guo (culture PCSG 530).

Notes — *Diaporthe sojiae* was first reported on pods and stems of soybean, and subsequently reported on a wide range of hosts. It was also reported on some fruit trees in China, such as *Vitis* spp. (Dissanayake et al. 2015) and *Citrus* spp. (Huang et al. 2015). In this study, 11 isolates were identified as belonging to this species, and this is the first report of *D. sojiae* responsible for pear shoot canker.

Compared with the description of the ex-type isolate FAU635, isolate PSCG 486 has shorter asci (33.5–39.5 × 6.5–9.5 vs 38.5–46.5 × 7–9 µm), slightly larger ascospores (10.5–13 × 3.5–4.5 vs 9.5–12 × 3–4 µm), and longer conidiogenous cells (8–14 vs 0.5–1 µm). Besides, beta conidia of isolate PSCG 486 were found to be hyaline, aseptate, multi-guttulate, filiform, curved, tapering towards both ends, 14.5–23 × 1–2 µm, mean ± SD = 18.8 ± 2.1 × 1.4 ± 0.2 µm, L/W ratio = 13.4.

Diaporthe spinosa Y.S. Guo & G.P. Wang, *sp. nov.* — MycoBank MB830659; Fig. 19

Etymology. From Latin *spinus* 'spiny', referring to its spiny perithecial necks.

Sexual morph on fennel stems. *Ascomata* black, deeply embedded in fennel stems surface, 702–1404 mm diam, densely clustered in groups, multiple tapering spiny perithecial necks protruding through substrata, 1235–1864 mm long. *Perithecia* oval to subglobose, dark brown, 67–215 µm, ostiolate. *Asci* fasciculate, unitunicate, 30.5–38.5 × 6–9 µm, 8-spored, sessile, elongate to clavate. *Ascospores* hyaline, two-celled, often biguttulate, elliptical to fusiform, 9.5–11.5 × 3–4 µm, mean ± SD = 10.5 ± 0.6 × 3.4 ± 0.3 µm, L/W ratio = 3.1 (n = 30). *Asexual morph* on alfalfa stems. *Pycnidial conidiomata* globose, solitary, exposed on the alfalfa stems surface, dark brown to black, 124–172 µm diam. *Conidiophores* hyaline, smooth, 1-septate, densely aggregated, unbranched, ampulliform, 6–9 × 3–4.5 µm. *Conidiogenous cells* phialidic, hyaline, terminal, cylindrical, straight, 8–29 × 1.5–2.5 µm, tapered towards the apex. *Alpha conidia* hyaline, aseptate, fusiform to oval, acutely round at both ends, biguttulate or multi-guttulate, 5.5–8 × 2–3.5 µm, mean ± SD = 7 ± 0.6 × 2.6 ± 0.3 µm, L/W ratio = 2.7 (n = 50). *Beta conidia* hyaline, aseptate, multi-guttulate, filiform, curved, tapering towards both ends, 18.5–30.5 × 1–1.5 µm, mean ± SD = 25.1 ± 2.8 × 1.3 ± 0.1 µm, L/W ratio = 19.3 (n = 38). *Gamma conidia* not observed.

Culture characteristics — Colony on PDA with fluffy mycelium, panniform, aerial mycelium white, reverse amber coloured, being darker at the centre and lighter at the edge. Colony diam 62.5–67.5 mm in 3 d at 28 °C. On OA, colony with entire margin, citrine green in the centre with a white margin.

Materials examined. CHINA, Jiangsu Province, Nanjing City, on branches of *P. pyrifolia* cv. Cuiquan, 22 Aug. 2016, Y.S. Guo (holotype HMAS 248151,

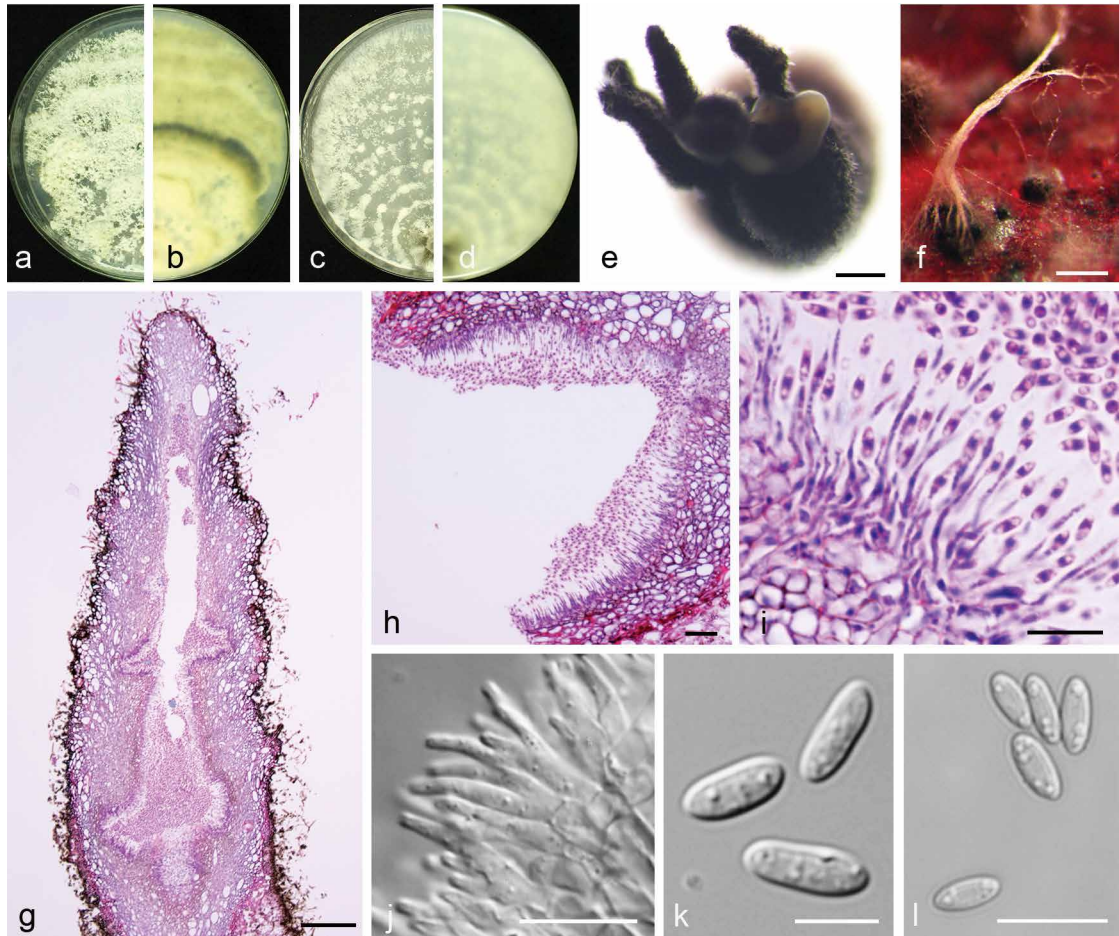


Fig. 22 *Diaporthe velutina* (PSCG 134). a–d. Front and back view, respectively of colonies on PDA (a, b) and OA (c, d); e–f. conidiomata; g–h. section view of conidiomata; i–j. conidiophores; k–l. alpha conidia. — Scale bars: e–f = 200 μ m; g = 100 μ m; h = 20 μ m; i–j, l = 10 μ m; k = 5 μ m.

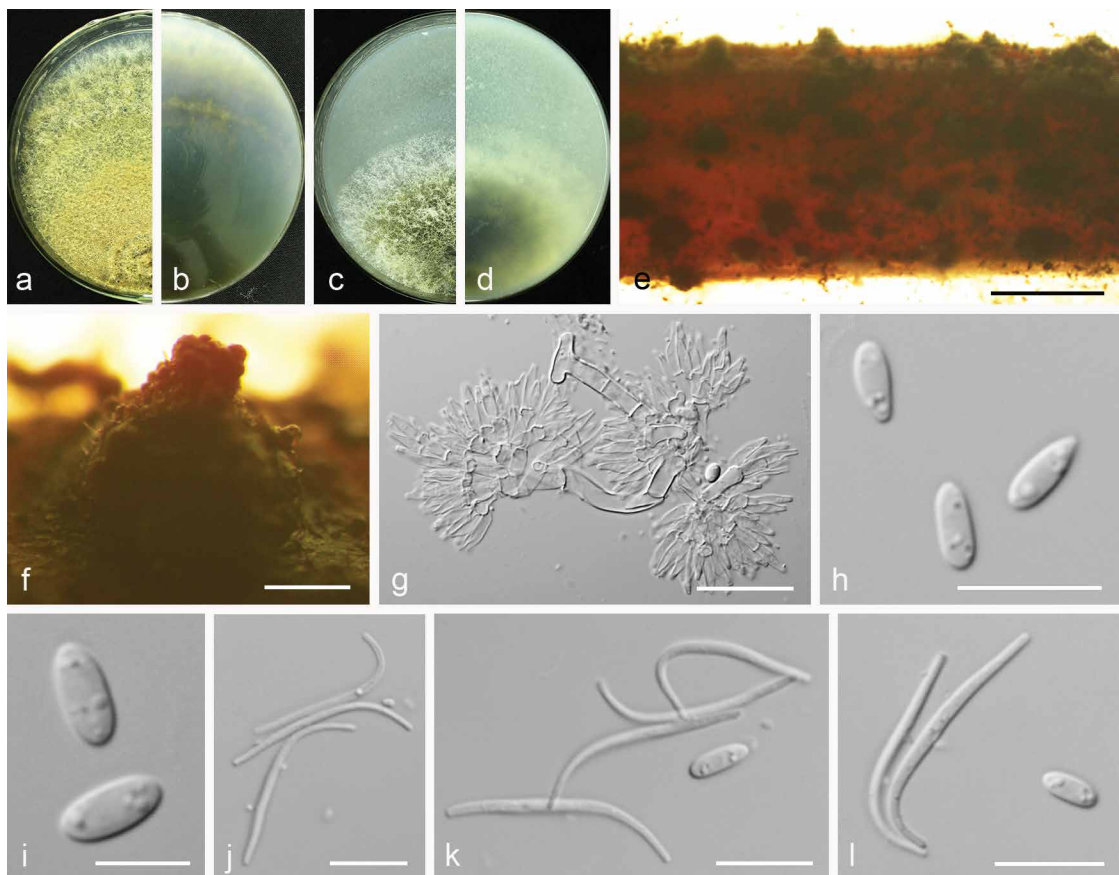


Fig. 23 *Diaporthe zaobaisu*. a–d. Front and back view, respectively of colonies on PDA (a, b) and OA (c, d); e. conidiomata on alfalfa stems; f. conidiomata; g. conidiophores; h–i. alpha conidia; j. beta conidia; k–l. alpha and beta conidia (a–h. isolate PSCG 033; i–l. PSCG 032). — Scale bars: e = 2 mm; f = 200 μ m; g = 20 μ m; h, j–k = 10 μ m; i = 5 μ m.

culture ex-type CGMCC 3.19602 = PCSG 383); *ibid.*, culture PCSG 388; Zhejiang Province, Hangzhou City, on branches of *P. pyrifolia* cv. Cuiguan, 7 Mar. 2016, Y.S. Guo (PCSG 279); Guizhou Province, Guizhou City, on branches of *P. pyrifolia* cv. Yuanhuang, 8 Nov. 2017, Y.S. Guo (PCSG 491).

Notes — *Diaporthe spinosa* forms a well-supported, independent clade in the *D. arecae* species complex (Fig. 4). It contains four isolates which are separated into two branches, with the former (PCSG 383, PCSG 279) differing from the latter (PCSG 388, PCSG 491) by unique fixed alleles in three loci including ITS positions 340 (C), 342 (G), 346 (A), 347 (A), 349 (G), 380 (T), *CAL* positions 368 (G), and *HIS* positions 162 (C), 163 (A), 191 (T), 193 (C), 194 (C), 195 (T), 205 (A), 213 (C), 404 (C), 417 (T), but without obvious differences in morphology of the asexual morph. *Diaporthe spinosa* is most closely related to *D. pescicola* and *D. fulvicolor*, but *D. spinosa* and *D. pescicola* can be clearly differentiated from the latter by 43 different unique fixed alleles in *CAL* loci, and 15 different unique fixed alleles in *CAL* loci can also distinguish *D. spinosa* from *D. fulvicolor*. This species differs from *D. pescicola* in its smaller conidiomata (124–172 vs 637–881 µm), and from *D. fulvicolor* in its shorter alpha conidia (5.5–8 × 2–3.5 vs 7–9 × 2–3 µm).

Diaporthe taoicola Dissanayake et al., *Mycosphere* 8: 543. 2017 — Fig. 20

Description & Illustration — Dissanayake et al. (2017).

Materials examined. CHINA, Zhejiang Province, Hangzhou City, on branches of *P. pyrifolia* cv. Cuiyu, 7 Mar. 2016, Y.S. Guo (culture PSCG 292); Guizhou Province, Guiyang City, on branches of *P. pyrifolia* cv. Jinqiu, 7 Mar. 2017, Y.S. Guo (culture PSCG 413); *ibid.*, on branches of *P. pyrifolia* cv. Yuanhuang, 8 Nov. 2017, Y.S. Guo (culture PSCG 485).

Notes — *Diaporthe taoicola* was first described from diseased shoots of *Prunus persica* in Hubei province, China (Dissanayake et al. 2017). In this study, four isolates clustered together with the ex-type culture of *D. taoicola* (MFLUCC 16-0117) in the multi-locus phylogenetic tree (Fig. 4), and this is the first report of *D. taoicola* responsible for pear shoot canker.

Diaporthe unshiuensis F. Huang et al., *Fungal Biol.* 119: 344. 2015 — Fig. 21

Description & Illustration — Huang et al. (2015).

Materials examined. CHINA, Fujian Province, Sanming City, on branches of *P. pyrifolia* cv. Minfu, 10 Nov. 2014, Q. Bai (culture PSCG 120); *ibid.*, on branches of *P. pyrifolia* cv. Huanghua, 10 Nov. 2014, Q. Bai (PSCG 128); *ibid.*, on branches of *P. pyrifolia* cv. Cuiyu, 25 Oct. 2017, Y.S. Guo (PSCG 468); Hubei Province, Wuhan City, on branches of *P. pyrifolia* cv. Cuiguan, 1 Sept. 2014, Q. Bai (PSCG 059); Jiangsu Province, Zhenjiang City, on branches of *P. pyrifolia* cv. Kousui, 18 Nov. 2017, Y.S. Guo (PSCG 511).

Notes — *Diaporthe unshiuensis* was initially described from twigs of asymptomatic *Fortunella margarita* in Zhejiang province, China (Huang et al. 2015). In this study, 14 isolates were identified as belonging to this species, and this is the first report of *D. unshiuensis* responsible for pear shoot canker. Bai et al. (2015) identified some of the isolates as *P. longicolla*, but they were re-identified as *D. unshiuensis* in this study.

Diaporthe velutina Y.H. Gao & L. Cai, *IMA Fungus* 8: 178. 2017 — Fig. 22

Description & Illustration — Gao et al. (2017).

Materials examined. CHINA, Fujian Province, Sanming City, on branches of *P. pyrifolia* cv. Huanghua, 10 Nov. 2014, Q. Bai (culture PSCG 134).

Notes — *Diaporthe velutina* was originally described from diseased leaves of *Neolitsea* sp. in Jiangxi province, China (Gao et al. 2017). In this study, one isolate (PSCG 134) clustered to-

gether with the ex-type culture of *D. velutina* (CGMCC 3.18286) in the multi-locus phylogenetic tree (Fig. 4), and this is the first report of *D. velutina* responsible for pear shoot canker. In this study, pycnidial conidiomata on alfalfa stems were globose, solitary or aggregated, exposed on the host surface, dark brown to black, 328–890 µm diam. Pycnidial conidiomata on PDA, OA or fennel stems were black, densely clustered in groups, with multiple tapering pycnidial necks protruding through substrata.

Diaporthe zaobaisu Y.S. Guo & G.P. Wang, *sp. nov.* — MycoBank MB830660; Fig. 23

Etymology. Referring to the host variety (*P. bretschneideri* cv. Zaobaisu), from which the fungus was isolated.

Sexual morph not observed. *Asexual morph* on alfalfa stems. *Pycnidial conidiomata* globose or irregular, solitary or aggregated, exposed on the alfalfa stems surface, dark brown to black, 235–445 µm diam. *Conidiophores* hyaline, smooth, 1-septate, densely aggregated, cylindrical, straight, 6–13 × 2.5–4 µm. *Conidiogenous cells* phialidic, hyaline, terminal, ampulliform, 8.5–12 × 2.5–3 µm, tapered towards the apex. *Alpha conidia* hyaline, aseptate, fusiform, biguttulate, 5.5–8.5 × 2–3 µm, mean ± SD = 6.4 ± 0.7 × 2.3 ± 0.2 µm, L/W ratio = 2.8 (n = 50). *Beta conidia* hyaline, aseptate, filiform, curved, tapering towards both ends, 21.5–28 × 1–1.4 µm, mean ± SD = 24.5 ± 1.5 × 1.1 ± 0.1 µm, L/W ratio = 22.3 (n = 41). *Gamma conidia* not observed.

Culture characteristics — Colonies on PDA flat with entire margin, colony honey in the centre with fluffy aerial mycelia and pale white margin; reverse with dull green pigment in the centre. Colony diam 40–44 mm in 3 d at 28 °C. On OA, colonies cottony, dense, greenish olivaceous in the centre; reverse dark herbage green.

Materials examined. CHINA, Yunnan Province, Kunming City, on branches of *P. bretschneideri* cv. Zaobaisu, 17 Oct. 2014, Q. Bai (holotype HMAS 248152, culture ex-type CGMCC 3.19598 = PSCG 031); *ibid.*, culture PSCG 032 and PSCG 033.

Notes — The three isolates studied form a well-supported independent clade distinct from known *Diaporthe* species. *Diaporthe zaobaisu* is most closely related to *D. baccae*, *D. rhusicola*, *D. foeniculina*, *D. neotheicola* and *D. ravennica*, but differentiated from them in ITS (9 different unique fixed alleles by *D. baccae*, 5 by *D. rhusicola*, 11 by *D. foeniculina*, 11 by *D. neotheicola* and 2 by *D. ravennica*) and *TEF* loci (21 different unique fixed alleles by *D. baccae*, 20 by *D. rhusicola*, 20 by *D. foeniculina*, 28 by *D. neotheicola* and 20 by *D. ravennica*). Moreover, *D. zaobaisu* differs from *D. baccae* in having shorter conidiophores (6–13 × 2.5–4 vs 20–57 × 2–3 µm) and conidiogenous cells (8.5–12 × 2.5–3 vs 9–23 × 1–2 µm) (Lombard et al. 2014). Alpha conidia are smaller than in *D. foeniculina* (5.5–8.5 × 2–3 vs 8.5–9 × 2–2.5 µm) and *D. ravennica* (5.5–8.5 × 2–3 vs 7–10.5 × 1.5–3 µm) (Udayanga et al. 2014a, Thambugala et al. 2016). Pycnidial conidiomata are smaller than in *D. foeniculina* (235–445 vs 400–700 µm) and *D. neotheicola* (235–445 vs 420–730 µm) (Santos & Phillips 2009, Udayanga et al. 2014a).

Prevalence of *Diaporthe* species

Prevalence analyses revealed that *D. eres* (248 isolates, 54.7 % of the total isolates) is the dominant species associated with pear shoot canker, followed by *D. hongkongensis* (57 isolates, 12.6 %, isolated from Guizhou, Jiangxi, Fujian and Zhejiang), *D. sojae* (43 isolates, 9.5 %, isolated from Guizhou, Hubei, Jiangsu, Jiangxi and Zhejiang), *D. unshiuensis* (38 isolates, 8.4 %, isolated from Guizhou, Hubei, Jiangsu, Shandong, Fujian and Yunnan), *D. fusicola* (21 isolates, 4.6 %, isolated from Guizhou, Jiangsu, Jiangxi, Fujian and Zhejiang), and *D. cercidis* (12 iso-

lates, 2.6 %, isolated from Chongqing, Jiangsu and Zhejiang) (Fig. 24a). The remaining 13 species account for 7.5 % of the total isolates, with each less than 1 % prevalence (Fig. 24a).

Analysis of the abundance of *Diaporthe* species in the sampling areas revealed only two species identified from the north of the Yangtze River and 19 from the south, revealing obvious species diversity in the south (Fig. 24b). Analysis of the abundance of *Diaporthe* species on pear species revealed 15 species from *P. pyrifolia* and seven from *P. bretschneideri*, respectively (Fig. 24c), with only one species (*D. eres*) on the remaining pear species *P. communis* and *P. ussuriensis*. These findings might be due to the small samples obtained (with 20 and two samples collected in the field, respectively), since symptomatic branches were far less observed than these of *P. pyrifolia* and *P. bretschneideri*.

Pathogenicity and host range

The host range of the 19 *Diaporthe* species was accessed by inoculating mycelial discs onto detached shoots of five pear varieties (i.e., *P. pyrifolia* cv. Hohsui, *P. bretschneideri* cv. Xuehua, *P. ussuriensis* cv. Hanxiang, *P. communis* cv. Docteur Jule Guyot and *P. sinkiangensis* cv. Kuerlexiangli). At 11 d post inoculation (dpi), all *Diaporthe* isolates caused lesions on the inoculated shoots of *P. pyrifolia*, *P. ussuriensis*, *P. communis*, inducing reddish to black shoot canker symptoms, except for a *D. sojae* isolate (PSCG 510) inducing no lesions on

P. bretschneideri, and a *D. zaobaisu* isolate (PSCG 031) and a *D. parvae* isolate (PSCG 034) on *P. ussuriensis* (Fig. 25). The lesion lengths varied significantly among the different isolates. *Diaporthe fusicola* and *D. chongqingensis* caused larger lesions (22–28 mm) on all the tested varieties, followed by the *D. eres* complex (7.6–14 mm), and the remaining isolates induced shorter lesions (1.5–10.5 mm). Most isolates induced longer lesions (longer than 10 mm) on the shoots of *P. pyrifolia* (13 isolates), *P. bretschneideri* (9) and *P. sinkiangensis* (7), while shorter lesions were observed on the shoots of *P. communis* (average 5 mm) and *P. ussuriensis* (5.6 mm). However, lesions longer than 10 mm were observed on *P. ussuriensis* (*D. eres* (PSCG092), *D. spinosa* (PSCG388) and *D. fusicola* (PSCG371, PSCG118)) and *P. communis* (*D. eres* (PSCG322), *D. fusicola* (PSCG371, PSCG118) and *D. chongqingensis* (PSCG435)) (Fig. 25). In parallel, no lesions developed on the twigs that were inoculated with PDA discs as control.

One isolate of each species was further inoculated on intact pear seedlings (*P. pyrifolia* cv. Cuiguan) (Fig. 26). These results showed that all the isolates started to induce black lesions after 10 dpi. The lesions turned reddish and significant differences were evident among different species by 25 dpi ($F = 8.735$, $P < 0.001$). The induced symptoms matched the ones observed in the field. *Diaporthe chongqingensis*, *D. fusicola* and *D. eres* are highly aggressive (lesion lengths more than 8 mm). No lesions were induced in the control branches inoculated with PDA

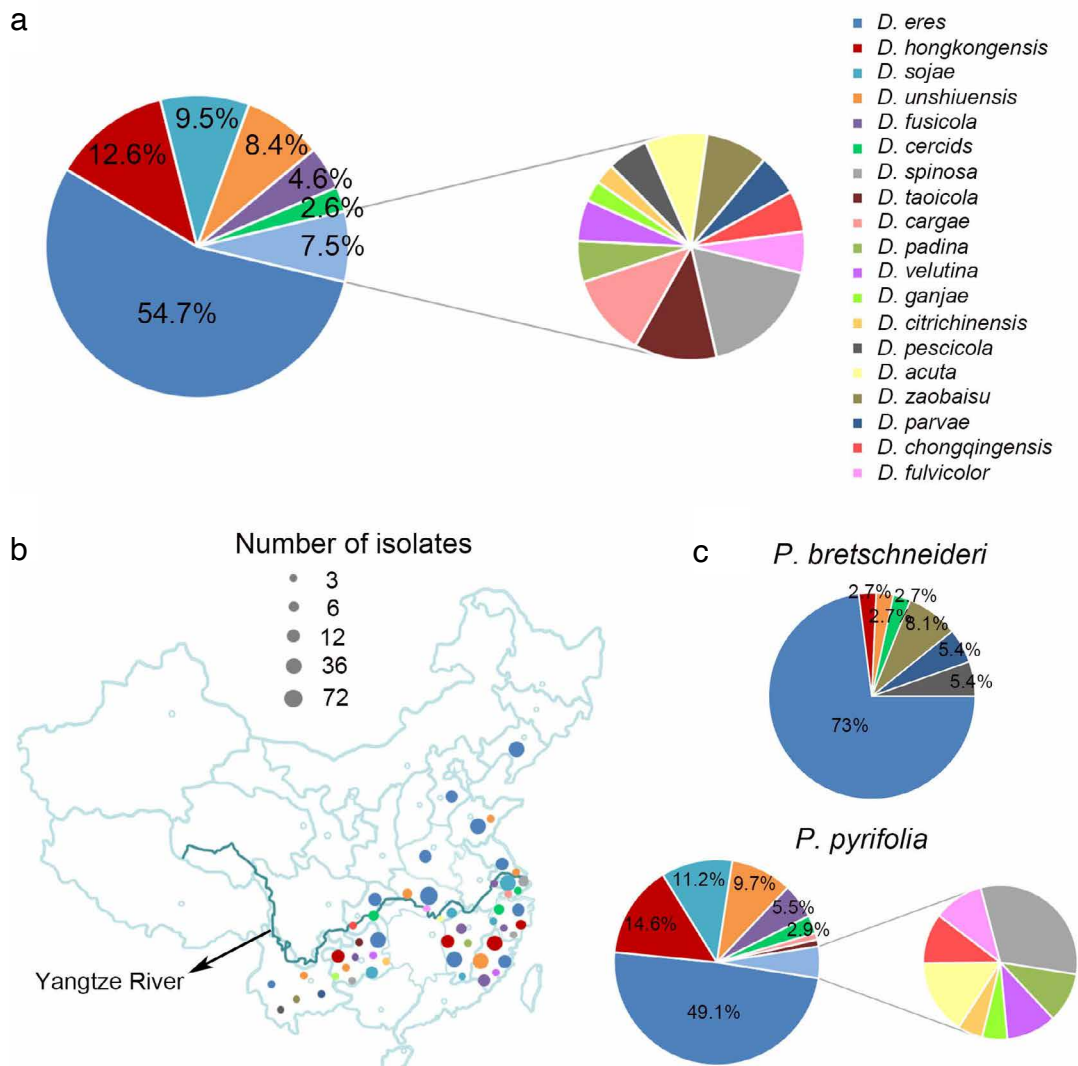


Fig. 24 The prevalence of *Diaporthe* species isolated from pear. a. Overall isolation rate (%) of *Diaporthe* species; b. distribution of *Diaporthe* species in China, each coloured circle represents one species, and the size of the circle indicates the number of isolates; c. isolation rate (%) of *Diaporthe* species from *P. pyrifolia* and *P. bretschneideri*, respectively.

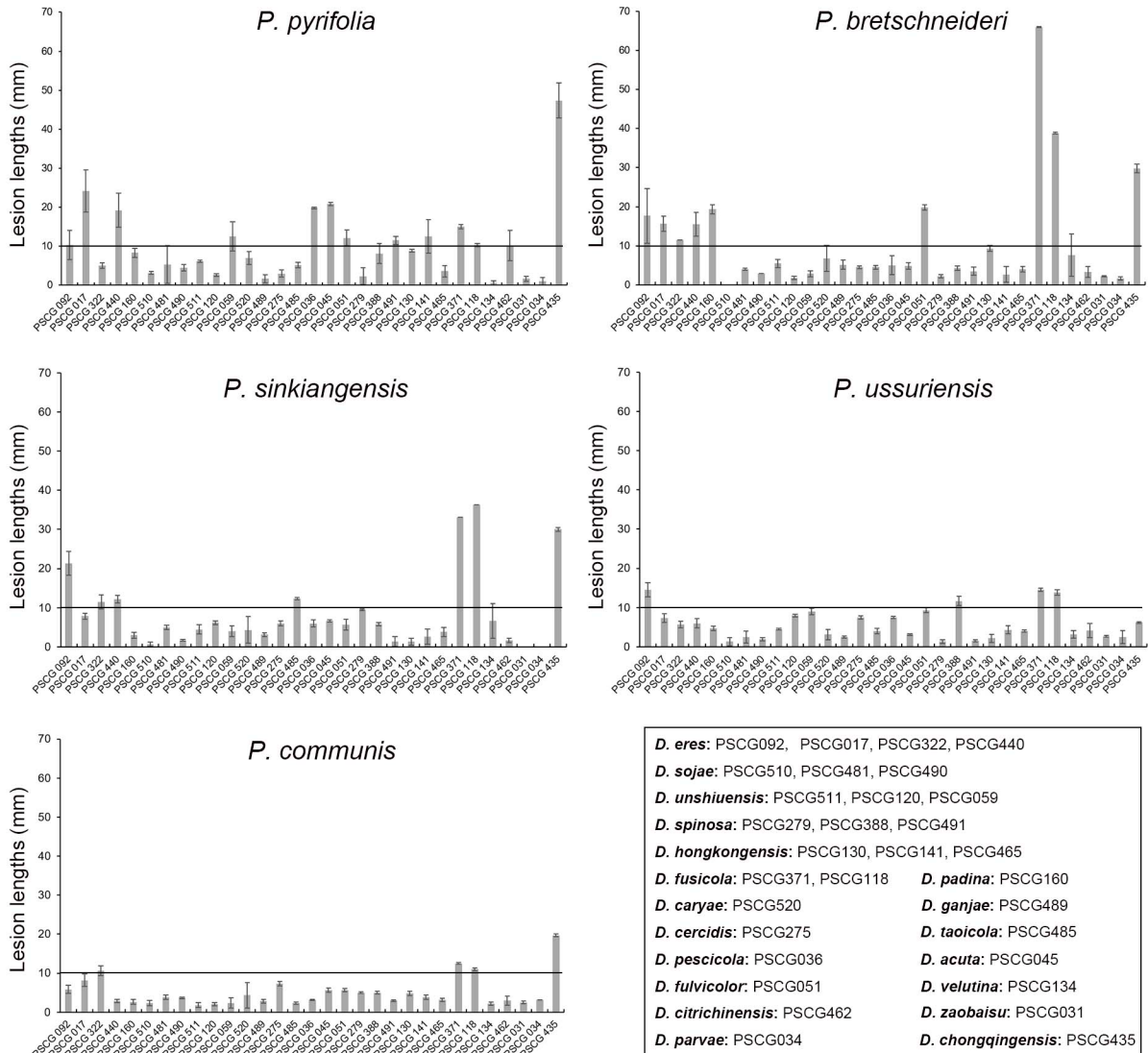


Fig. 25 Lesion lengths on wounded pear twigs (*P. pyrifolia* cv. Hohsui, *P. bretschneideri* cv. Xuehua, *P. ussuriensis* cv. Hanxiang, *P. communis* cv. Docteur Jules Guyot and *P. sinkiangensis* cv. Kuerlexiangli) at 11 dpi induced by mycelia plugs of 31 representative isolates of 19 *Diaporthe* species.

plugs. All branches showing canker symptoms induced by the inoculations were subjected to fungal isolation, and the results showed that the obtained colonies matched the inoculated ones in morphology and ITS sequence data.

Host range was accessed on fruit trees including apple, peach, kiwifruit and citrus by inoculating the detached shoots with mycelium discs of one representative isolate from each *Diaporthe* species. The results showed that 13 species (including *D. acuta*, *D. caryae*, *D. cercidis*, *D. chongqingensis*, *D. citrichinensis*, *D. eres*, *D. fulvicolor*, *D. fusicola*, *D. ganjae*, *D. pescicola*, *D. spinosa*, *D. taicola* and *D. unshiuensis*) infected all plants, resulting in lesions ranging from 1.5–49 mm on apple, 1.2–53 mm on peach, 1.2–53 mm on kiwifruit and 2–12 mm on citrus (Fig. 27). Of these, *D. fusicola* induced the longest lesions (32 mm) on four hosts compared to other species (less than 18.5 mm), as did *D. spinosa* (53 mm) on peach, *D. pescicola* (53 mm) on kiwifruit and *D. chongqingensis* (45 mm) on apple. Whereas *D. padina* and *D. parvae* infected all plants except for citrus, so did *D. velutina* except for peach, and *D. sojae* and *D. hongkongensis* except for kiwifruit. *Diaporthe zaobaisu* only infected citrus and apple, inducing lesions 3 and 2 mm long on their shoots, respectively.

Mating-type test

The mating-types of these 113 isolates were identified by PCR amplification of the mating genes (*MAT1-2-1* and *MAT1-1-1*).

These results showed that all *D. sojae* isolates are homothallic since both mating genes were detected in the same isolates; all the isolates of *D. caryae*, *D. pescicola*, *D. spinosa*, *D. taicola* and *D. velutina* are heterothallic since only one of the mating genes was detected. For the remaining species (*D. eres*, *D. unshiuensis*, *D. hongkongensis*, *D. cercidis*), both mating genes were detected in some isolates while only one was detected in the remaining isolates of the same species, suggesting that they contain potentially homothallic as well as heterothallic isolates (Table 1).

DISCUSSION

Diaporthe species have been extensively investigated on several hosts (Gomes et al. 2013, Gao et al. 2017), but not yet on pear. Up to now, only eight species have been reported infecting pear, i.e., *D. ambigua*, *D. infecunda*, *D. terebinthifolii*, *D. foeniculacea* and *D. oxe* on *P. communis*, *Phomopsis theicola* and *D. nobilis* complex on *P. pyrifolia* and *D. eres* on *P. communis* (Smit 1996, Cloete et al. 2011, Santos et al. 2017b, Bertetti et al. 2018). In this study, we conducted extensive surveys of *Diaporthe* species associated with pear shoot canker in the major production provinces in China. Multi-locus phylogenetic and morphological analyses revealed 12 species (from 453 isolates) belonging to three *Diaporthe* species complexes, including the *D. eres* complex (*D. eres* and *D. padina*), *D. sojae*

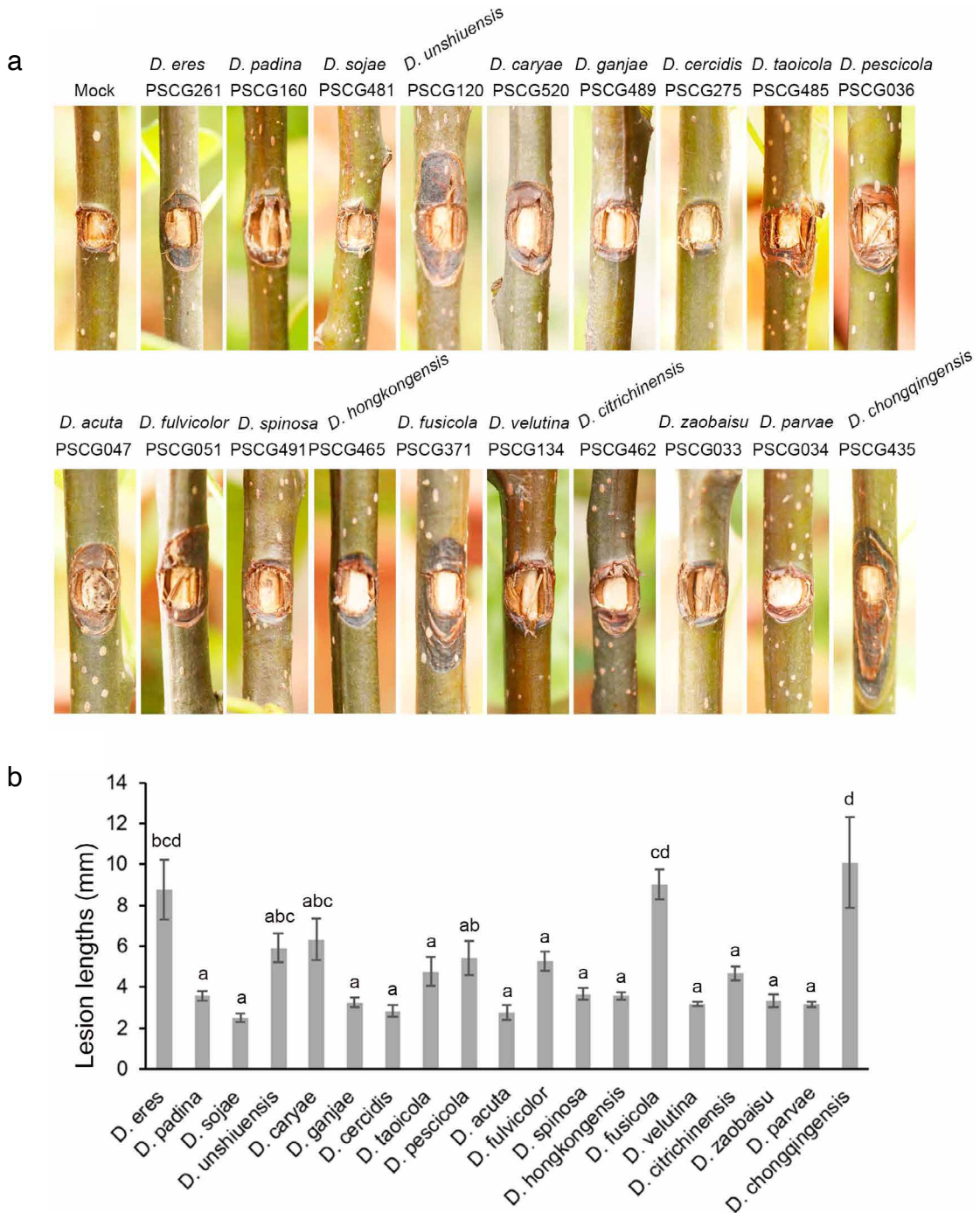


Fig. 26 Symptoms and lesion lengths induced by inoculation of wounded pear seedlings (*P. pyrifolia* cv. Cuiguan) at 25 dpi with mycelia plugs of representative isolates of 19 *Diaporthe* species. a. Representative symptoms as photographed at 25 days post inoculation (dpi); b. mean lesions lengths from six replicates of branches measured at 25 dpi. Statistical analysis was performed with SPSS Statistics 21.0 by one-way analysis of variance, and means were compared using Tukey's test at a significance level of $P = 0.05$. Letters over the bars indicate the significant difference at the $P = 0.05$ level.

complex (*D. caryae*, *D. ganjae*, *D. sojiae* and *D. unshiuensis*), and *D. arecae* complex (*D. acuta*, *D. cercidis*, *D. fulvicolor*, *D. pescicola*, *D. spinosa* and *D. taoicola*), and seven singleton species (*D. chongqingensis*, *D. citrichinensis*, *D. fusicola*, *D. hongkongensis*, *D. parvae*, *D. velutina* and *D. zaobaisu*). Of the 19 species, six species are newly described here, namely *D. acuta*, *D. chongqingensis*, *D. fulvicolor*, *D. parvae*, *D. spinosa* and *D. zaobaisu*. These species are all responsible for pear shoot canker, which could be confirmed following Koch's postulates. To our knowledge, this is the first report that these species infecting pear are responsible for pear shoot canker besides *D. eres*.

Recently, *Diaporthe* species identification has been advanced by phylogenetic analysis based on multilocus DNA phylogeny

including *TEF*, *TUB*, *HIS* and *CAL* genes (Santos et al. 2017a). Here, we resolved the *Diaporthe* species (*P. fukushii*, *D. eres*, *P. amygdali*, *P. longicolla* and *D. neotheicola*) that were previously identified based on phylogenetic analysis of *TEF*, *ACT* and ITS (Bai et al. 2015). Our results showed that these four species were incorrectly identified, and we reassigned isolates identified as *P. fukushii* to *D. eres*, *P. amygdali* to *D. fusicola*, *P. longicolla* to *D. unshiuensis*, and *D. neotheicola* to *D. velutina* (Fig. 2–4). Similarly, *D. biguttusis*, *D. camptothecicola*, *D. ellipticola*, *D. longicolla*, *D. mahothocarpus* and *D. momicola* clustered with *D. eres* (Fig. 2), suggesting that they are synonyms of *D. eres*, as previously proposed (Fan et al. 2018, Yang et al. 2018). Additionally, the ITS locus has been shown to be less

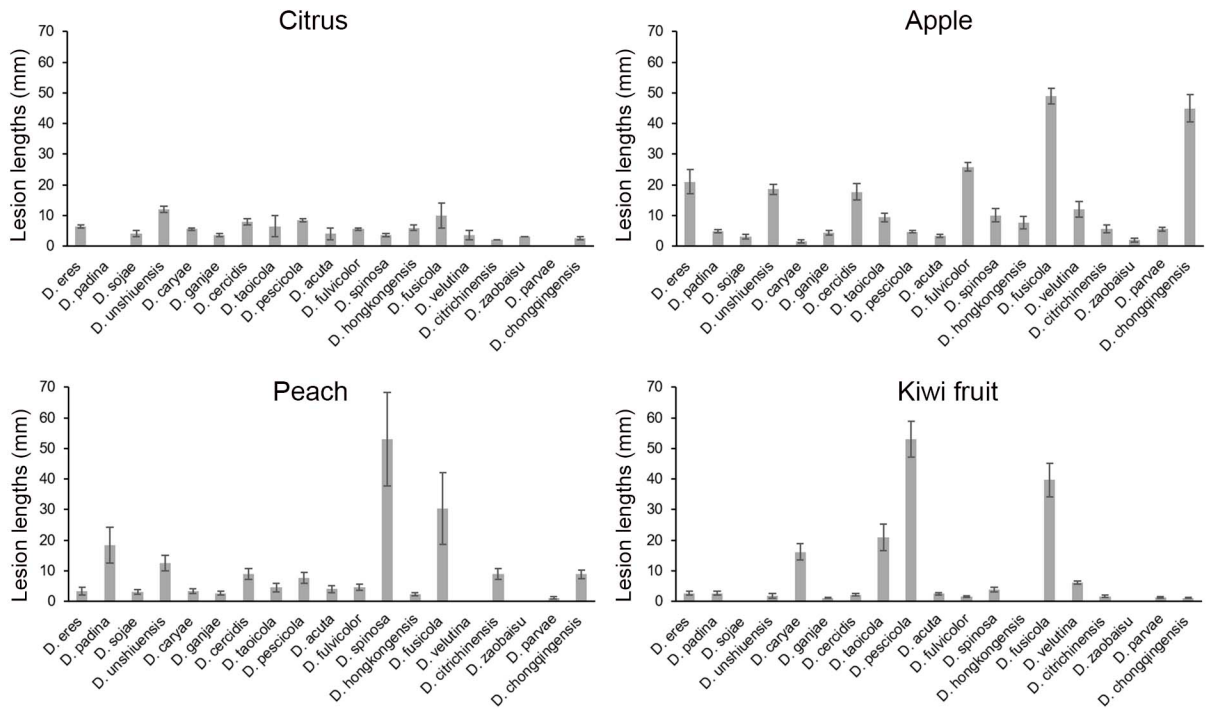


Fig. 27 Lesion lengths on wounded citrus, apple, peach and kiwifruit twigs at 11 dpi induced by mycelia plugs of representative isolates of 19 *Diaporthe* species.

optimal for closely related species (Farr et al. 2002, Gomes et al. 2013), especially in the *D. eres* complex (Santos et al. 2017a). Therefore, the ITS region was excluded from the phylogenetic analysis for the *D. eres* complex, which resulted in a well-supported phylogenetic tree (Fig. 2). However, for the *D. sojae* and *D. arecae* complexes, the phylogenetic analysis was still resolved with all these loci (Huang et al. 2013, Udayanga et al. 2014a, 2015). Furthermore, three new species (i.e., *D. acuta*, *D. fulvicolor* and *D. spinosa*) were identified as belonging to the *D. arecae* complex (Fig. 4).

Although the taxonomy of *Diaporthe* species has relied more heavily on molecular characteristics rather than on morphology (Castlebury et al. 2003, Crous & Groenewald 2005, Udayanga et al. 2012), we have noticed that most *Diaporthe* species exhibited morphological characteristics closely corresponding to their DNA phylogeny. For example, colonies of *D. eres* often secreted grey olivaceous pigments (Fig. 10, 15), *D. arecae* umber pigments (Fig. 5, 7, 11, 17, 19), while *D. sojae* lacked pigments (Fig. 13, 18, 21). Furthermore, their alpha conidial morphologies differed among these species complexes. Of those, most isolates in the *D. eres* complex exhibited short rod-like alpha conidia, *D. sojae* had oval conidia with obtusely rounded ends, and *D. arecae* had acutely rounded ends. In a previous study, gamma conidia were discovered for *D. limonicola*, which were hyaline, multiguttulate, fusiform to subcylindrical with an acute or rounded apex (Guarnaccia & Crous 2017). It is worthy to note that such conidia were also observed for *D. eres* (isolate PSCG 041) in this study (Fig. 10).

The prevalence analysis revealed that *D. eres* is the most prevalent species in China, which is consistent with observations made in our previous study (Bai et al. 2015), and corresponds to its biological trait of wide host range, since it infects many plants in the *Rosaceae* (Farr & Rossman 2018). Moreover, *Diaporthe* species are closely linked to the sampling area, with a higher diversity (19 species) in the south of the Yangtze River than that in the north (2). It might be due to the fact that the climate in the south is humid and warm, suitable for the survival and prevalence of *Diaporthe* species, while drought and extremely low temperatures in the north, especially in Gansu, Shanxi and Xinjiang, are unsuitable for *Diaporthe*. Moreover,

P. pyrifolia trees are dominantly cultivated in the south, and are susceptible to infection by *Diaporthe* species. No *Diaporthe* species were detected from the pear samples collected in the north provinces including Gansu, Shanxi and Xinjiang. Instead, *Botryosphaeria* spp. were readily isolated from these samples, which induced stem canker following inoculation on pear stems, suggesting that these samples might be infected by pear stem canker instead of pear shoot canker.

Since *Diaporthe* spp. have an endophytic, saprobic or pathogenic lifestyle, we determined their pathogenicity to pear by inoculating colonised mycelial discs on shoots of five different pear species. These results showed that they are all pathogenic and responsible for pear shoot canker by fulfilling the Koch's postulates. Moreover, these isolates showed significantly different virulence spectra related to species and host plants. For example, *D. fuscicola* isolates were highly aggressive to *P. bretschneideri*, whereas *D. parvae* was only slightly aggressive on the same *Pyrus* species; *D. chongqingensis* isolates were aggressive to most of the tested *Pyrus* plants, but obviously less to *P. ussuriensis*. Additionally, the host ranges of these *Diaporthe* species also showed a clear diversity among them, exemplified by the fact that some infected all test plants, while others not. It is worth to note that most *Diaporthe* species have a wide host range, indicating that these species also pose threats to other fruit trees, as previously described (Gomes et al. 2013, Dissanayake et al. 2015). In fact, *Diaporthe* spp. have been reported infecting many plants resulting in severe diseases, e.g., seed decay of soybean (Sun et al. 2013), canker and twig dieback of jujube (Zhang et al. 2018), cordon dieback of kiwifruits (Díaz & Latorre 2018), and shoot canker diseases of citrus or grapevines (Van Niekerk et al. 2005, Huang et al. 2013), and of *Rosaceae* plants, e.g., peach (Dissanayake et al. 2017), apple (Abreo et al. 2012), blackberry (Vrandecic et al. 2011), and almond (Diogo et al. 2010).

In previous studies, 22 *Diaporthe* species have been characterised based on their mating type, revealing that most of the species are heterothallic except for *D. ambigua* which is homothallic, and *D. viticola* which is mixed (Santos et al. 2010). Recently, *D. foeniculina*, *D. pyracanthae*, *D. malorum*, and *D. eres* were also identified as being heterothallic (Santos et al. 2017b).

Similarly, most of the species obtained in this study are heterothallic, with one species, *D. sojae*, being homothallic. Correspondingly, almost all of the obtained *Diaporthe* species were asexual, but *D. sojae* also produced ascospores with viable ascospores. It is worth to note that four species (*D. unshiuensis*, *D. hongkongensis*, *D. cercidis* and *D. eres*) were identified to be homo- as well as heterothallic, and the identification for *D. eres* differs from the previous report, which described *D. eres* as exclusively heterothallic (Santos et al. 2017b). For the heterothallic identification, we cannot exclude the possibility that one mating gene was undetected due to variation among isolates. For example, *D. spinosa* produced sexual sporocarps from single conidia, suggesting it to be homothallic, but only one mating type gene was detected (Table 1). Finally, the mating types detected by these primers need further confirmation since they might be inactive, or change due to mutation.

This study represents the most intensive investigation and the first resolution with multi-locus phylogenetic analysis of *Diaporthe* species infecting *Pyrus* plants, revealing six novel species that infect pear and are responsible for pear shoot canker. This study also characterises the taxonomic, morphological and biological diversity of *Diaporthe* spp. associated with different *Pyrus* spp. in China, with regards to geographical location, host range and mating type. As such it provides useful information to help understand the ecology of the *Diaporthe* spp. infecting pear, as well as for the control of pear shoot canker.

Acknowledgements This study was financially supported by the fund of Integrated Research and Demonstration of Reduction of Fertilizer and Pesticide but Efficiency Enhancement for Pear Cultivation in the Yangtze River Basin (no. 2018YFD0201406), the earmarked fund for Pear Modern Agro-Industry Technology Research System (CARS-28-15) of the Chinese Ministry of Agriculture and the Fundamental Research Funds for the Central Universities (no. 2662016PY107). The authors thank Lei Cai for critical suggestions and Fang Liu for technical guidance in the morphological descriptions.

REFERENCES

- Abreo E, Martínez S, Sessa L, et al. 2012. Phomopsis cotoneastri as a pathogen associated with trunk cankers and death of young apple trees cv. Cripps Pink. *Journal of Phytopathology* 160: 434–436.
- Bai Q, Wang GP, Zhai LF, et al. 2015. Biological and molecular characterization of five Phomopsis species associated with pear shoot canker in China. *Plant Disease* 99: 1704–1712.
- Bertetti D, Guarnaccia V, Spadaro D, et al. 2018. First report of fruit rot in European pear caused by Diaporthe eres in Italy. *Plant Disease* 102: 1651.
- Carbone I, Kohn LM. 1999. Method for designing primer sets for speciation studies in filamentous ascomycetes. *Mycologia* 91: 553–556.
- Castlebury LA, Farr DF, Rossman AY, et al. 2003. Diaporthe angelicae comb. nov., a modern description and placement of Diaportheopsis in Diaporthe. *Mycoscience* 44: 203–208.
- Choi YW, Hyde KD, Ho WH. 1999. Single spore isolation of fungi. *Fungal Diversity* 3: 29–38.
- Cloete M, Fourie PH, Damm U, et al. 2011. Fungi associated with die-back symptoms of apple and pear trees, a possible inoculum source of grapevine trunk disease pathogens. *Phytopathologia Mediterranea* 50: S176–S190.
- Crous PW, Groenewald JZ. 2005. Hosts, species and genotypes: opinions versus data. *Australasian Plant Pathology* 34: 463–470.
- Crous PW, Groenewald JZ, Risède J, et al. 2004. Calonectria species and their cylindrocladium anamorphs species with sphaeropedunculate vesicles. *Studies in Mycology* 50: 415–430.
- Crous PW, Groenewald JZ, Shivas RG, et al. 2011. Fungal Planet description sheets: 69–91. *Persoonia* 26: 108–156.
- Crous PW, Verkley GJM, Groenewald JZ, et al. (eds). 2019. Fungal Biodiversity. Westerdijk Laboratory Manual Series 1. Westerdijk Fungal Biodiversity Institute, Utrecht, The Netherlands.
- Crous PW, Wingfield MJ, Burgess TI, et al. 2016. Fungal Planet description sheets: 469–557. *Persoonia* 37: 218–403.
- Díaz GA, Latorre BA. 2018. First report of cordón dieback of kiwifruits caused by Diaporthe ambigua and D. australafricana in Chile. *Plant Disease* 102: 446.
- Diogo ELF, Santos JM, Phillips AJL. 2010. Phylogeny, morphology and pathogenicity of Diaporthe and Phomopsis species on almond in Portugal. *Fungal Diversity* 44: 107–115.
- Dissanayake AJ, Liu M, Zhang W, et al. 2015. Morphological and molecular characterisation of Diaporthe species associated with grapevine trunk disease in China. *Fungal Biology* 119: 283–294.
- Dissanayake AJ, Zhang W, Liu M, et al. 2017. Diaporthe species associated with peach tree dieback in Hubei, China. *Mycosphere* 8: 533–549.
- Fan XL, Yang Q, Bezerra JDP, et al. 2018. Diaporthe from walnut tree (Juglans regia) in China, with insight of the Diaporthe eres complex. *Mycological Progress* 17: 841–853.
- FAO – Food and Agricultural Organization of the United Nations, China. 2017. Pear fruits fresh and processed: annual statistics. <http://www.fao.org/faostat/en/#data/QC>.
- Farr DF, Castlebury LA, Rossman AY. 2002. Morphological and molecular characterization of Phomopsis vaccinii and additional isolates of Phomopsis from blueberry and cranberry in the eastern United States. *Mycologia* 94: 494–504.
- Farr DF, Rossman A. 2018. Fungal databases, systematic mycology and microbiology laboratory. ARS, USDA. <http://nt.ars-grin.gov/fungaldata-bases/>.
- Ferradini N, Lancioni H, Torricelli R, et al. 2017. Characterization and phylogenetic analysis of ancient Italian landraces of pear. *Frontiers in Plant Science* 8: 751.
- Freeman S, Katan T, Shabi E. 1996. Characterization of Colletotrichum gloeosporioides isolates from avocado and almond fruits with molecular and pathogenicity tests. *Applied and Environmental Microbiology* 62: 1014–1020.
- Fu M, Crous PW, Bai Q, et al. 2019. Colletotrichum species associated with anthracnose of Pyrus spp. in China. *Persoonia* 42: 1–35.
- Gao YH, Liu F, Cai L. 2016. Unravelling Diaporthe species associated with Camellia. *Systematics and Biodiversity* 14: 102–117.
- Gao YH, Liu F, Duan W, et al. 2017. Diaporthe is paraphyletic. *IMA Fungus* 8: 153–187.
- Gao YH, Su YY, Sun W, et al. 2015. Diaporthe species occurring on Lithocarpus glabra in China, with descriptions of five new species. *Fungal Biology* 119: 295–309.
- Glass NL, Donaldson GC. 1995. Development of primer sets designed for use with the PCR to amplify conserved genes from filamentous ascomycetes. *American Society for Microbiology* 61: 1323–1330.
- Gomes RR, Glienke C, Videira SIR, et al. 2013. Diaporthe: a genus of endophytic, saprobic and plant pathogenic fungi. *Persoonia* 31: 1–41.
- Grasso FM, Marini M, Vitale A, et al. 2012. Canker and dieback on Platanus × acerifolia caused by Diaporthe scabra. *Forest Pathology* 42: 510–513.
- Guarnaccia V, Crous PW. 2017. Emerging citrus diseases in Europe caused by species of Diaporthe. *IMA Fungus* 8: 317–334.
- Guarnaccia V, Crous PW. 2018. Species of Diaporthe on Camellia and Citrus in the Azores Islands. *Phytopathologia Mediterranea* 57: 307–319.
- Guarnaccia V, Groenewald JZ, Woodhall J, et al. 2018. Diaporthe diversity and pathogenicity revealed from a broad survey of grapevine diseases in Europe. *Persoonia* 40: 135–153.
- Hillis DM, Bull JJ. 1993. An empirical test of bootstrapping as a method for assessing confidence in phylogenetic analysis. *Systematic Biology* 42: 182–192.
- Huang DH, Zhou CH, Xu L, et al. 2014. New diseases of Jiangxi precocious pear shoot canker and its comprehensive prevention and control measures. *Xiandai Horticulture* 1: 67–68.
- Huang F, Hou X, Dewdney MM, et al. 2013. Diaporthe species occurring on citrus in China. *Fungal Diversity* 61: 237–250.
- Huang F, Udayanga D, Wang X, et al. 2015. Endophytic Diaporthe associated with Citrus: a phylogenetic reassessment with seven new species from China. *Fungal Biology* 119: 331–347.
- Katoh K, Standley DM. 2013. MAFFT multiple sequence alignment software version 7: improvements in performance and usability. *Molecular Biology and Evolution* 30: 772–780.
- Kumar S, Stecher G, Tamura K. 2016. MEGA7: Molecular evolutionary genetics analysis version 7.0 for bigger datasets. *Molecular Evolutionary Genetics Analysis* 33: 1870–1874.
- Lombard L, Van Leeuwen GCM, Guarnaccia V, et al. 2014. Diaporthe species associated with Vaccinium, with specific reference to Europe. *Phytopathologia Mediterranea* 53: 287–299.
- Marin-Felix Y, Hernández-Restrepo M, Wingfield MJ, et al. 2019. Genera of phytopathogenic fungi: GOPHY 2. *Studies in Mycology* 92: 43–133.
- Nasu H, Hatamoto M, Date H, et al. 1987. Pear fruit rot caused by agents of Japanese pear canker, Phomopsis fukushii and blossom end rot of European pear phomopsis sp. *Annals of the Phytopathological Society of Japan* 53: 630–637.

- Nirenberg HI. 1976. Untersuchungen über die morphologische und biologische Differenzierung in der Fusarium-Sektion *Liseola*. Mitteilungen aus der Biologischen Bundesanstalt für Land- und Forstwirtschaft Berlin-Dahlem 169: 1–117.
- Nitschke T. 1870. *Pyrenomyces Germanici* 2. Eduard Trewendt, Breslau, 245.
- Nylander JAA. 2004. MrModelTest v. 2. Program distributed by the author. Evolutionary Biology Centre, Uppsala University.
- Rambaut A. 2014. FigTree, v. 1.4.2. Institute of evolutionary biology. University of Edinburgh. <http://tree.bio.ed.ac.uk/software/figtree/>.
- Rayner RW. 1970. A mycological colour chart. Commonwealth Mycological Institute, Kew, UK.
- Ronquist F, Huelsenbeck JP. 2003. MrBayes 3: Bayesian phylogenetic inference under mixed models. *Bioinformatics* 19: 1572–1574.
- Santos JM, Correia VG, Phillips AJ. 2010. Primers for mating-type diagnosis in *Diaporthe* and *Phomopsis*: their use in teleomorph induction in vitro and biological species definition. *Fungal Biology* 114: 255–270.
- Santos JM, Phillips AJL. 2009. Resolving the complex of *Diaporthe* (*Phomopsis*) species occurring on *Foeniculum vulgare* in Portugal. *Fungal Diversity* 34: 109–123.
- Santos JM, Vrandecic K, Cosic J, et al. 2011. Resolving the *Diaporthe* species occurring on soybean in Croatia. *Persoonia* 27: 9–19.
- Santos L, Alves A, Alves R. 2017a. Evaluating multi-locus phylogenies for species boundaries determination in the genus *Diaporthe*. *PeerJ* 5:e3120. doi: <https://doi.org/10.7717/peerj.3120>.
- Santos L, Phillips AJL, Crous PW, et al. 2017b. *Diaporthe* species on Rosaceae with descriptions of *D. pyracanthae* sp. nov. *Mycosphere* 8: 485–511.
- Silva GJ, Souza TM, Barbieri RL, et al. 2014. Origin, domestication, and dispersing of pear (*Pyrus* spp.). *Advances in Agriculture* 2014: 1–8.
- Smit WA. 1996. A new canker disease of apple, pear, and plum rootstocks – caused by *Diaporthe ambigua* in South Africa. *Plant Disease* 80: 1331–1335.
- Smith H, Wingfield MJ, Crous PW, et al. 1996. *Sphaeropsis sapinea* and *Botryosphaeria dothidea* endophytic in *Pinus* spp. and *Eucalyptus* spp. in South Africa. *South African Journal of Botany* 62: 86–88.
- Sun S, Kim MY, Chaisan T, et al. 2013. *Phomopsis* (*Diaporthe*) species as the cause of soybean seed decay in Korea. *Journal of Phytopathology* 161: 131–134.
- Swofford D. 2002. PAUP 4.0 b10: Phylogenetic analysis using parsimony (*and other methods). Computer programme. Sinauer Associates, Sunderland, MA, USA.
- Tanaka S, Endo S. 1930. Studies on a new canker disease of Japanese pear trees caused by *Phomopsis fukushii* n. sp. *Transactions of the Tottori Society of Agricultural Sciences* 2: 123–134.
- Thambugala KM, Daranagama DA, Phillips AJL, et al. 2016. Microfungi on tamarix. *Fungal Diversity* 82: 239–306.
- Thompson SM, Tan YP, Young AJ, et al. 2011. Stem cankers on sunflower (*Helianthus annuus*) in Australia reveal a complex of pathogenic *Diaporthe* (*Phomopsis*) species. *Persoonia* 27: 80–89.
- Udayanga D, Castlebury LA, Rossman AY, et al. 2014a. Species limits in *Diaporthe*: molecular re-assessment of *D. citri*, *D. cytosporrella*, *D. foeniculina* and *D. rudis*. *Persoonia* 32: 83–101.
- Udayanga D, Castlebury LA, Rossman AY, et al. 2014b. Insights into the genus *Diaporthe*: phylogenetic species delimitation in the *D. eres* species complex. *Fungal Diversity* 67: 203–229.
- Udayanga D, Castlebury LA, Rossman AY, et al. 2015. The *Diaporthe sojae* species complex: phylogenetic re-assessment of pathogens associated with soybean, cucurbits and other field crops. *Fungal Biology* 119: 383–407.
- Udayanga D, Liu X, Crous PW, et al. 2012. A multi-locus phylogenetic evaluation of *Diaporthe* (*Phomopsis*). *Fungal Diversity* 56: 157–171.
- Udayanga D, Liu X, McKenzie EHC, et al. 2011. The genus *Phomopsis*: biology, applications, species concepts and names of common phytopathogens. *Fungal Diversity* 50: 189–225.
- Van Niekerk JM, Groenewald JZ, Farr DF, et al. 2005. Reassessment of *Phomopsis* species on grapevines. *Australasian Plant Pathology* 34: 27–39.
- Van Rensburg JCJ, Lamprecht SC, Groenewald JZ, et al. 2006. Characterisation of *Phomopsis* spp. associated with die-back of rooibos (*Aspalathus linearis*) in South Africa. *Studies in Mycology* 55: 65–74.
- Vrandecic K, Jurkovic D, Cosic J, et al. 2011. First report of cane blight on blackberry caused by *Diaporthe eres* in Croatia. *Plant Disease* 95: 612–612.
- Wang HY, Han XF, Gao JJ, et al. 2011. The cause of severe occurrence of pear shoot canker and its comprehensive control technology. *Chinese Horticulture Abstracts* 7: 164–165.
- White TJ, Bruns T, Lee S, et al. 1990. Amplification and direct sequencing of fungal ribosomal RNA genes for phylogenetics. In: Innis MA, Gelfand DH, Sninsky JJ, et al. (eds), *PCR protocols: a guide to methods and applications*: 315–322. Academic Press, San Diego, California.
- Wu J, Wang ZW, Shi ZB, et al. 2013. The genome of the pear (*Pyrus bretschneideri* Rehd.). *Genome Research* 23: 396–408.
- Yang Q, Fan XL, Guarnaccia V, et al. 2018. High diversity of *Diaporthe* species associated with dieback diseases in China, with twelve new species described. *MycologyKeys* 39: 97–149.
- Zhang QM, Yu CL, Li GF, et al. 2018. First report of *Diaporthe eres* causing twig canker on *Zizyphus jujuba* (Jujube) in China. *Plant Disease* 102: 1458.
- Zhao DY, Xu K, Yuan JC, et al. 2016. Analysis on the current situation of production and sales of world pear's main country of origin and its development. *China Fruits* 2: 94–100.

Appendix Number of samples and *Diaporthe* isolates collected from 12 regions in China.

Province	Number of samples	Number of isolates
Chongqing	11	16
Fujian	37	83
Guizhou	21	53
Hebei	18	10
Henan	11	10
Hubei	46	87
Jiangsu	35	47
Jiangxi	18	44
Liaoning	25	21
Shandong	27	40
Yunnan	8	12
Zhejiang	29	30
Total	286	453